Organisation de Coopération et de Développement Économiques
Organisation for Economic Co-operation and Development

26-Nov-2010

_____
English text only

NUCLEAR ENERGY AGENCY
COMMITTEE ON THE SAFETY OF NUCLEAR INSTALLATIONS

Core Exit Temperature (CET) Effectiveness in Accident Management of Nuclear Power Reactor

October 2010

JT03293388

ORGANISATION FOR ECONOMIC CO-OPERATION AND DEVELOPMENT

The OECD is a unique forum where the governments of 33 democracies work together to address the economic, social and environmental challenges of globalisation. The OECD is also at the forefront of efforts to understand and to help governments respond to new developments and concerns, such as corporate governance, the information economy and the challenges of an ageing population. The Organisation provides a setting where governments can compare policy experiences, seek answers to common problems, identify good practice and work to co-ordinate domestic and international policies.

The OECD member countries are: Australia, Austria, Belgium, Canada, Chile, the Czech Republic, Denmark, Finland, France, Germany, Greece, Hungary, Iceland, Ireland, Israel, Italy, Japan, Korea, Luxembourg, Mexico, the Netherlands, New Zealand, Norway, Poland, Portugal, the Slovak Republic, Slovenia, Spain, Sweden, Switzerland, Turkey, the United Kingdom and the United States. The European Commission takes part in the work of the OECD.

OECD Publishing disseminates widely the results of the Organisation's statistics gathering and research on economic, social and environmental issues, as well as the conventions, guidelines and standards agreed by its members.

This work is published on the responsibility of the Secretary-General of the OECD.
The opinions expressed and arguments employed herein do not necessarily reflect the official
views of the Organisation or of the governments of its member countries.

NUCLEAR ENERGY AGENCY

The OECD Nuclear Energy Agency (NEA) was established on 1st February 1958 under the name of the OEEC European Nuclear Energy Agency. It received its present designation on 20th April 1972, when Japan became its first non-European full member. NEA membership today consists of 28 OECD member countries: Australia, Austria, Belgium, Canada, the Czech Republic, Denmark, Finland, France, Germany, Greece, Hungary, Iceland, Ireland, Italy, Japan, Korea, Luxembourg, Mexico, the Netherlands, Norway, Portugal, the Slovak Republic, Spain, Sweden, Switzerland, Turkey, the United Kingdom and the United States. The European Commission also takes part in the work of the Agency.

The mission of the NEA is:

– to assist its member countries in maintaining and further developing, through international co-operation, the scientific, technological and legal bases required for a safe, environmentally friendly and economical use of nuclear energy for peaceful purposes, as well as

– to provide authoritative assessments and to forge common understandings on key issues, as input to government decisions on nuclear energy policy and to broader OECD policy analyses in areas such as energy and sustainable development.

Specific areas of competence of the NEA include safety and regulation of nuclear activities, radioactive waste management, radiological protection, nuclear science, economic and technical analyses of the nuclear fuel cycle, nuclear law and liability, and public information.

The NEA Data Bank provides nuclear data and computer program services for participating countries. In these and related tasks, the NEA works in close collaboration with the International Atomic Energy Agency in Vienna, with which it has a Co-operation Agreement, as well as with other international organisations in the nuclear field.

COMMITTEE ON THE SAFETY OF NUCLEAR INSTALLATIONS

Within the OECD framework, the NEA Committee on the Safety of Nuclear Installations (CSNI) is an international committee made of senior scientists and engineers, with broad responsibilities for safety technology and research programmes, as well as representatives from regulatory authorities. It was set up in 1973 to develop and co-ordinate the activities of the NEA concerning the technical aspects of the design, construction and operation of nuclear installations insofar as they affect the safety of such installations.

The committee's purpose is to foster international co-operation in nuclear safety amongst the NEA member countries. The CSNI's main tasks are to exchange technical information and to promote collaboration between research, development, engineering and regulatory organisations; to review operating experience and the state of knowledge on selected topics of nuclear safety technology and safety assessment; to initiate and conduct programmes to overcome discrepancies, develop improvements and research consensus on technical issues; and to promote the co-ordination of work that serves to maintain competence in nuclear safety matters, including the establishment of joint undertakings.

The clear priority of the committee is on the safety of nuclear installations and the design and construction of new reactors and installations. For advanced reactor designs the committee provides a forum for improving safety related knowledge and a vehicle for joint research.

In implementing its programme, the CSNI establishes co-operate mechanisms with the NEA's Committee on Nuclear Regulatory Activities (CNRA) which is responsible for the programme of the Agency concerning the regulation, licensing and inspection of nuclear installations with regard to safety. It also co-operates with the other NEA's Standing Committees as well as with key international organizations (e.g. the IAEA) on matters of common interest.

AUTHORS

Coordinator:

Ivan TÓTH, AEKI, Hungary

Participating Ogganizations and Authors:

Robert PRIOR

Oddbjörn SANDERVAG, SSM, Sweden

Klaus UMMINGER, AREVA NP GmbH, Germany

Hideo NAKAMURA, JAEA, Japan

Nikolaus MUELLNER, Marco CHERUBINI, Alessandro DEL NEVO, Francesco D'AURIA, U. Pisa, Italy

Jörg DREIER, PSI, Switzerland

Jose Ramon ALONSO, CSN, Spain

Abdallah AMRI, OECD-NEA

TABLE OF CONTENTS

EXECUTIVE SUMMARY

Background

The Task on the Core Exit Temperature (CET) thermocouple effectiveness in Accident Management (AM) was initiated based on a discussion held by the CSNI Working Group on Analysis and Management of Accidents (WGAMA) in September 2007. The discussion focused on results of the test 6-1 performed in the frame of the OECD ROSA/LSTF project simulating a vessel head small break loss-of-coolant accident (SBLOCA) under an assumption of total failure of the high pressure injection (HPI) system. The test had to be terminated prematurely to avoid excessive overheating of the core. It was noted that core uncovery had started well before CET thermocouples indicated superheating and the temperature increase rate in the core was higher than shown by the CET. The results suggested that the response of the CET thermocouples could be inadequate to initiate the relevant AM actions. Moreover, examples of CET response in other tests, e.g. in LOFT, PKL and LSTF seemed to confirm this observation.

In order to address this issue, the CSNI approved a WGAMA activity in December 2007 with the objectives to review and consolidate background knowledge of CET application in AM and to provide conclusions and recommendations for possible further work.

Approach

The principal mechanism for the discussion of the CET reliability in AM was through three technical meetings and exchanges by e-mails which addressed the following items:

- Collection and review of the design basis of CET application for AM procedures through a survey of the CET use in the NEA member countries.

- Review of pertinent experimental results (from LOFT, ROSA/LSTF, PKL and PSB-VVER) focusing on delay times between CET and core temperature rise. Though test results in experimental facilities may help to understand CET behavior, one should be cautious when extrapolating facility results to power reactors. This is why scaling and transposition issues were addressed and discussed.

- Conclusions and recommendations for further work.

Main Conclusions

a) CET readings use for AM in the member countries, and associated Technical Bases

The Task Group has conducted an international survey on CET use for AM. The main conclusions of this survey are as follow:

Most of the plants at the surveyed organizations use CET readings for AM. However, the scope and extent of their use is quite different from country to country; and something that is really significant, in countries

using more than one unique technology (i.e. vendor), use of CET for AM could also be quite different from plant to plant.

In general, member countries have reported a generalized use of CET in EOP (preventive AM), in the transition from EOP to SAMG, in SAMG (mitigative AM) and, in some cases, in Emergency Planning.

The questions and responses to the survey were not sufficiently detailed to derive the exact technical basis for the definition of all set-point values. Criteria based on sub-cooling, saturation, onset of superheating and/or significant superheating, were reported by most of the surveyed organizations. In order to remedy this shortcoming, a discussion of the technical (physical) bases for the major classes of set-point and CET usage was provided in Section 2.7.

Another important topic investigated in the survey was the relationship between CET Readings and Maximum Cladding Temperature. A significant fraction of the responses indicated that specific analysis had been performed to address this issue, but some of them felt the model validation was not fully adequate. Consistently with that, some of the responses expressed that either "delayed response" or "accuracy" was a concern.

b) Review of experimental facilities results

The group has extensively reviewed information from different sources and experiments where delays and differences between CET and cladding temperature readings had been observed: these include relevant experiments performed in LOFT, PKL, PSB-VVER facilities and thirteen ROSA/LSTF experiments. The following conclusions have been obtained from this review:

- Delays in CET responses compared to actual cladding temperatures had been already identified earlier in different experiments. Especially, LOFT results had been carefully analyzed to gain insights about this issue and their impact on plant safety.

- The use of the CET measurements has some limitations in detecting inadequate core cooling and core uncovery: if CET reading indicates superheating it is in all cases with a certain time delay (ranging from 20 to several 100 s) and it is always significantly lower (up to several 100 K) than the actual maximum cladding temperature.

- CET performance strongly depends on the accident scenarios and the flow conditions in the core.

- The main causes affecting CET delays, which were present in all the experimental facilities and for most of the scenarios, are the following: radial temperature profiles (both in and above the core), cooling effect of the unheated structures in the upper part of and above the core, poor heat transfer from the rod surface to the surrounding steam due to low steam velocities during core boil-off and water backflow from the hot legs during core heat-up due to steam condensation in SG tubes, pressurizer water fall down or from hot leg ECC injection.

- Besides that, there are other relevant aspects very specific to the facility design, like the actual CET location or behavior that is scenario-dependent, like the hot steam chimney effect in RPV Top Head breaks and the downward core flow in the case of RPV bottom head break.

- The number of experiments for scenarios starting from shutdown and/or low reactor water level conditions is limited. However, PKL and ROSA tests have shown that CET delays in these conditions can be even more pronounced than in tests starting from nominal power due to colder structures in the upper part of the core.

c)   Applicability of experimental results to real plant conditions

A relevant conclusion drawn from the data in the reviewed experiments deals with the consequences of CET delays for the effectiveness of the AM strategies included in the different EOP/SAMG packages existing in the nuclear industry.

Qualitative application/extrapolation of the CET response to reactor scale is possible. However, direct extrapolation in quantitative terms to the reactor scale should be avoided in general or done with special care due to limitations of the experimental facilities in terms of geometrical details, unavoidable distortion in the scaling of the overall geometry, and of the heat capacity of structures.

According to the results of the experiments and the subsequent analysis, and at least for scenarios starting at power conditions, it seems that the observed delays should not affect severely the effectiveness of most existing AM actions, but it must be underlined that concerns about CET functionality for general use in AM are well founded. It should be realized that an increase in the CET temperature is the ultimate indication of an inadequate core cooling and of an already started core heat-up. No CET temperature increase during a transient does not guarantee adequate core cooling: accident scenarios cannot be excluded, in which the CET indication of inadequate core cooling is significantly delayed, especially for some scenarios, such as RPV Top Head and Lower Head Breaks and cases with water backflow from the hot legs. These scenarios should deserve special attention.

Nevertheless, taking into account the delay and the temperature difference in the CET behavior, a CET temperature increase above saturation temperature, in particular in combination with other measurements, is well capable to detect a core heat up and is therefore an important element in the context of AM procedures.

After reviewing the different international approaches to AM, it seems that it is not possible to *a priori* fully discard the possibility of having, in a real nuclear power plant, a similar response as the one observed in ROSA Project Test 6.1, provided the applicable AM action initiation rely only on CET readings, which is not always the case.

In this sense it is interesting to remark that most of the AM strategies analyzed by the group, but not all, rely on a combination of CET readings and other instrumentation indications (normally, Reactor Vessel and/or Steam Generator water level) to define the initiation of the different AM recovery actions. This approach, when appropriately implemented, makes the AM more reliable because the specific draw-backs of each individual instrumentation system do not use to be coincident for a particular scenario.

d)   Impact on AM procedure set points

In view of the Task Group's results with respect to CET delay, the question may be raised about the consequences for the effectiveness of AM strategies relying on CET signals, widely used in the nuclear industry.

In order to judge whether the effects discussed in this report have an impact on AM measures and set-points already in place, one would need to understand whether the definition of a given CET set-point took into account all relevant effects and uncertainties (like known physical reasons affecting heat transfer from the core to CET location, instrumentation accuracy/bias etc.). Did the AM developer use computer codes and models that were able to correctly represent these effects? Or maybe he did not address them specifically, but the set-point has included margin which would more than compensate?

Obviously, to answer these questions goes well beyond the present mandate of the Task Group and it could even be argued whether – due to a large number of plant specific aspects – it fits to the activity of an

OECD task group. However, a feasible activity within such a task group could consist in developing a "best practice" methodology as recommended below.

Recommendations for future work

Based on the previous conclusions, it is recommended to continue with the activities related to the CET effectiveness in AM, including the following:

- The conclusions of the present report indicate the importance of dealing appropriately with the associated phenomena and uncertainties when performing analytical studies in support of AM strategies. Existing models used to calculate time delays between core temperature and CET readings may not be fully validated – this is also evident from the responses received to the questionnaire. Computer codes normally used for this type of analysis may not have enough "resolution" to accurately calculate some relevant phenomena affecting this particular issue. It is therefore recommended to verify whether or not state-of-the-art codes and their underlying models applied in support of AM procedure development are able to reproduce the delays and differences between rod surface temperatures and CET readings.

- The above activity could take the form of an ISP based on one or two pertinent experiments. PKL or ROSA/LSTF tests reviewed here could be candidates. The activity could have the following objectives:

  o Assessment of physical models to predict heat transfer modes affecting CET behavior.

  o Development of a "best practice guideline" for the nodalisation approach of the uncovered core section up to the point of CET location.

  o Based on comparison with test results, assessment of the possible impact of 3D effects, not modeled in these codes.

  o If the 3D effects turn out to have an important contribution to time delay or delta-T, development of proposals, how these effects can be modeled e.g. by the help of CFD codes.

- Investigate the problem of CETs issue "scaling" (methods of extrapolating) from experimental facilities size, like LSTF, to commercial PWR reactors. The investigation could include both experimental and analytical aspects and would focus on the influence of reflux water from hot legs onto CETs as well as on the 3D flow behaviour in the upper part of the core. Large scale experiments are proposed for phenomena investigation and data preparation for code validation.

Besides that, the conclusions drawn by this group should be disseminated among stakeholders on AM (utilities, vendors, etc) in order to give them the opportunity of reviewing the robustness of the existing AM packages to cope with situations like the ones discussed in this report.

1.   INTRODUCTION

The Core Exit Temperature (CET) thermocouple indication is widely used for initiation of Accident Management (including emergency operating procedures and severe accident management) in many countries although CET set points may vary among reactor types and designs. However, since the CET is important for Accident Management (AM) actions initiation, it is important to understand the behavior of the CET in order to assess its reliability.

As a matter of fact, the test 6-1 performed in the OECD ROSA/LSTF project simulating a vessel head small break loss-of-coolant accident (SBLOCA) under an assumption of total failure of the high pressure injection (HPI) system, had to be terminated prematurely to avoid excessive overheating of the core. It was noted that the test 6-1 results showed that the core uncovery had started significantly early before the CET thermocouples indicated superheating and that the temperature increase rate was higher in the core than in the CET. The results suggested that the response of the CET thermocouples could be inadequate to initiate the relevant AM actions.

In addition, 4 LOFT experiments (experiment L2-5 which was a large break LOCA in the cold leg with rapid pump coastdown, experiment L8-1 that was a 4 inch small break in the cold leg, experiment L5-1 which was an intermediate size (14 inch) cold leg break with low head accumulator injection and experiment L8-2 which was an intermediate size (14 inch) cold leg break with delayed accumulator injection) have been analyzed. They confirm that there may be scenarios in which CET indications would be inadequate to initiate the corresponding AM actions. Moreover, examples of CET response compiled from data obtained earlier in BETHSY, LSTF, PKL and PSB-VVER facilities seem to confirm this observation.

Possible reasons and hypothesis to explain this observation have been proposed; they are mainly related to a possible cooling of the CET thermocouples by steam generators reflux water, persistence of liquid film on the CET thermocouples surface combined with low steam velocities, or thermodynamic non-equilibrium between steam and water droplets.

Though test results in experimental facilities may help to understand CET behaviour, one should be cautious when extrapolating facility results to power reactors. For example, it is noted that the CET thermocouples are generally installed much closer to the core in the experiments than in the power plants - in LOFT only one inch above the core. Therefore, it may not be assumed that the CETs in the plant behave more favourably than in the experiments. In general, the scaling and transposition issues should be addressed and discussed.

In order to address the CET reliability and effectiveness in AM, WGAMA proposed late 1997 an activity which was approved by the CSNI with the objective to prepare a status report covering the following items:

- Collection and review of the design basis of CET application for AM procedures in different countries;

- Review of pertinent experimental results focusing on delay times between CET and core temperature rise;

- Conclusions and recommendations for further work, if needed.

Though some concerns about 3-D effects have been raised, which would require detailed analytical evaluations, they are considered outside the scoping nature of the present activity, and may be addressed later if needed. Also thermocouple design issues are excluded, as these are too plant specific to be covered in an international context and within a short time activity.

Co-operation with ROSA and PKL Projects is encouraged as it would be beneficial in order to draw relevant conclusions and recommendations for possible further work on this issue.

The activity started during the first quarter of 2008 with a call for nominations. Nominations were received from AREVA-France, AREVA-Germany, Belgium (TRACTEBEL), Hungary (KFKI AEKI, PAKS NPP), Italy (University of Pisa), Japan (JAEA), Korea (KINS), Slovenia (Slovenian Nuclear safety Administration), Spain (CSN) and Switzerland (PSI). Though Sweden did not nominate any expert, important input came from O. Sandervag (SMS). This provides the adequate number of participants for a Task Group which includes utilities, designers/vendors, research institutes, technical support organizations and regulators.

The Task Group, lead by I. Tóth (KFKI AEKI), also WGAMA Chairman, met three times in order to address CET issues:

- First meeting on April 23-24, 2008 in Budapest during which the Task Group discussed the presentations on the different countries' status in CET use for AM, the available experimental data for confirmation of CET use in AM including the effect of CET thermocouple location. The Group could also prepare a Questionnaire which was distributed to WGAMA members.

- Second meeting held on September 22, 2008 in Paris to discuss the answers to the Questionnaire received from 17 organizations and the available experimental investigations relevant to CET effectiveness in AM. A detailed plan for the preparation of the draft report, including its outline, was also discussed and agreed.

- Third meeting held on April 17, 2009 in Paris to discuss the available chapters of the report and the preliminary conclusions and to define the work plan to complete the activity.

The report presents the outcome of the Task Group meetings and the results of its review of the background knowledge of CET application in AM, with some recommendations for further work, according to the following outline:

- Chapter 1: Introduction, including background of the activity, scope and issues, and report outline;

- Chapter 2 which addresses design basis of CET application for AM procedures in different NEA member countries;

- Chapter 3 which reviews pertinent experimental results from BETHSY, LOFT, PKL and ROSA/LSTF. RELAP5 simulation of PSB-VVER SBLOCA test is also presented in order to evaluate the code performance in terms of CET modeling. Finally, a synthesis of relevant experimental results is proposed;

- Chapters 4 and 5 summarize the conclusions and recommendations proposed by the Task Group.

2. DESIGN BASIS OF CET APPLCATION FOR AM PROCEDURES IN DIFFERENT COUNTRIES

2.1 INTRODUCTION

The WGAMA Task Group on CET is entrusted to prepare a status report covering collection and review of the design basis of CET application for Accident Management procedures in different countries. To evaluate this, a questionnaire was prepared and distributed to WGAMA members. The questions asked in this survey were the following:

1- Is CET used for accident management in your country?

2- If yes, for what purposes?

(Please, identify in your response, and briefly describe, the most relevant AM procedures which rely on CET readings).

3- If you have set points for CET use, please provide the values and describe the basis.

4- How do you account of the fact that the CET is not the cladding temperature?

5- In case you perform supporting calculations, please describe the way you model the CET readings. Have you made comparison with experiments to support the approach?

6- Do you have any specific concerns associated with the use of CET in accident management?

This section of the report presents the responses to the survey.

It should be noted that the scope of the Working Group includes use of core exit temperature instrumentation during response to an accident or incident, in the context of plant stabilisation and recovery (management of and accident situation). It includes both "preventive" accident management (normally, the response to an event in which core damage has not occurred), and 'mitigative accident management (response to 'severe accidents' – those in which core/fuel damage has occurred).

The scope of the investigation does NOT include the use of core exit temperature instrumentation during normal operation, or its use to support the implementation of an off-site emergency plan (though mention may be made of such applications if relevant).

2.2 PARTICIPATION IN THE SURVEY

2.2.1 Summary of Participation in the Survey

Participation in the survey is summarised in table 1.

A good overall and general spectrum of response was received, with a wide range of countries and organisations participating, including utilities, regulators, TSOs and vendors.

Table 1 – Summary of Participation in the WGAMA CET Survey

Country	Organisation	Type of Org
Belgium	Tractebel	U (TSO)
Finland	RNSA	R
France	EDF	U
	IRSN	R(TSO)
Germany	AREVA	V
Hungary	NPP Paks	U
Japan	MHI	V
Korea	KINS	R(TSO)
Netherlands	KCB/EPZ	U
	VROM/KFD	R
Slovenia	SNSA	R
Spain	ANAV	U
	CNAT	U
	CSN	R
Sweden	SKI	R
Switzerland	HSK	R
USA	NRC	R

CET GAMA - Response to Questionnaire

Total responses received: 17
Regulatory bodies: 9
Utilities: 6
Vendors: 2
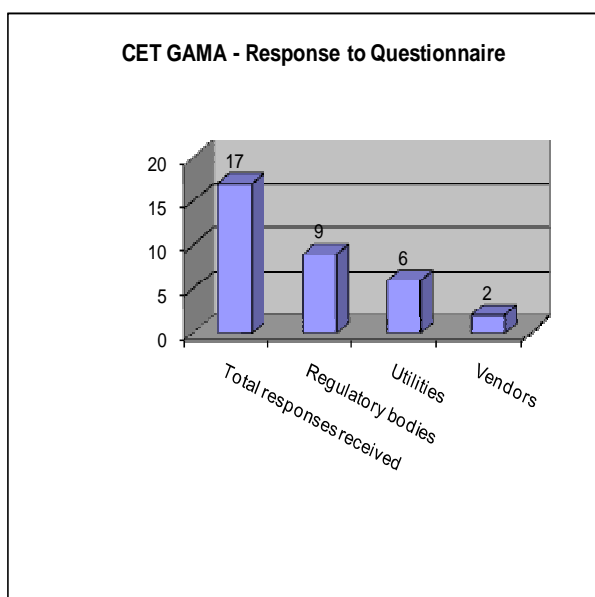
R : Regulatory bodies
U : Utilities
V : Vendors

CET GAMA - Response to Questionnaire
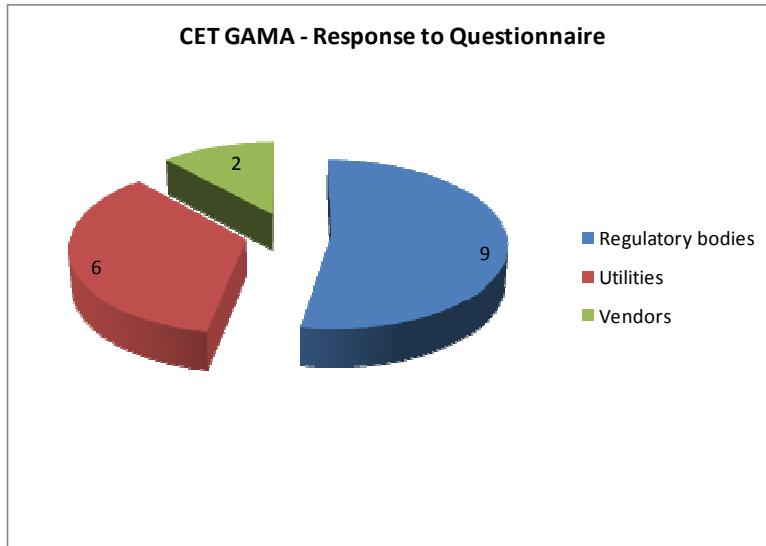
2.3 GENERAL USE OF CORE EXIT TEMPERATURE IN SURVEYED COUNTRIES

2.3.1 Introduction

The first two questions in the survey were designed to identify the function in the members' accident management programs which rely on the core exit thermocouples. These questions were:

1- Is CET used for accident management in your country?

and

2- If yes, for what purposes?

(Please, identify in your response, and briefly describe, the most relevant AM procedures which rely on CET readings).

The responses to these questions are presented by country. 13 countries were represented.

2.3.2 Identified Uses and Results of Survey

Considering all the responses, the following areas of use of CET within accident management were identified by the participants:

- The CET are used *within* Emergency Operating Procedures (EOPs) (i.e. within the preventive accident management regime, before core damage has occurred). All 13 responses indicated that this is the case in their country.

- The CET are used as the primary indication to initiate the transition from EOPs to Severe Accident Management Guidance (SAMG) (i.e. the transition from preventive to mitigative accident management). 12 of the 13 countries represented responded that this is the case in their country.

- The CET are used within SAMG (i.e. within the mitigative accident management regime, after core damage has occurred) in order to cue certain checks and/or actions. This is the case in 9 of the 13 countries. (Finland, France, Germany and Japan indicated that this is *not* done in their countries).

- The CET are used as one of the inputs to categorise an emergency (assign an Emergency Action Level or EAL) by emergency planning staff. This was the case for 4 participants (Hungary, US, Slovenia and The Netherlands), but this was volunteered information and so it is not possible to conclude that this is *not* done in the other nine participating countries. Also, as has been noted above, use of CET in Emergency Planning (i.e. the planning of off-site actions to protect the public) is not within the scope of this working group, and so this application is not discussed in detail in subsequent report sections.

- The CET are used as one of the inputs used to perform a Core Damage Assessment or CDA by Emergency Planning staff. (This is an evaluation of the degree of core damage which may be used as an input to the source term used to identify appropriate off-site protective actions (PAs). This was the case for 2 participants (US and Slovenia), but this was volunteered information and so it is not possible to conclude that this is *not* done in the other ten participating countries. Also, as has been noted above, use of CET in Emergency Planning (i.e. the planning of off-site actions to protect the public) is not within the scope of this working group, and so this application is not discussed in detail in subsequent report sections.

The summarized response to these questions is shown in table 2.

Table 2 – Use of CET by Participating Countries

Question 1- Is CET used for accident management in your country?

Question 2- If yes, for what purposes?

(Please, identify in your response, and briefly describe, the most relevant AM procedures which rely on CET readings).

Country	Organisation / type		Q1 - CET used?	Q2 -		Purposes		
				EOP	EOP-SAMG	within SAMG	EP - EAL	EP - CDA
Belgium	Tractebel	U(TSO)	Yes	Yes	Yes	Yes		
Finland	RNSA	R	Yes	Yes	Yes	No		
France	EDF	U	Yes	Yes	Yes	No		
	IRSN	R(TSO)	Yes	Yes	Yes	No		
Germany	AREVA	V	Yes	Yes	Yes (planned)	No		
Hungary	NPP Paks	U	Yes	Yes	Yes	Yes	Yes	No
Japan	MHI	V	Yes	Yes	No	No		
Korea	KINS	R(TSO)	Yes	Yes	Yes	Yes		
Netherlands	KCB/EPZ	U	Yes	Yes	Yes	Yes	Yes	No
	VROM/KFD	R	Yes	Yes	Yes	Yes	Yes	No
Slovenia	SNSA	R	Yes	Yes	Yes	Yes	Yes	Yes
Spain	ANAV	U	Yes	Yes	Yes	Yes		
	CNAT	U	Yes	Yes	No	No		
	CSN	R	Yes	Yes	Yes	Yes		
Sweden	SKI	R	Yes	Yes	Yes	Yes		

| Switzerland | HSK | R | Yes | Yes | Yes | Yes | | |
| USA | NRC | R | Yes | Yes | Yes | Yes | Yes | Yes |

CET GAMA - Use of CET by Country

13   13   12   9   4   2

14
12
10
8
6
4
2
0

Countries represented
Use within EOPs
EOP: SAMG transition
Use within SAMG
Emergency Planning (EAL)
Emergency Planning (CDA)
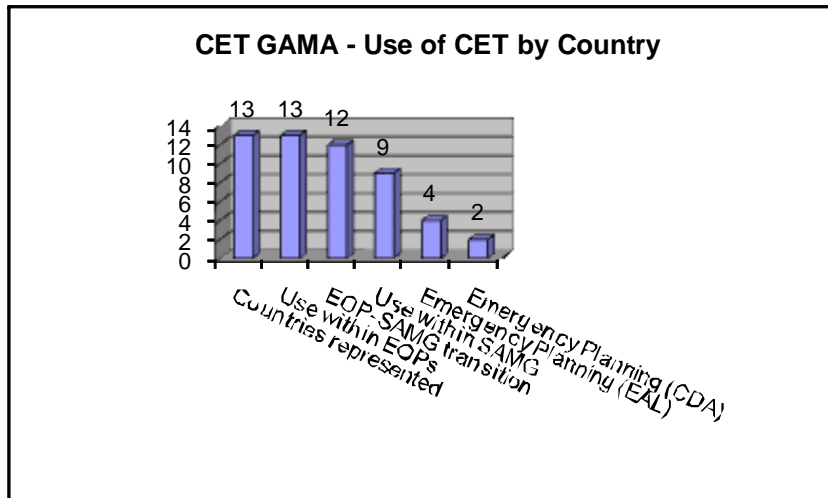
2.4   DETAILED USE, SET-POINT VALUES AND BASIS

2.4.1   Introduction

The third question of the survey deals with the more detailed usage of CETs and requests information on the basis and values of set-points used:

3- If you have set-points for CET use, please provide the values and describe the basis.

From the responses received, a summary of the basis for EOPs and SAMGs in the different countries was made, and also of the detailed uses of the CET. These are presented in this section. Where possible from the responses, the values of set-points used are included, but this was not possible for all responses.

2.4.2   Identified Detailed Uses and Results of Survey

The basis for EOP and SAMG packages in use in participating countries fell into two main classes:

- A plant or design specific basis

- A package based on a vendor or owners group generic approach which has been adapted to the specific plant

Detailed uses of the CET within these EOP and SAMG packages identified by the responding participants were classed as follows:

- Quantifying subcooling margin (number of degrees by which a given measurement is below the saturation temperature at the prevailing pressure)

- Detecting loss of subcooling margin (or, onset of saturation conditions)

- Detecting onset of superheated conditions (temperature rising above saturation temperature at prevailing pressure)

- Quantifying amount of superheat (or, detecting that superheat has exceeded a certain value)

- Determining that core has been successfully re-covered (reflooded) and cooled following an event in which core damage has occurred

The summarized response to this question is shown in table 3.

2.4.3   Discussion

The questions and responses to the questionnaire were not sufficiently detailed to derive the exact technical basis for the calculation of all set-point values. However, in spite of this, section 2.7 has been prepared which provides a discussion of the technical (physical) bases for the major classes of set-point and thermocouple usage.

Table 3 – Detailed CET Use and Set-point Bases
Question 3: If you have set points for CET use, please provide the values and describe the basis

Country	Organisation / Type		AM Basis					Q3 - Set-points basis				
			EOP	EOP-SAMG	within SAMG	EP - EAL	EP - CDA	subcooling margin	loss of subcooling	onset of super heat	significant superheat	core reflooded/cooled in SAM
Belgium	Tractebel	U (TSO)	Adapted WOG 370°C FR-C.2 650°C FR-C.1	Adapted WOG 650°C from FR-C.1, FR-S.1 and ECA-0.0 700°C in SPI-N2	Adapted WOG 370°C for core cooling recovery 355°C in SPI-N1/2				Yes	Yes	Yes	Yes
Finland	RNSA	R	Pl specific Typ.:10°C subcooling margin (Lov)	Pl specific 450°C (Lov) 650°C for depressurisation (OL3)				Yes	Yes		Yes	

France	EDF IRSN	U R (TSO)	Adapted EDF/Areva	Pl specific 1100C for existing plant, 650°C forEPR	No			Yes	Yes		Yes	No
Germany	AREVA	V	Pl specific 400°C for feed and bleed	~600C (planned)					Yes	Yes	Yes	
Hungary	NPP Paks	U	Adapted WOG 370°C FR-C.2 550°C FR-C.1	Adapted WOG 1100°C from FR-C.1 and FR-S.1 800°C from ECA-0.0	Adapted WOG 370°C for core cooling recovery	Yes	No	Yes	Yes	Yes	Yes	Yes
Japan	MHI	V	350°C for degraded core cooling (onset of superheat)								Yes	

| Korea | KINS | R (TSO) | Adapted WOG cooldown rate in EOPs 370°C FR-C.2 650°C FR-C.1 (inferred) | Adapted WOG 650°C from FR-C.1, FR-S.1 and ECA-0.0 | Adapted WOG 370°C for core cooling recovery (inferred) | | | Yes | Yes | Yes | Yes | Yes |

Country	Organisation / Type		AM Basis					Q3 - Set-points basis				
			EOP	EOP-SAMG	within SAMG	EP - EAL	EP - CDA	subcooling margin	loss of subcooling	onset of superheat	significant superheat	core reflooded/cooled in SAM
Netherlands	KCB/EPZ VROM/ KFD	U R	Adapted WOG subcooling margin 370°C FR-C.2 650°C FR-C.1	Adapted WOG 650°C from FR-C.1, FR-S.1 and ECA-0.0	Adapted WOG 370°C for core cooling recovery	Yes		Yes	Yes	Yes	Yes	Yes
Slovenia	SNSA	R	Adapted WOG subcooling margin 354°C FR-C.2 650°C FR-C.1	Adapted WOG 650°C from FR-C.1, FR-S.1 and ECA-0.0	Adapted WOG 354°C for core cooling recovery	Yes	Yes	Yes	Yes	Yes	Yes	Yes

Spain	ANAV	U	Adapted WOG subcooling margin 380°C FR-C.2 650°C FR-C.1	Adapted WOG 650°C from FR-C.1, FR-S.1 and ECA-0.0	Adapted WOG 380°C for core cooling recovery			Yes	Yes	Yes	Yes	Yes
	CNAT	U	Pl specific / Areva 340°C – adequate core cooling Trending					Trend	Trend			
	CSN	R	see utility responses above									
Sweden	SKI	R	Adapted WOG subcooling margin 370°C FR-C.2 650°C FR-C.1	Adapted WOG 650°C from FR-C.1, FR-S.1 and ECA-0.0	Adapted WOG 370°C for core cooling recovery			Yes	Yes	Yes	Yes	Yes

| Switzerland | HSK | R | Adapted WOG (KKB) | Adapted WOG (KKB) 620°C (KKG) 650°C (KKB) | Adapted WOG (KKB) | | | Yes | Yes | Yes | Yes | Yes |

Country	Organisation / Type		AM Basis					Q3 - Set-points basis				
			EOP	EOP-SAMG	within SAMG	EP - EAL	EP - CDA	subcooling margin	loss of subcooling	onset of superheat	significant superheat	core reflooded/cooled in SAM
USA	NRC	R	Adapted OG approaches	Adapted OG approaches (eg, 650°C in WOG SAM 10°C superheat in CEOG SAM)	Adapted OG approaches (eg 870°C for certain CHLAs in CEOG SAM)	Yes[1]	Yes[2]	Yes	Yes	Yes	Yes	Yes

.

In this table, a blank field indicates that information was not available or provided in the questionnaire response.

Note 1: Example EAL set-points include:

- 655 K (382 ℃) – potential loss of fuel clad barrier, etc.

- 922 K (650 ℃) – loss of fuel clad barrier, etc.

- 366K (93 ℃) and 5 ℃ increase – shutdown system degradation

Note 2: Westinghouse CDAGs require plant-specific set-points, but generic values are recommended, including:

- 922 K (650 ℃) - cladding damage while depressurized

- 1033 K (760 ℃) - cladding damage

- 1366 K (1090 ℃) - potential for significant fission product release

2.5   RELATION BETWEEN CORE EXIT TEMPERATURE AND PEAK CLADDING TEMPERATURE AND ITS MODELLING

2.5.1   Introduction

Questions 4 and 5 deal with the use of core fluid channel exit temperature to indicate actual temperature of the fuel rods in the core. While it is generally accepted that the CET do not provide a direct measurement of the parameter of interest (the highest cladding temperature, since this affects geometry, coolability and oxidation/hydrogen generation concerns), it is also generally the case that the CET provide the 'most direct' measurement of fuel temperature status. Of interest is how (or if) the relation between actual cladding temperature and core fluid channel exit temperature is addressed in the accident management procedures, and in case this is investigated via analyses (simulations) how this is done and to what extent the models used are validated.

Survey questions 4 and 5 were:

4- How do you account of the fact that the CET is not the cladding temperature?

5- In case you perform supporting calculations, please describe the way you model the CET readings. Have you made comparison with experiments to support the approach?

2.5.2   Addressing the Relationship between CET and Maximum Cladding Temperature – Results of Survey

Question 4 dealt with how the participants had addressed the fact that the core exit temperature is not a direct measurement of fuel/clad temperatures. The results are shown in table 4, and fall into the following categories:

"Total responses":

Some responses/organisations quoted more than one of the categories listed below. Where this is the case, the responses were treated independently. There are therefore considered to be 14 total responses to question 4.

"Known from calculations and models":

This response indicates that the participant believes that it is important to know the relation between core exit temperature and maximum cladding temperature, but also that they felt that existing models and analyses allow this relation to be adequately quantified. 5 participants responded in this manner.

"Only detect loss of cooling".

These participants recognised the issues under discussion, but felt that knowing the relationship between core exit temperature and peak cladding temperature is not very important if the only purpose of using the measurement is to determine a severe loss of core cooling. 3 participants responded in this manner.

"Appropriate set-point choice":

This response indicates that the participants felt that the relationship under discussion is important, but can adequately be accounted for by selecting and adjusting (downwards normally) appropriate set-point values. Certain responses indicated that warnings are included in the procedures/guidelines to alert users to the fact that CET do not measure directly fuel temperatures. 3 participants responded in this manner.

"Alternative instrumentation":

This response implies that the 'uncertainties' associated with the use of CET to infer fuel/clad temperature can be (and, presumably have been) addressed by using a backup, diverse instrument. This was usually reactor vessel level. 2 participants responded in this manner.

"Not addressed":

No specific measures are taken to address this point. 1 participant responded in this manner.

Question 5 (see table 4) asked whether participants had performed specific analyses to address this issue, and in particular to define the choice of set-points. It also asked whether the users of the associated models felt that those models were adequately validated for this type of application.

Of the 12 responses, 6 do perform analyses, but feel the model validation is not adequate, 4 do not perform such calculations, and 2 perform the calculations and also feel the models are adequately validated.

2.5.3   Discussion

The responses to question 4 revealed a wide range of approaches. At one end, using a thoroughly validated model to calculate set-points, or applying suitably conservatively estimated margins to the nominal set-point value appear to be the techniques which address the CET issue the most in current AM approaches. At the other, some approaches do not consider specifically the performance of the CET, or provide simple warnings within the guidance. (Here it is noted that warnings included in the procedures/guidelines to alert users may not be the best practice if it simply puts the burden of set-point uncertainty on the operator.)

Some approaches do not attempt to identify any narrow range of core conditions, but simply try to detect a 'gross' loss of core cooling. The response 'only detect loss of cooling' would seem to imply that action to be taken based on this information is not urgent – or at least may be adequately taken over a wide range of degraded conditions.

From the answers to question 5, it is evident that the CET issue is of importance, since a significant fraction of respondents indicated that calculations are performed. However, it is also notable that only two organisations felt that the associated models were adequately validated. Results of calculations presented at working group meetings clearly indicate the sensitivity of the results, and particularly the timing, to the modelling assumptions.

Table 4 - Relationship between CET and Maximum Cladding Temperature

Question 4:

How do you account of the fact that the CET is not the cladding temperature?
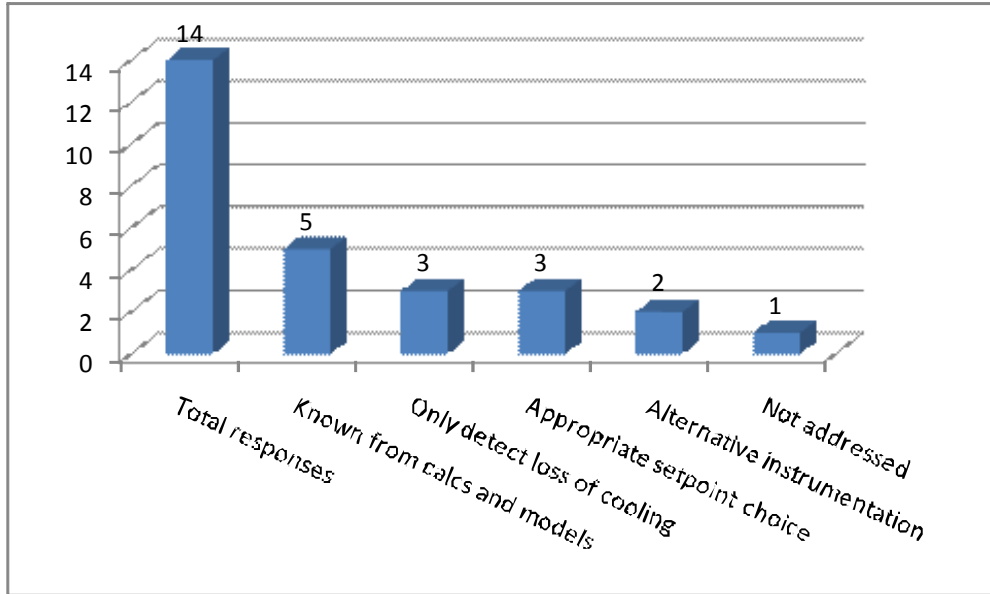
Question 5:

In case you perform supporting calculations, please describe the way you model the CET readings. Have you made comparison with experiments to support the approach?
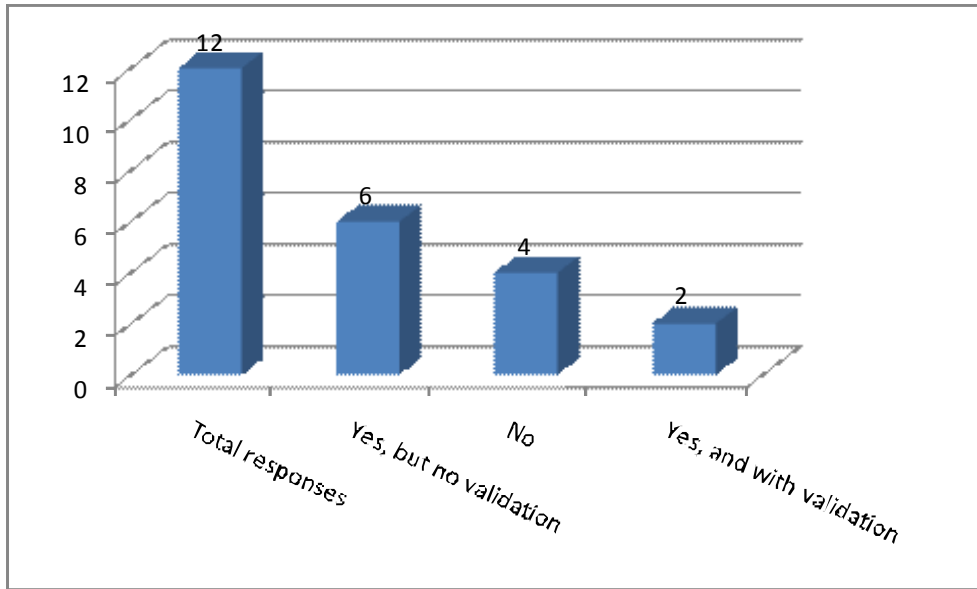
2.6   SPECIFIC ISSUES WITH USING CET IN ACCIDENT MANAGEMENT

2.6.1   Introduction

Question 6 of the survey asked participants if there were any aspects of using CET in accident management procedures which raised any specific issues and what these were:

6 - Do you have any specific concerns associated with the use of CET in accident management?

2.6.2   Specific Issues with Use of CET – Results of Survey

Responses to this question are summarised in table 5.

"Total responses":

Some responses/organisations quoted more than one of the categories listed below. Where this is the case, the responses were treated independently. There are therefore considered to be 23 total responses to question 6.

Concerns fell into the following categories:

"No concern":

The organisation has no specific concern with the use of CET in AM, or a concern exists but was resolved by use of appropriate guidance (for example, not using CET above temperature at which their survivability/reliability is doubtful). There were 8 such responses.

"Survivability":

CET are used, but there is a concern over the survivability of the thermocouples in a severe accident environment. 4 responses identified this as a concern.

"Accuracy":

The accuracy of thermocouples is known to decrease as temperature increases, and within harsh environments. These respondents felt that more should be understood about this aspect. 4 responses identified this as a concern.

"Delayed response / representativeness":

The concern is that either the thermocouples respond with a certain delay compared with the heatup rate in the core during a severe accident, potentially leading to late diagnosis or decision to take actions, and/or, that the thermocouple readings do not represent adequately the conditions in the core which are required to be known. 4 responses identified this as a concern.

"Reliability, availability, power supply":

Responses essentially related to concerns over the availability of the instrumentation are grouped under this heading. 3 responses identified this as a concern.

2.6.3 Discussion

- The idea behind this question was whether the countries believe, there is a "delay-type" concern for their plants. The diversity of responses seems to indicate that the question was interpreted in a much wider context and the delay-issue might have been overshadowed by that. However, it is notable that six responses claimed either "delayed response" or "accuracy" as concerns, indicating that this issue is of significant concern.

- It should be noted that treating "concerns" as independent, regardless of the number identified by a given respondent, may lead to a misleading impression, tending to suggest a greater concern than may actually exist. (A response 'no concern' is treated as a single response. A response "yes: survivability, accuracy, availability" is treated as three responses). When considered by country, the results for this question indicate that out of thirteen countries responding, six indicated "no concern" (see inset in table 5).

- "Qualification" of CET instrumentation was not mentioned in responses, though survivability is clearly an issue for some. This may be because most responses concern existing plants where (in general) no equipment is qualified for severe accident conditions.

Table 5 – Specific Concerns Related to Use of CET in AM

Question 6:

Do you have any specific concerns associated with the use of CET in accident management?
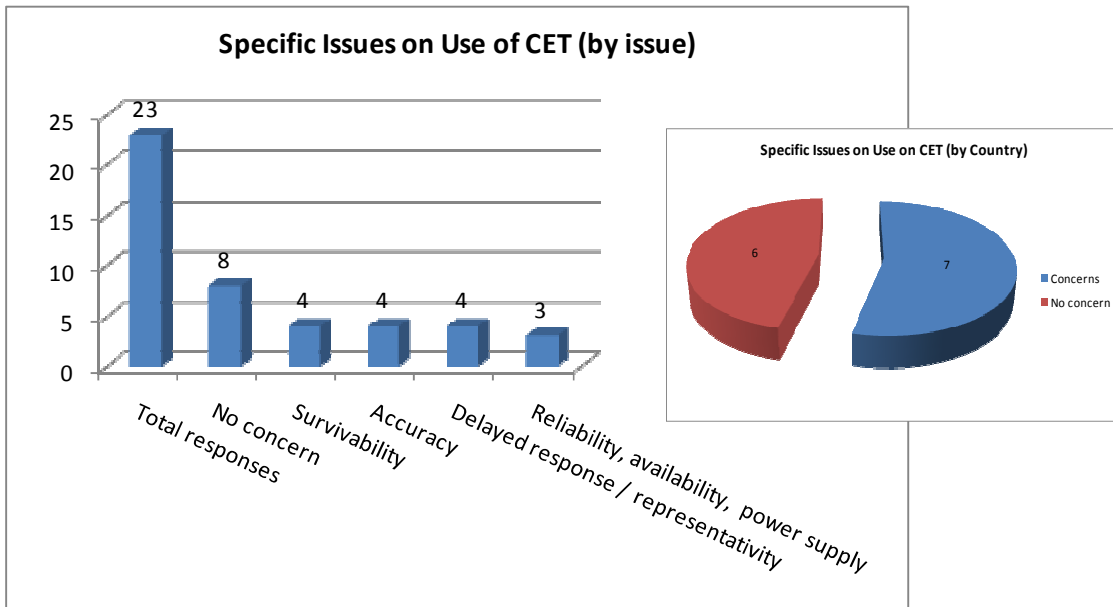
2.7   DISCUSSION OF TECHNICAL BASIS FOR CET SET-POINTS

2.7.1   Introduction

This section discusses the technical basis for some types of CET set-point used in AM. Examples are provided; however, it should be noted that these are examples only – they are not intended to be exhaustive.

Detailed uses of the CET within EOP and SAMG packages which were identified by the responding participants were discussed in section 2.4 and presented in table 3. They were classed as follows:

- Quantifying subcooling margin (number of degrees by which a given measurement is below the saturation temperature at the prevailing pressure)

- Detecting loss of subcooling margin (or, onset of saturation conditions)

- Detecting onset of superheated conditions (temperature rising above saturation temperature at prevailing pressure)

- Quantifying amount of superheat (or, detecting that superheat has exceeded a certain value)

- Determining that core has been successfully re-covered (reflooded) and cooled following an event in which core damage has occurred

In this section, each of these is treated in turn. A short discussion is provided, together with examples of the technical basis used to calculate the set-point values. Many set-point technical bases are developed by the reactor vendor as part of a generic AM package. The plant specific values of the set-points are then adapted for the specific plant application during an AM implementation phase. (An additional conservatism is sometimes added during this phase as a utility checks uncertainties in its specific parameters/instrumentation against the vendor's generic values but usually does not change the vendor's values).

Information available to the working group from vendors on this topic was limited.

2.7.2   Quantification of Subcooling Margin and Detection of Loss of Subcooling Margin

The instruction will check that reactor system subcooling > x°C. The subcooling is a function of pressure and temperature. Generally pressure indication and CET are used (though some PWRs may use hot leg temperature instruments), and generally there is a direct display of subcooling margin within the control room.

This check ensures that the primary system is subcooled: the pressure and temperature are independently controlled and there is margin to saturation conditions. This in turn ensures that the primary system is single (liquid) phase, and there is no steam formation / accumulation within the vessel or primary system. Cooling of the fuel elements is by initially subcooled water and there is no bulk boiling in the core region.

x may be zero + instrumentation errors (detection of loss of subcooling). The addition of iInstrument errors is normally made such that the indicated value >x° ensures that the true value is >0°. While CET accuracy is generally good, the accuracy of the pressure indication may impose relatively large values of 'x' in order to be sure that subcooling is >0. This is particularly an issue at low pressures for some designs.

There are situations where a certain positive subcooling margin is required, in which case x may be > 0 + instrument errors. This is often the case when an action is foreseen which will cause a reduction in subcooling. In such a case, a preceding step will often instruct operators to establish a certain subcooling margin (if it is not already present) before taking the foreseen action. An example is tripping/terminating safety injection during a small LOCA or SGTR which will cause a reduction in subcooling, but which is necessary to re-establish normal pressure and inventory control during the

recovery phase. Such a step would normally be preceded by an instruction to increase subcooling (normally by reducing temperature using SGs) to ensure subcooling is not lost when the SI is reduced.

Absence of subcooling margin does not imply core damage or even core uncovery, but does indicate a deviation from the preferred core cooling regime. A negative response to the check on subcooling described in 2.6.2 will generally lead to the need to take immediate action to restore subcooling margin. (For example, restarting a tripped safety injection pump).

All EOPs for PWRs use this type of set-point. This type of usage is only found within Emergency Operating Procedures. This type of set-point is not treated in detail here as its use is unlikely to be impacted by the delay phenomenon which is the primary concern of this report.

2.7.3   Detection of Onset of Superheated Conditions

There is no means that superheated steam conditions can exist within a PWR primary system unless there is direct heating of steam by fuel elements within the core. Thus detecting onset of superheat at the core exit is, in principle, a direct indication that core uncovery has occurred.

The detection of superheated conditions will also normally be performed within emergency procedures, although it may be associated with a direct transition to or initiation of severe accident management guidance. This depends on the scope and structure of the EOP and SAMG package.

Also, depending on the approach, the intention may be either to detect the onset of superheat as soon as possible after it occurs, or, a set-point may be used which bounds a range of conditions, all of which indicate that core uncover has occurred at some time before the check. An example of each of these is described below.

In the Combustion Engineering Owners Group (CEOG) approach to SAMG, the criterion >10°C superheat is used as an indication of core uncovery, and if it occurs, SAMG are initiated. However, in this approach, EOP use continues in parallel, and other set-points are used for initiating specific actions within the SAMG (examples: implementing candidate high level action to depressurize the reactor coolant system, CET > 870ºC; implementing candidate high level action to flood the reactor cavity, CET > 870ºC).

The approach recognises that core uncovery does not mean core damage, but that core damage may be imminent. Using a relatively low entry value to SAMG is acceptable since EOP use is continued in parallel.

In the Westinghouse Owners Group (WOG) EOPs, CET are used as one of the main methods to monitor the core cooling safety function. In particular, the generic value of >370°C is used to indicate degraded core cooling, and initiate a specific procedure aimed at rapidly restoring cooling. (Note that this is NOT the transition criteria to SAMG in the WOG approach – this is based on a higher temperature, described below).

The 370°C set-point is a temperature, not a superheat. Depending on the prevailing pressure, the actual superheat at this condition may vary considerably. However, in all cases, this condition indicates "core uncovered". The use of a single temperature is deliberate in order to improve ease of use of the procedures. It means that a specific set of thermo-hydraulic conditions are not searched for, rather a general degradation, applicable to a range of conditions.

The basis for this set-point value is that the temperature is above saturation at the highest possible pressure in the system (taken as the design pressure). This guarantees that superheat is present and that the core has been uncovered. Some plants modify slightly the value such that it is exactly T_{sat} at the plant specific design pressure

2.7.4   Quantification of Amount of Superheat

Most of the criteria for transition between EOP and SAMG fall into this category. However, it is unusual for a specific amount of superheat to be used. Rather a condition indicating "significantly superheated conditions" is used. The choice of the set-point basis varies widely between approaches (see figure 2-1), and there are numerous factors which explain this variation, mainly in terms of the scope of the actions contained within the EOP and SAMG. (A more detailed discussion and comparison of these transition criteria is provided in refs [1, 2]).

Section 2.6.4 has mentioned the CEOG's use of 'onset of superheat' as a condition for entry to SAM. Two further examples (spanning the full range of values used in different approaches) are provided below.

The WOG EOP use a value of CET>650°C (generic PWR value, sometimes adapted for specific applications) as an indication of 'Inadequate Core Cooling'. This diagnosis is performed within EOP, but if the condition occurs, it signals entry to the last 'utlimate' procedure, which contains a small number of measures to attempt rapid restoration of core cooling, and which, if these measures are unsuccessful, instructs a transition to SAMG. WOG do not allow simultaneous EOP and SAMG use, and so once the transition takes place, actions for recovery are as defined in SAMG and EOP are no longer used. (This impacts on the choice of criterion for transition, since it is important not to transition too early).

The basis for the selection of the value is analytical. Analysis of specific BDBA events, including sensitivity studies on recovery of safety injection was performed, which showed that for generic W plant, around 10 minutes were available after reaching this temperature, before recovery of injection could not be guaranteed effective. The analysis shows that at 650C, the core is deeply uncovered (~75%) but value depends on sequence (in particular, this is a function of pressure). However, as described above, in the WOG approach, a single value is chosen for all sequences.

Figure 2-1

SAM Entry Condition Comparison
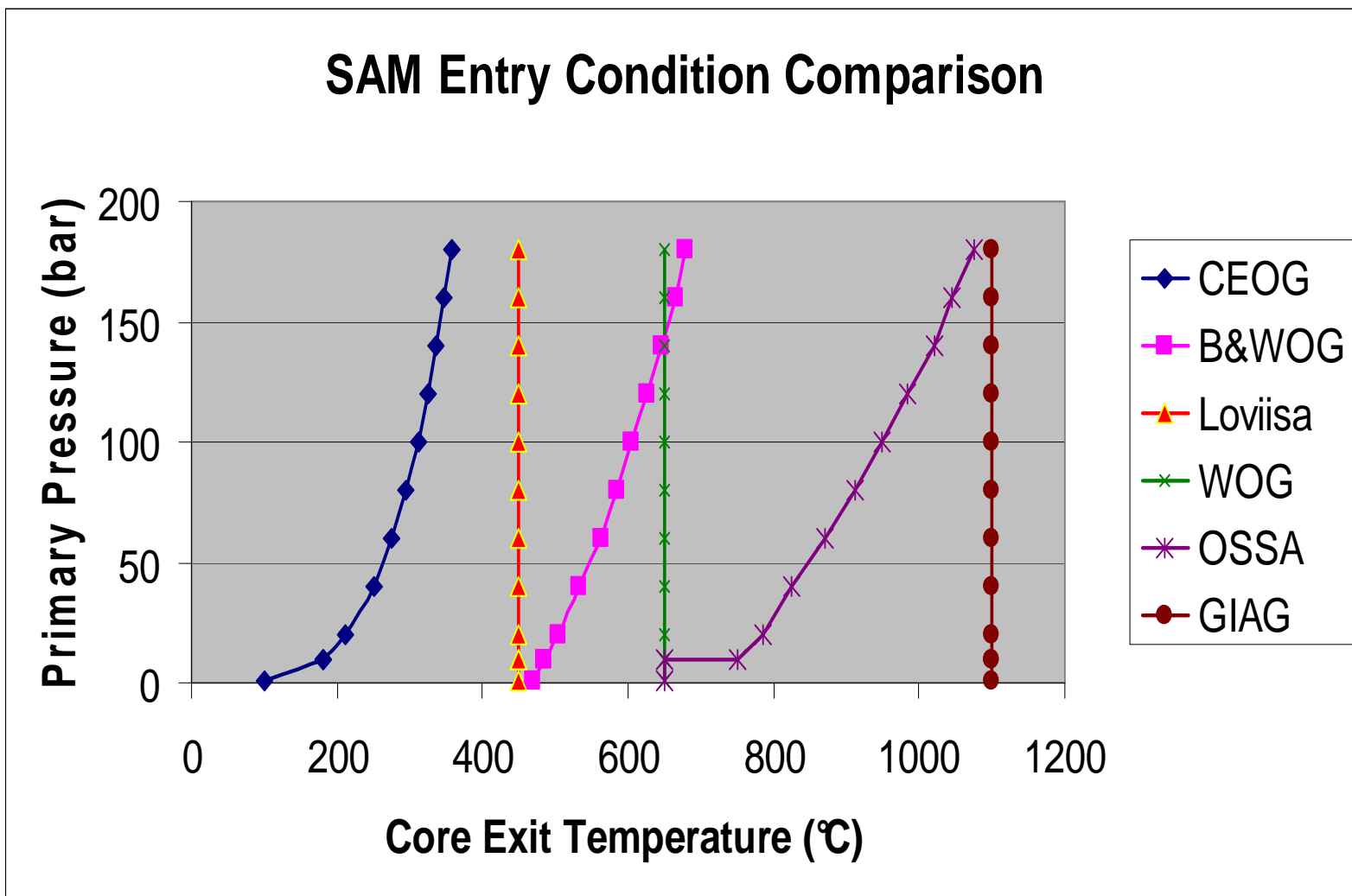
Some plant specific studies have led to modification of this set-point (e.g. some VVER-440 at 550C).

In the EDF GIAG (the SAM for existing French plants) (ref [3]), the entry condition criterion is taken as CET>1100°C. This is one of the highest values used by any approach for EOP-SAMG transition. It is intended to indicate that release from the fuel matrix has begun (fuel damage is already occurring), and that cladding temperatures have reached around 1350 – 1500°C. EOPs deal with appropriate actions before this point is reached, and so once again, the scope of EOP and SAMG actions is important in choosing the set-points. This set-point is also not trying to "detect" a specific set of T/H or fuel conditions, rather to indicate that loss of cooling AND onset of fuel damage have occurred.

The AREVA-SAS severe accident management concept for the EPR ('OSSA', described in ref [4] and [5]) uses an entry criterion based on T_{CET} as a function of pressure corresponding to a given clad temperature. (Note that this is a concept approach – individual EPR reactors will review and possibly modify their entry conditions). The resulting curve is developed from analysis and the chosen clad temperature is a value above which reflood cannot be shown conclusively to restore cooling, taking into account recent reflood experimental data.

Of interest with respect to this example (and also some others) is the use of a temperature set-point that is a function of pressure. The "true" concern when developing the entry condition is the cladding temperature, but the core exit temperature must be used as the most direct available means to infer this temperature. The CET reading at a given peak cladding temperature is a strong function of system pressure, for two reasons:

- the amount of superheat (at a given temperature) is a function of pressure (saturation curve effect);
- the temperature difference between the clad and the fluid (the heat transfer effectiveness) is also a function of the pressure.

Available models can be (and are) used to calculate the relation for a given plant and a set of different conditions. However, the SAM guidance developer is faced with the choice between using a single temperature value, or using a temperature which is a function of pressure. The former has the advantage of simplicity and ease of use, but the disadvantage that the chosen value must encompass and cover a relatively wide range of conditions. The latter may arguably be more complex to use, but will ensure that the core conditions at the transition criterion are very close, regardless of the sequence or system pressure. Both approaches are used. EOP-SAMG Transition Set-points which are a function of Pressure include CEOG (accounts for saturation curve function of pressure), and B&W, and AREVA-OSSA (which both account for the saturation effect and for the relation between T_{clad} and T_{CET}).

Of importance in this discussion is that none of the approaches described explicitly allows for a "time delay" in response of CETs, although most approaches do include "margin" to allow for unspecified uncertainties. In addition, numerous approaches rely on analyses, which contain models (of varying sophistication) of the response of the CETs.

2.7.5 Determination that Core has been Successfully Re-covered (reflooded) and Cooled

The results of the survey reported in earlier sections indicate that there is no real consensus on the use of CET *after* entry to SAMG. Amongst the respondents, only those with WOG SAMG declare this as a use for CETs. This nonetheless represents a large fraction of respondents. Within the WOG approach to SAM, there is an 'exit criterion' which allows discontinuation of the SAMG once conditions have been stabilised and releases terminated or minimised. Four plant parameters must be within certain limits, and controlled, to meet this criterion. One of the parameters is core exit temperature, which must have been reduced below 370°C (generic PWR value). The basis for this value is the same as described in section 2.6.4, but it should be remembered that for entry to the WOG SAMG, CET must have exceeded 650°C; thus a value of 370°C (and stable or decreasing), although indicating that the core may be still uncovered, is considered appropriate to indicate that core cooling has been restored and core temperature is controlled.

Most other approaches do not use CET *after* the entry to SAMG because the instrumentation is expected to fail at some (uncertain) point during a severe core heatup. (WOG addresses this by providing guidance on use of other parameters in case failure of CETs is apparent).

2.8   IDEAL DEVELOPMENT OF AM PROCEDURE SET-POINTS

In order to assure that the AM measure selected for the given situation be successful the developer has to select a method to define an appropriate set-point for initiating the action as explained and illustrated in Section 2.7. If the cladding temperature was directly measurable, it would be relatively easy to select a set-point, such that the time taken to initiate the action plus the time taken for the action to have the desired effect, are allowed for (i.e. to avoid exceeding x degrees, this action must be taken before clad temperature exceeds (x-y) degrees.). An example is primary system depressurisation, where the time allowance would be based on (a) the time needed to perform the action to open the pressuriser valves, plus (b) the time taken for the system to depressurise to a particular pressure allowing primary injection to occur, plus (c) the time required for the injection to be effective in arresting the clad temperature increase. This total time allowance would then be combined with an expected cladding heatup rate to obtain the temperature margin, y.

However, since the cladding temperature is not known directly, and must be inferred from CET readings, this introduces a further "allowance" into the set-point - so it should be reduced further (x-y-z degrees) to account for all the known contributors to the difference between indicated CET and true clad temperatures.

One of the contributors to '"z" will be due to the fact that core exit fluid temperature will always be less than highest clad temperature – for physical reasons, because of the delta-T driving the heat transfer from the clad to the fluid and from the fluid to the thermocouple measuring the CET (and possibly two-phase non-equilibrium effects). These physical phenomena are described in detail in Section 3.5.1. This contributing factor ($z1$) is caused by physical reasons that are understood and can in principle be modelled – so the AM developer should take it into account.

There may be instrumentation accuracy/bias concerns - i.e. perhaps there are mechanisms that would cause a CET to under- or over-read even in a steady temperature environment (regardless of any transient delay effect). These need to be considered too ($z2$).

And finally, there are apparently some mechanisms which lead to a delayed response and, if the temperature is increasing, we obtain an under-prediction (at any given time) due to a delayed response. Presumably, the size of the under-prediction depends on the actual rate of temperature increase which is influenced by several physical processes pointed-out in 3.5.1. This contribution is $z3$.

So, ideally, the AM developer should calculate his set-point of $(x – y – z1 – z2 – z3)$.

In order to better understand the nature of the allowance "z" experimental results focusing on the differences between core cladding temperatures and CET signals will be investigated in the next chapter.

REFERENCES FOR CHAPTER 2

[1] Vayssier, G., Wike, C., "Principles and Fundamentals of Accident Management", IAEA training Seminar "Overview of Severe Accidents and Accident Management", Trnava, Slovakia, June 2 - 4, 2003.

[2] Prior R., "The Transition to Severe Accident Management", to be presented at the OECD/NEA Workshop on Implementation of Severe Accident Management Measures (ISAMM-2009), Paul Scherrer Institute, Villigen, Switzerland, October 26 - 28, 2009.

[3] Chatry 1997, "Management of Incidents and Accidents in the French PWR (Instrumentation)", Chatry J. P., lecture L.10.4 at the IAEA/ANL Interregional Training Course on Prevention and Mitigation of Accidents at Nuclear Power Plants, Argonne National Labs., February 1997.

[4]   "MAAP Analysis, International Severe Accident Management Guidelines", SARNET Course Nuclear Reactor Severe Accident Analysis: Applications and Severe Accident Management, Session 21, Budapest, April 2008

[5] Sauvage, E., et al, "An Optimized Approach to Severe Accident Management: EPR Application", Proceedings of ICAPP '06, Reno, NV USA, June 4-8, 2006, Paper 6382

3. REVIEW OF CET PERFORMANCE IN EXPERIMENTS

3.1 BACKGROUND AND HISTORY

The idea of using core exit thermocouples for accident management emerged after the TMI-2 accident. The TMI-2 reactor had been equipped with core exit temperatures but the instrumentation was not used or tested for assisting in managing the accident. This accident triggered a number of actions from the regulatory side. NRC developed an action plan to implement the lessons learned [1]. A very detailed regulatory guide was developed to define the requirements on the inadequate core cooling conditions [2]. This regulatory guide contains a detailed list of instrumentation required that in fact became a standard for and a basis for backfitting existing plants.

Prior to this regulatory guide the NRC "determined that an instrumentation system for detection of inadequate core cooling consisting of upgraded subcooling margin monitors, core-exit thermocouples, and a reactor coolant inventory tracking system is required for the operation of pressurized water reactor facilities [3]."

The core exit temperatures play an important role for initiating the accident management measures and the safety concern is that such measures could be so delayed that recovery actions would be less effective. In this Chapter a review is made of pertinent experimental results focusing on discrepancies between CET readings and core temperature measurements during conditions that can be addressed by accident management. Beyond the collection of experimental data showing significant core superheat from different integral-type test facilities the focus was also to supply physical explanation for the CET behaviour by reviewing the physical phenomena playing an important role. Obviously, location of CET measurements may be very different in test facilities as compared to plants and the scaling ratio of the facilities may lead to distortions: these effects have to be assessed as well.

After screening the availability of experimental data it was decided to review results of the following facilities:

- It was an experiment performed at the LOFT (Loss of Fluid Test) facility that first raised the question of the reliability of measured core exit temperatures as an indicator of inadequate core cooling. During the L2-5 experiment it was noted that – although substantial core uncovery occurred – the CETs did not indicate temperatures beyond saturation. LOFT experiments with significant core uncovery have been reviewed.

- One of the tests performed within the OECD/NEA ROSA Project, Test 6-1, a vessel head SBLOCA indicated significant discrepancy between CET and the hottest core temperatures that called for a reinvestigation of the issue. Results of twelve relevant LSTF tests have been analyzed with the aim to improve understanding of CET performance during various transients.

- Logically, tests performed at the German PKL facility – a rig that serves as basis of another OECD/NEA project – were also included in the review, although the number of tests with substantial core overheating is limited.

- The Russian test facility PSB has just concluded a test campaign in the framework of an OECD/NEA project and it was proposed to be included in the review.

- There was a proposal in the task group to gather information from the BETHSY facility as well. CEA Grenoble was contacted and a short note on the CET issue in BETHSY was received [4]. From the note it can be derived that it was not in the scope of BETHSY to represent CET measurement locations as they can be found in plants. Fluid temperatures were measured at core outlet and in the upper plenum, but core outlet temperatures showed strongly heterogeneous values in cases with core heat-up. This can be explained by the specific design of the upper core support plate not representing any NPP-typical geometry. Although fluid temperatures did indicate some superheat, when cladding temperatures reached higher values, they were strongly influenced by water coming from the upper plenum and directed by the core support plate towards the middle of the core. There is little information about fluid temperatures above the fuel bundle in the test reports and they are never compared with corresponding cladding temperatures. Due to the non-typical fluid measurements for NPP conditions and the fact that a comparison of CET with cladding temperatures would have been possible only by the analysis of the archived experimental data, no further steps were undertaken by the group for BETHSY.

References

[1] NUREG-0737, "Clarification of TMI Action Plan Requirements."

[2] Regulatory Guide 1.97. Instrumentation for light-water-cooled nuclear power plants to assess plant and environs conditions during and following an accident, Revision 3, May 1983

[3] Generic letter no. 82-28. Inadequate core cooling instrumentation system

[4] P. Bazin: Informations relatives à la température sortie cœur dans BETHSY

3.2 THE LOFT EXPERIMENTS

3.2.1 The LOFT facility

The LOFT test facility simulated a typical 4-loop PWR ([1] and [2]). It had a nuclear core with a thermal power of 55 MW, a primary coolant system and emergency core cooling systems (ECCS). It included a secondary coolant heat removal system and a blowdown suppression system. The reactor core consisted of nine fuel assemblies, each containing 15 x 15 fuel pins of standard dimensions except that the fuel had half length and the four corner assemblies were truncated to triangular shape. The reactor design allowed removal and insertion of the centre fuel module.

The primary circuit contained two loops referred to as the intact loop and the broken loop. The intact loop contained a pressurizer and a steam generator that could remove the generated heat. The broken loop contained normally the simulated break and had pump and steam generators simulators to provide the appropriate hydraulic resistance.

The ECCS had a high pressure injection system (HPIS), an accumulator system and a low pressure injection system (LPIS). The ECCS water could be injected into the cold leg, hot leg downcomer and the lower plenum. Simulated pipe breaks could occur both in the broken loop and the intact loop.

The facility was extensively instrumented with instrumentation that in part was specially developed for the facility. Of particular interest for the present study is the monitoring of cladding temperatures and fluid temperatures. For most of the experiments the exit thermocouples were located just 1 inch above the top of the fuel rods. This arrangement is expected to respond quicker to core uncovery than CETs for typical commercial PWRs which may be installed longer downstream of the core or, for instance, inside thimble tubes.

3.2.2 The LOFT test program

In the beginning of the test program the Large Break LOCA was considered to be the major hazard and the program was focused on such transients. A number of large break nonnuclear tests were carried out between 1976 and 1978. The first two nuclear large breaks were carried out in December 1978 and May 1979. These tests showed much earlier rewet and much lower clad temperatures than had been expected. Although some of these differences could have been caused by atypicalities as compared to a commercial plant, it was concluded that the results demonstrated the significant conservatisms in the licensing rules. This was later further confirmed by another two large break tests.

After the accident in TMI-2 the program was redirected to investigate accidents in which the time scale was large enough for operator intervention to be an important factor. The goal of the testing was also to investigate methods and systems to help recovery and to minimize the consequences of an accident.

From May 1979 until end of 1982 a total of 26 nuclear tests were performed. In addition to one large break LOCA, seven test were carried out on small break LOCAs in response to the TMI-2 accident. A total of 13 tests were carried out addressing anticipated transients. The tests were rather mild but the probability of occurrence was so high that some of the transients could be expected to occur within the lifetime of a plant. Five tests were carried out on anticipated transients with multiple failures that potentially could be more severe that the design basis accidents. The cost of the LOFT project was about $ 1M per week and the ACRS recommended to decommission the facility in 1983.

It was clear that the LOFT project was of international interest and an OECD project was formed and carried out at a slower budgetary pace with active support from international participants. Under the OECD project two large break LOCAs which were expected to complement each other with respect to emergency core cooling assumptions were conducted. One experiment addressed loss of feedwater and three tests were devoted to small break LOCAs. The project was terminated by two experiments with fission product release. The last experiment was carried out on July 3, 1985 and fuel temperatures of more than 2100 K for several minutes were achieved in the center module. The project provided a significant addition to the international database of large scale experimental data on reactor safety.

3.2.3 Selection of experiments from the experiments sponsored by NRC for CET functional assessment study

Since the objective is to address the function of CETs under conditions that are typical for an accident management situation, the experiments selected all had a significant core uncovery. An excellent compilation and analysis of the CET functionality in the experimental series supported by NRC was done by Adams and McCreery, references [3] and [4]. The observations and conclusions in this Section from these experiments are taken from their work.

The following four experiments were selected for judgement in [3]:

- Experiment L2-5 which was a large break LOCA in the cold leg with rapid pump coastdown. After the first refill the core was allowed to uncover a second time. It was the second uncovery that was analyzed with respect to CET functionality.

- Experiment L8-1 that was a 4 inch small break in the cold leg with a rapid core uncovery and reflood initiated after experiment L3-6.

- Experiment L5-1 which was an intermediate size (14 inch) cold leg break with low head accumulator injection.

- Experiment L8-2 which was an intermediate size (14 inch) cold leg break with delayed accumulator injection.

3.2.4 Results from the series of experiments sponsored by NRC [3]
3.2.4.1 Large cold leg break (L2-5)

This was the experiment that first raised the question of the reliability of measured core exit temperatures as an indicator of inadequate core cooling. During the experiment a second heat up occurred. The collapsed level in the core was about half the core height when the heat up began at 190 s into the transient. The core quenching was initiated at 380 s into the transient.

As an example a typical core exit temperature and a clad temperature at low elevation are shown in Figure 3.2.1. Although the core was in dryout conditions, the CETs did not show temperatures beyond saturation during the core uncovery period. The CETs started to show superheat at about the same time as the quench began.
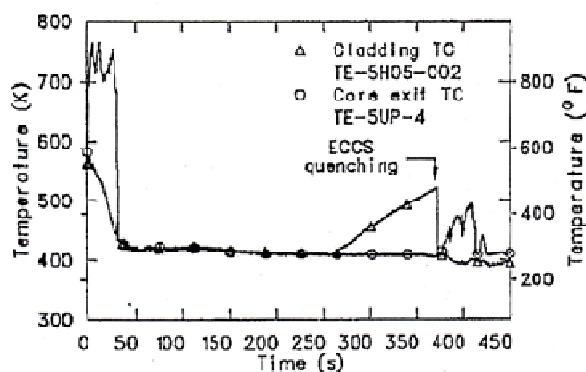
Figure 3.2.1 Cladding temperature at low elevation in the core and
typical core exit temperature during experiment L2-5. Reproduced from [3]

The difference between the maximum core temperature and the CET was 425 K. The corresponding difference between the uppermost clad temperature measurement and the CET was 65 K. The fact that CET readings showed saturation during the whole core heatup was explained by a possible water film deposited at the surfaces in the upper plenum which covered the thermocouples until the film had drained. The delay could also have been caused by very small velocities in the upper plenum until the ECCS water started to vaporize in the hot core.

3.2.4.2 Small cold leg break L8-1

The experiment was conducted to measure the effect of pump operation on primary coolant response and the pumps were operated during the whole blowdown phase. When the pumps were running the core was cooled. When the pumps were turned off at 2370 s, stratification occurred uncovering the entire core.

Comparisons of core temperatures at two elevations and typical core exit temperatures are depicted in Figure 3.2.2. The maximum clad temperatures occurred at start of core quench at 2466 s. The time delay between initiation of core uncovery and core exit temperature response was 35 s. The difference between the maximum core temperature and the CET was 125 K. The corresponding difference between the uppermost clad temperature measurement and the CET was 15 K. The experiment demonstrated that CET respond more to saturated conditions or cladding temperatures near the core exit rather than the hottest temperatures in the core.
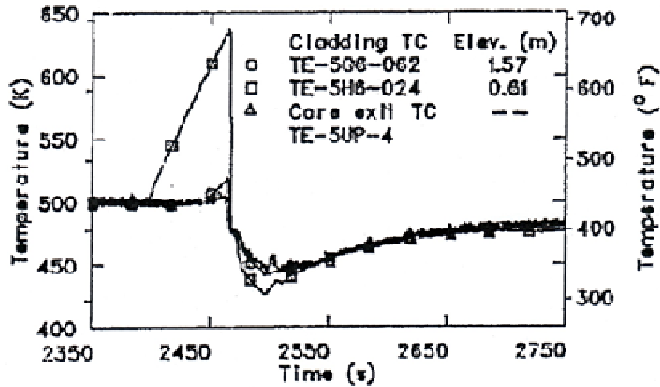
Figure 3.2.2 Cladding temperature at intermediate and high elevations in the
core and typical core exit temperature during experiment L8-1. Reproduced from [3].

3.2.4.3   Intermediate cold leg break L5-1

The experiment was performed to investigate operation of ECCS for an intermediate break. Saturation of the primary system was quickly reached. The pumps were turned off shortly after scram.

Comparisons of core temperatures at two elevations and core exit temperatures are depicted in Figure 3.2.3.
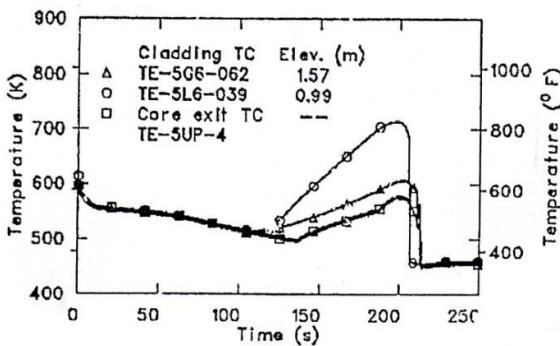
Figure 3.2.3 Cladding temperature at intermediate and high elevations in the
core and typical core exit temperature during experiment L5-1. Reproduced from [3].

Core uncovery occurred at 108 s and continued until 214 s. The time delay between initiation of core uncovery and core exit temperature response was 28 s. The difference between the maximum core temperature and the CET was 135 K. The corresponding difference between the uppermost clad temperature measurement and the CET was 95 K.

3.2.4.4   Intermediate cold leg break L8-2

This experiment was quite similar to L5-1. The main difference was that the ECCS was delayed so that the core uncovery lasted 95 s longer. The time delay of the CET and the difference to uppermost clad temperature was similar to results of experiment L5-1.

Comparisons between clad temperatures and typical core exit temperatures are presented in Figure 3.2.4. The difference between the CET and the maximum clad temperature was 340 K. These experiments demonstrated that CET responded more to saturated conditions or cladding temperatures near the core exit rather than the hottest temperatures in the core.
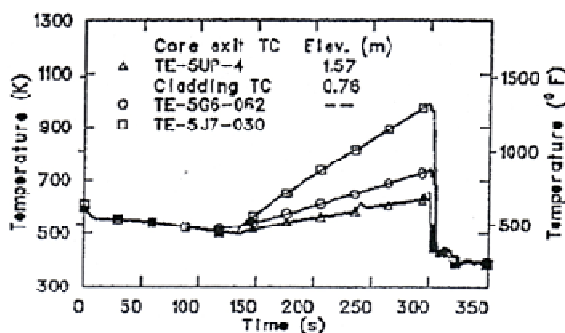
Figure 3.2.4 Cladding temperature at intermediate and high elevations in the core and
typical core exit temperature during experiment L8-2. Reproduced from [3].

3.2.5   Discussion of results of first LOFT test series [3]

It was hypothesized that the differences in delay of the CET to show superheat could be attributed to the depressurization rate during core uncovery. This could have the effect that the water on the thermocouples would evaporate faster with higher depressurization rate.

The general conclusion was that the core exit thermocouples had limitations in detecting core uncovery. There was a significant delay between the actual core uncovery and the response of the thermocouples.

Another limitation was that the measured core exit temperatures were several hundred K below the maximum cladding temperatures in the core. This was explained as the vapour superheat was limited by saturation temperatures or the cladding temperatures near the outlet which were much lower than the maximum clad temperatures.

The general conclusion of [3] in is that any procedure that relies on the response of the core exit temperatures to monitor core uncovery should take these two limitations into account. There may be accident scenarios in which these thermocouples would not detect inadequate core cooling that precede core damage.

3.2.6 The OECD LOFT Experiments [1] and [2]

Conclusions and compilations of the CET functionality in the OECD LOFT experiments were based on review of references [1], [2] and [5] through [9].

Two tests of particular interest from the OECD LOFT project were selected.

- The LP-SB-3 which was a small break in the cold leg without high pressure safety injection. The test was characterized as a slow boil off of the core inventory and corresponding clad temperature increase

- The first part of the fission product release experiment LP-FP-2. The experiment was a simulation of a break in the low pressure injection system outside the containment with simultaneous failure to isolate the system.

- All equipment not needed for the conduct of the experiment, such as pump and steam generator simulators in the broken loop, had been deleted.

A candidate was also the first fission product experiment LP-FP-1. The experiment was a simulation of an accident with fuel failure which led to fission product release into the coolant. The temperature rise would typically be terminated by ECCS injection. The experiment simulated a Large Break LOCA with delayed ECC injection. There was an unplanned early injection of water into the upper plenum and these partly compromised conclusions with respect to CET functionality. The very first experiment in the OECD LOFT experiments was a loss feedwater with high pressure safety injection to tests the feed and bleed procedure through the PORVs. No core uncovery occurred in this test.

3.2.6.1 Small cold leg break LP-SB-3

The experiment simulated a cold leg break with no high pressure injection available. The experiment was designed mainly for investigation of plant recovery effectiveness using secondary feed and bleed during core uncovery. One objective was also to investigate the heat transfer characteristics when core uncovery occurs during slow boil-off conditions with pressure over the accumulator setpoint.

The reactor scrammed on low pressure at about 9 s after initiation of the break. The pumps were running until 1 600 s. After pump trip stratification occurred and the depressurization rate increased because of uncovery of the break location. Core heat up began at 3 800 s. The maximum cladding temperature was 988 K. The core dryout was terminated by accumulator injection at 5588 s and the core was quenched at 5800 s.

Superheated vapour was detected by coolant thermocouples near the core exit. Temperatures measured in the so called upper end box showed both metal temperatures and fluid temperatures. Typical fluid temperatures measured above the various sections of the core are shown in Figure 3.2.5. The local differences were rather large and showed that local conditions could have a significant importance for the behaviour. It was noted that the temperatures measured above fuel assembly 4 was slightly lower than those for other bundles. This was attributed to the fact that bundle 4 was closer to the hot leg and therefore was more subject to condensate runback.
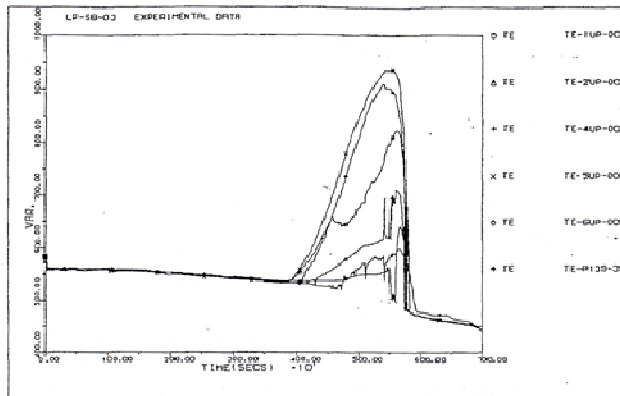
Figure 1. Figure 3.2.5 Typical temperatures near the upper end of the test
fuel assembly from experiment LP-SB-3. Reproduced from [5].

3.2.6.2   Fission product release experiment LP-FP-2

Experiment LP-FP-2 was the eighth and final experiment to be conducted in LOFT. Experiment LP-FP-2 was designed to simulate the system thermal-hydraulic and core uncovery conditions from rupture of a low-pressure injection system (LPIS) pipe. The primary objective of the experiment was to collect data on fission product behaviour. The experiment simulated an accident in which the fuel continued to overheat after cladding failure so that fission products were released both from the gap between fuel and cladding and from the fuel matrix itself.

The conduct of the experiment was rather complicated with repeated openings of two blowdown lines. The timeline for the experiment was thus not very representative of a real accident. The reactor was scrammed 24 s into the transient. The peripheral core heat up started at 662 s and the centre fuel module started overheating at 689 s. Measured cladding temperatures exceeded 2100 K at 1504 s and the transient was terminated by injection of ECCS water at 1783 s. The temperatures were in excess of 2100 K for several minutes and the peak temperatures were probably several hundred degrees higher that that. Material examinations showed material formations consistent with temperatures in the range of 2800 K and in local areas over 3000 K.
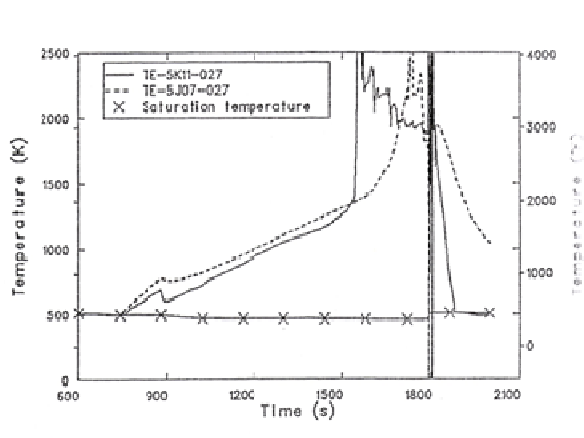
Figure 3.2.6 Measured clad temperatures during experiment LP-FP-2. Reproduced from [2]

Some cladding temperatures during core heat up are shown in Figure 3.2.6. Fluid temperatures in

the upper end box of the central fuel module are depicted in Figure 3.2.7. It is difficult to estimate the flow conditions in the upper plenum since the only measurements are the thermocouples. These measurements, indicating both metal and fluid temperatures, reveal a significant spread. Some thermocouples show departure from saturation at about the same time as the first core dryout occurs. The heatup rate of the fluid temperatures is much slower that in the fuel and some temperatures reach a maximum of about 1000 K for a short moment at about 1470 s. At this time typical core clad temperatures were in the order of 1500 K.
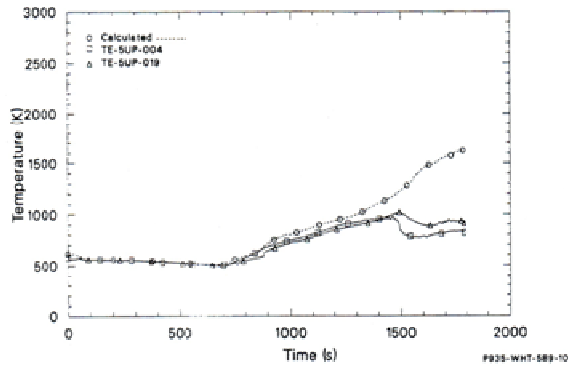
Figure 3.2.7 Measured fluid temperatures in the upper plenum during experiment LP-FP-2. Reproduced from [9].

When the core temperatures started runaway at about 1500 s (see Figure 3.6) and quickly exceeded 2100 K with a fission product release, the fluid temperatures in the upper plenum measured over the centre fuel module (Figure 3.7) actually started to decrease. The temperature was typically 700 K when quenching of the core occurred. For the peripheral bundles the temperatures were typically around 600 K when core quench began. A fluid temperature measured right above the central fuel module during core quench are depicted in Figure 3.2.8.The core quench caused a large excursion in the fluid temperature measurements. For a few seconds temperatures near 2000 K were observed followed by indication of saturation temperature.
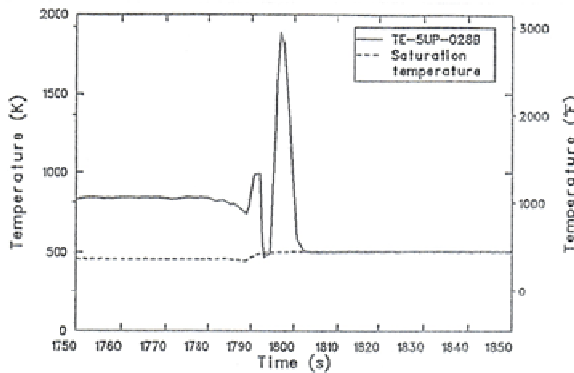
Figure 3.2.8. Upper plenum temperatures during core quench. Reproduced from [2]

There was no evidence in the test that the CET indication was very much delayed. It can be concluded though that the core exit temperatures were much lower than typical core temperatures. During the rapid oxidation phase the CET appeared essentially to be disconnected from core temperatures. Although relocation of the fuel changed the flow paths, it was judged that there was always a free flow path through the bundle and no complete blockage. The temperature excursion at core quench is probably explained by a violent flow up through the bundle that heated up the thermocouples.

3.2.7   Summary

Findings from the experiments in the LOFT facility indicate that the concerns for the functionality of the core exit thermocouples (CETs) in accident management situations are well-founded. For accident management it is important to identify occurrence of core uncovery and inadequate core cooling. For typical conditions that are important for accident management, for instance a propagating core uncovery, the LOFT results have indicated both a late response of the CETs and a slower heat up rate as compared to core temperatures. In LOFT the CET readings may be more indicative of saturation conditions or fuel temperatures near the exit. For extreme core temperatures the difference between the CETs and core temperatures may be several hundred K.

For core runaway conditions with rapid fuel oxidation, LOFT results indicated that the CETs essentially were disconnected from the core temperatures. This is perhaps a lesser problem since such conditions can not be well addressed by accident management measures. The temperatures excursion at reflood of an overheated core could be an indication that the steam velocity through the bundle may be a significant parameter when assessing CET performance.

References

[1] Fell, J., Modro, S.M., An Account of the OECD LOFT Project. OECD LOFT- T-3907. May 1990

[2] The OECD/LOFT Project: Achievements and Significant Results. Proceedings of an Open Forum sponsored by the OECD/NEA. 9-11 May, 1990.

[3] J.P.Adams, G E McCreery: "Detection of Inadequate Core Cooling with Core Exit Thermocouples: LOFT PWR Experience", NUREG/CR-3386 (Nov. 1983).

[4] J.P.Adams, G E McCreery: "Limitations of Detecting Inadequate Core Cooling with Core Exit Thermocouples" Trans. Am. Nucl. Soc., P.474-476, (1984).

[5] Alemberti, A., Comparison Report on OECD LOFT Experiment LP-SB-03, OECD LOFT-T-3606, February 1987.

[6] J. P. Adams, J. C. Birchley, N. Newman, D. Briney, E. W. Coryell, M. L. Carboneau: Quick-Look Report on OECD LOFT Experiment LP-F P-1. OECD LOFT- T-3704, March 1985

[7] A B Wahba, Thermal Hydraulic Experiment Analysis and Summary Report of OECD LOFT LP-FP-1, OECD-LOFT-T-3709, April 1986

[8] S Guntay, M Carboneau, Y Anoda. Best Estimate prediction for OECD LOFT Project Fission Product Experiment LP-FP-2. OECD LOFT-T-3803

[9] M Carboneau, V T Berta, M S Modro. Experiment Analysis and Summary Report for OECD LOFT Project Fission Product Experiment LP-FP-2, OECD-LOFT-T-3806, June 1989.

3.3 PKL TEST RESULTS CONCERNING CET EFFECTIVENESS

3.3.1 The PKL III test facility

3.3.1.1 General remarks

The large-scale test facility PKL (see Figure 3.3.1 and refs. [1-2]) is a scaled-down model of a pressurized water (PWR) reactor of KWU design of the 1300 MW class. Reference plant is Philippsburg 2 nuclear power plant. The PKL test facility models the entire primary side and essential parts of the secondary side (without turbine and condenser) of the reference plant. All elevations are scaled 1:1, volumes, power and mass flows are modeled by the scaling factor 1:145. The test rig is equipped – like the reference PWR – with 4 loops on the primary side (comprising a reactor coolant pump (RCP) and a steam generator (SG) each) symmetrically arranged around the reactor pressure vessel (RPV). The maximum pressure on the primary side is 45 bar.
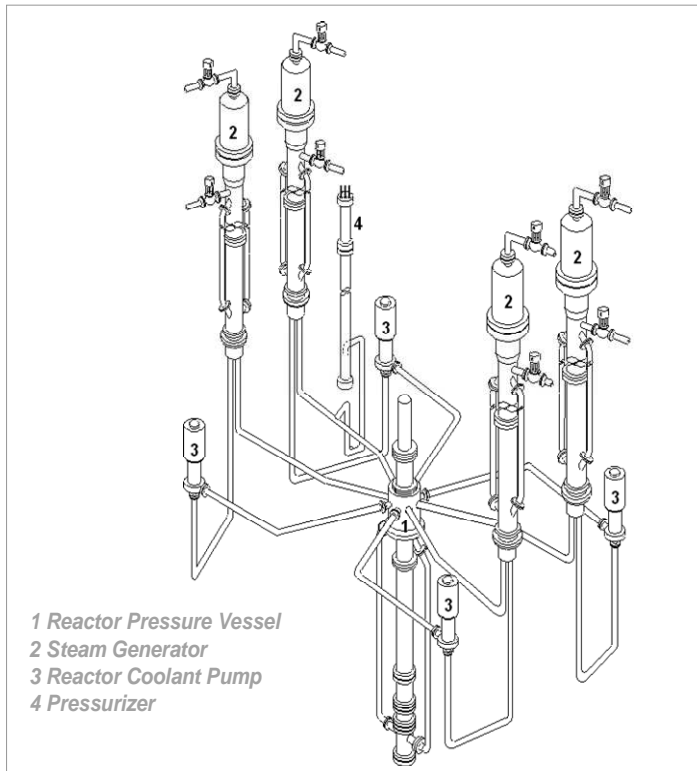
Figure 3.3.1 PKL III test facility

The PKL test facility was designed, built and commissioned by Siemens/KWU (now AREVA NP) in the seventies. At that time reactor safety research was centered above all on the theoretical and experimental analysis of large-break (LB) loss of coolant accidents (LOCAs), focussing on verifying the effectiveness of the emergency core cooling system (ECCS) required for controlling these accidents. In line with this

original objective and considering topical issues[1], the first PKL tests were carried out in the years from 1977 to 1986 in the course of the projects PKL I and PKL II which were sponsored by the German Ministry for Education, Science, Research and Technology (BMBF).

The PKL III project, which was started subsequently, had the main goal of investigating experimentally the thermal-hydraulic processes on the primary and the secondary side of a PWR during various accident scenarios with and without loss of coolant. Within the scope of this project tests concerning the investigations of transients were performed from 1986 to 1999 with additional support of the German Utilities operating PWRs. One focus of these activities was on the effectiveness of accident management measures being initiated manually by the operators after beyond design basis accidents [3].

Since 2001, the PKL project has been continued in the course of an international project initiated by the OECD. The major topics covered by the experiments up to now were boron dilution events following SB-LOCA and loss of residual heat removal under shut-down conditions.

3.3.1.2 PKL III relevant measuring instrumentation

In the PKL test facility the reactor core is modeled by a bundle of 314 electrically heated rods and 26 control rod guide thimbles. The core geometry is, like the SG geometry, constructed as an „actual section"; that is, the individual heated rods and U-tubes have the actual geometry, but the number of heated rods in the core and the number of U-tubes in the SG are reduced by the scaling factor 1:145, (volume and power scaling) as compared to the original plant. The total core power of 2.5 MW corresponds to 10 % of the rated thermal power.

The heater rods are arranged in three concentric zones (see Figure 3.3.2) which can be heated independently of another to enable radially variable power profiles across the test bundle to be simulated.

The core simulator used in the experiments described below was designed with a uniform axial power distribution.

The PKL III test facility features a detailed set of thermocouples (TC) used to acquire temperature signals from different locations within the RPV. Amongst others, the most significant measuring positions used for the determination and evaluation of the core exit temperature (CET) performance are:

> Heater rod wall temperatures: Sixteen rods are equipped with

Outer zone (133 heater rods)
Intermediate zone (118 heater rods)
Inner zone (63 heater rods)

Spacer 8 without vane
Unheated Length   LU 250
Spacer 4105
Spacer 3532
Spacer 2960
Spacer 2388
3900
Spacer 1816
Spacer 1244
Spacer 672
Unheated Length   LU 100
Spacer 100

● Heater rods with temperature measurement
○ Model of control rod guide thimble
● Thermocouples (TC) in subchannels along height

Figure 3.3.2 PKL III core simulator

---

[1] The accident at TMI-2 (USA, 1979) made scenarios with small breaks and multiple failures the subject of many investigations.

chromel-alumel-sheated TCs. The six TCs per rod are brazed into slots distributed over the heater rod length at different elevations (ME 1 - ME 7, see Figure 3.3.3). The thermocouples have an outside diameter of 0.5 mm.

> Sub-channel fluid temperatures: In the core between heater rods, the fluid temperature is measured at elevations in-plane with the corresponding cladding temperatures (ME 1 - ME 7). Additional fluid temperatures are installed above (ME 7.1 below the upper edge of heated length and ME 7.2 just below the upper core plate in the unheated region of the core). The exact position in the core is indicated by core coordinate grid and the elevation (see Figures 3.3.2-3.3.4). The TCs for the fluid temperature measurements have an outside diameter of 1.0 mm.

> Core exit temperature: The fluid temperature, which is in the following defined as CET, is measured directly above the upper core plate (15 mm above the upper core plate) and close to the center position (TF O10/P11, ME 8, see Figure 3.3.4). Several other TCs are available at the same elevation (ME 8, see Figure 3.3.11), due to their peripheral positions the maximum temperatures measured are lower. The upper core plate in PKL represents the fuel assembly top nozzle in the PWR plant (in PWRs the CET measurements are typically also installed above this fuel assembly top nozzle, however in a slightly larger distance to the plate and in some cases inserted in so called finger tubes).In order to get information about the radial temperature distribution above the upper core plate, additional temperature measurements are available in other radial positions in PKL.

> Temperatures in the upper plenum: Fluid and wall temperatures are measured by TCs in the upper plenum below and above the hot leg nozzles in different elevations and radial positions (e.g. TF UP ME 9.1: 530 mm above the upper core plate).
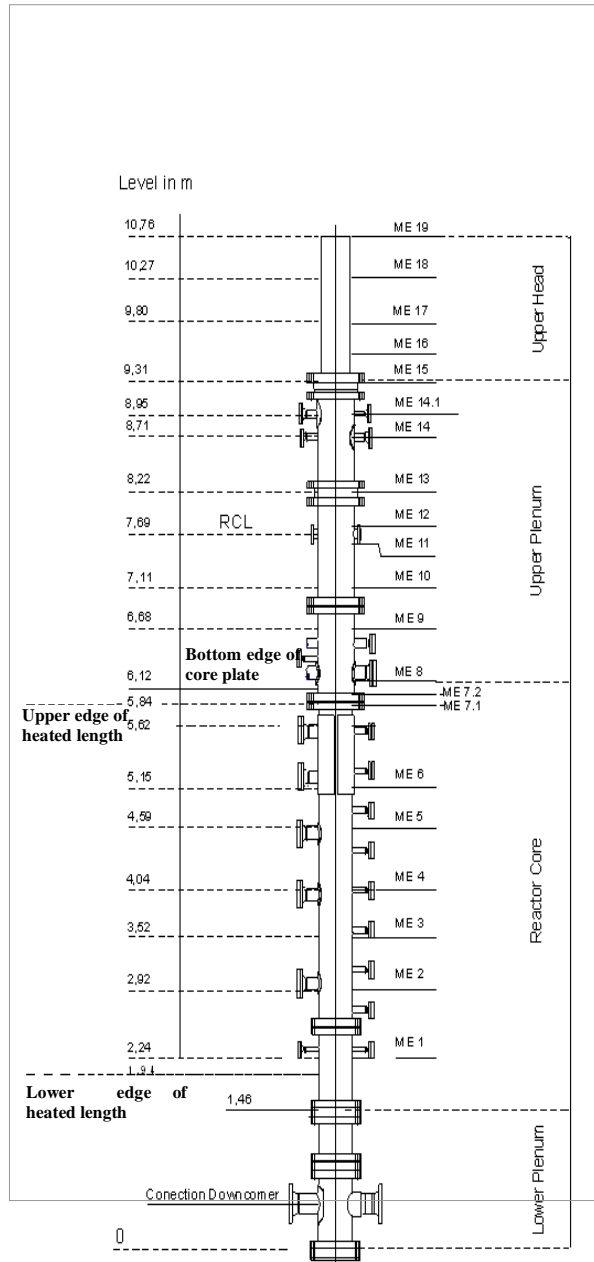
Figure 3.3.3 PKL III rod bundle vessel
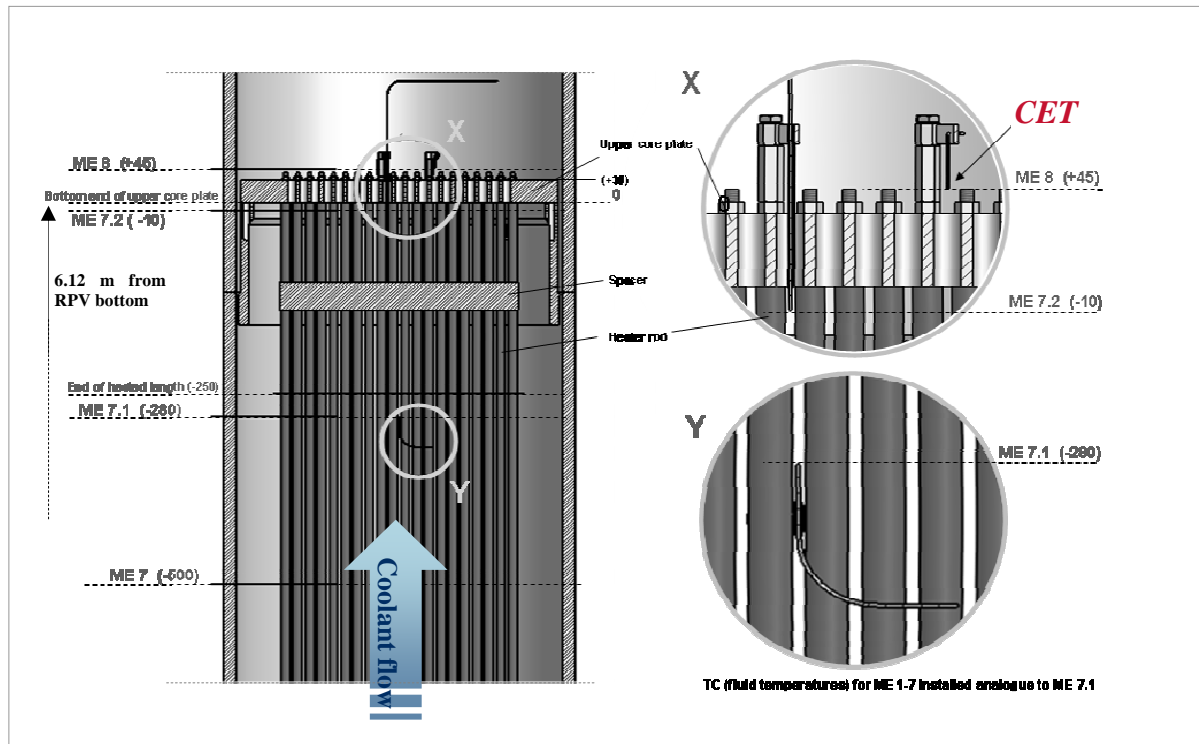
Figure 3.3.4 PKL III tempeature measurements in core simulator (heights given in mm)

3.3.2   Objective

The present summary provides an overview on the results of selected PKL III tests comprising phases of core uncovery which evolved from different background scenarios:

The main objective is the investigation of the performance of the CET during periods of core uncovery until recovery of core cooling and to provide answer to the question whether it reflects the situation in the core within acceptable margins.

3.3.3   Reference PKL III tests

The below-mentioned conclusions on the significance of the CET-fluid temperature for the determination of the situation in the core were drawn from the following PKL III tests:

> PKL III C5.2: Loss of feed water transients, e.g. as consequence of station blackout (SBO)

> PKL III D1.2: SB-LOCA transient with additional system failures (no HPSI, no automatically initiated secondary side cool down, hot leg ACCs only), late secondary side depressurization

> PKL III G1.1: Parameter study on heat transfer following loss of RHRS transients, i.e. with coolant inventory displacement from RPV (e.g. due to CCFL in SG-inlet chamber)

All tests feature phases of core uncovery and heat-up as a result of different background scenarios and under impact of different boundary conditions in the reactor cooling system (RCS):

-   Different pressure levels

- Steady state conditions (constant pressure) and transients (depressurization)
- Heat transfer
    - o Reflux condensation
    - o Blowdown via pressurizer relief and safety valves or via break
- With and without ECC injection into the hot legs

3.3.4 Station black out (SBO) test

3.3.4.1 Background

Test PKL III C 5.2 [3] simulated a station blackout transient and demonstrated the effectiveness of countermeasures (primary-, secondary side bleed-and-feed) to control the accident. The risk potential for core damage arising from station blackout transients is characterized by the loss of the secondary side feed-water supply, eventually followed by the complete boil-off of the SG secondary sides which results in the loss of the main heat sink. The loss of heat removal from the core results in a pressure and temperature rise on the primary side. The pressure rises up to ~ 176 bar until the pressurizer (PRZ) safety valve controls the pressure by discharge of primary inventory into the containment. Consecutively, the heat removal from the core is attended with a constant loss of primary inventory at constant high pressure. Without any countermeasures, this would eventually result in a high-pressure core meltdown scenario. Accident management (AM) measures (primary-, secondary side bleed-and-feed) manually initiated can be deployed to control the transient, and to prevent high pressure core meltdown.

In the case of total loss of feed water (e.g. station blackout conditions), the secondary side bleed-and-feed (B+F), initiated by the depressurization of the steam generator secondaries is the preferred measure in German PWRs to maintain or to re-establish the core cooling. It is foreseen to initiate the

Figure 3.3.5 Loss of feed water transient in a PWR without AM-Procedures (schematically)

secondary side B+F when the RCS is still almost filled with water (e.g. pressurizer level high), i.e. before core uncovery occurs. In the following this procedure is designated "early" secondary side bleed-and-feed (see Figure 3.3.5).

If the secondary side bleed and feed is seriously delayed or not possible due to whatever reasons primary side bleed and feed is initiated as an ultimate procedure to prevent high pressure core melt down scenarios.

Primary side B+F can be realized when the water level in the RPV (indicated by the liquid level probe in the upper part of the RPV as shown in Figure 3.3.6) drops below the hot leg nozzles. As an ultimate procedure primary side B+F must be performed at the latest when the core exit temperature exceeds 400°C (50K superheating).

Primary side bleed, i.e. depressurization is achieved by opening the pressurizer relief and safety valves. In the event of a station blackout only the accumulators (ACCs) are available for primary side feed. Due to the limited amount of water being available from the ACCs, core heat up is only delayed for a certain period of time. However, this time period can be used to complete the initially started secondary side emergency procedure.

3.3.4.2   Test Procedure

Test PKL III C5.2 was performed to demonstrate the effectiveness of a lately deployed secondary side bleed-and-feed following a primary side bleed-and-feed which was already initiated at 50 K of CET superheat. According to test objective it was postulated that the secondary side bleed-and-feed was significantly delayed so it was specified to follow the primary side bleed-and-feed. Consequently, the C5.2 test procedure featured a "late" secondary side bleed-and-feed deployed at already present extensive superheat at core outlet (see Figure 3.3.7).
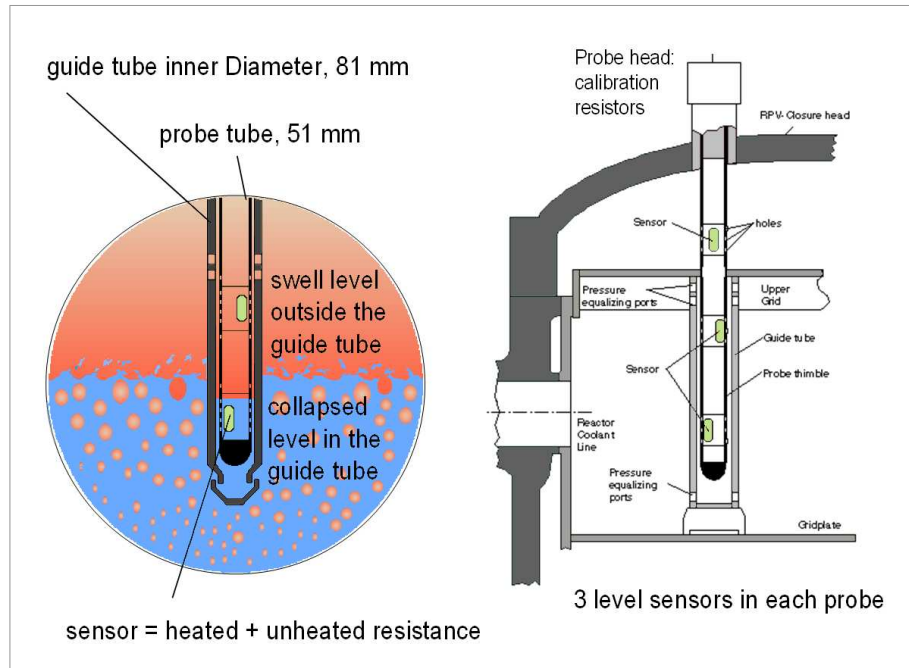
Figure 3.3.6 AREVA PWR - level probe: configuration with heated and non-heated resistances
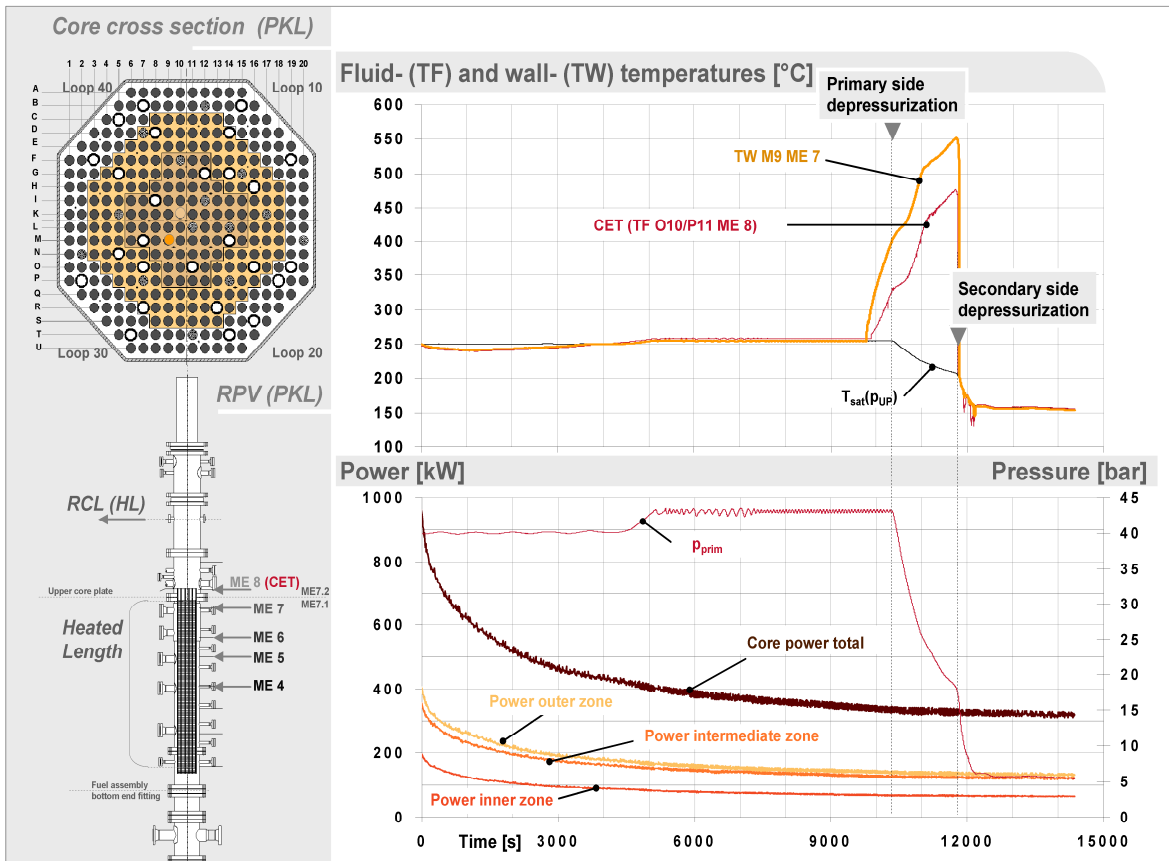
Figure 3.3.7 PKL SBO - Experiment

Due to the pressure limitation of the PKL III test facility, control of primary pressure by discharge of primary inventory and primary side bleed procedure were actuated at 43 bar.

The phase relevant for CET performance started with the onset of insufficient core cooling as the swell level drops below the upper edge of the heated length in the core and start of the core heat up (increase of rod wall temperature).

In principle the segment in the C5.2 transient relevant for the performance of the CET may be divided into four separate phases (see Figure 3.3.8):

Phase A: Loss of inventory at constant high primary pressure

Supposing, secondary side depressurization was not possible, the primary side pressure limitation resulted in discharge of coolant inventory via PRZ valve station at constant high primary pressure.

Phase A is characterized by heat removal from the core via evaporation of ambient coolant and discharge of saturated steam via PRZ safety valve. The primary coolant inventory constantly decreases. As the swell level in the core drops below the upper edge of the heated length the upper ends of the heater rods are no longer sufficiently cooled and the steam starts to superheat as it passes by. The resulting superheat of the steam is also recorded by the CET with a delay of about 100 s (see Figure 3.3.8, up to t = 10400 s).
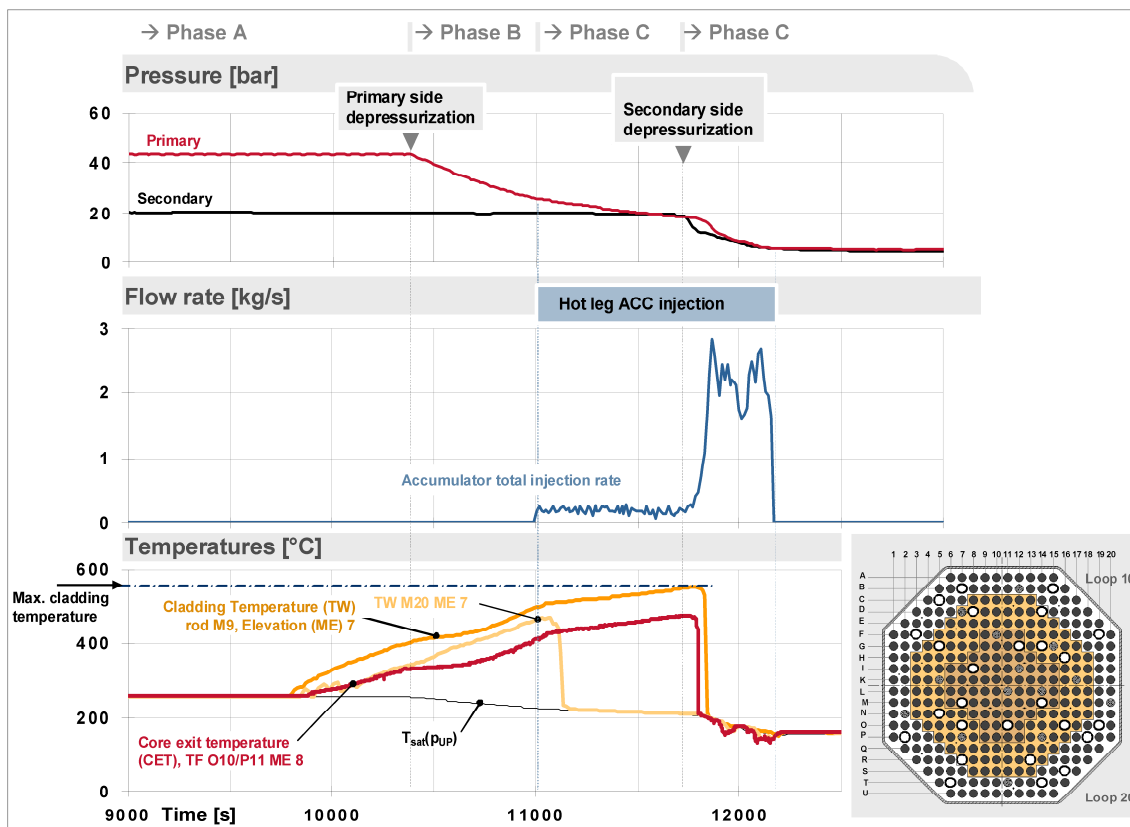
Figure 3.3.8 PKL SBO - Experiment

Phase B: Primary side depressurization

The primary side depressurization was performed as an ultimate action when the core exit temperature was superheated to more than 50K above saturation. Starting from the depressurization, the PRZ safety valves and the relief valve are kept open permanently. This led to a rapid pressure decrease on the primary side. After conduction of the depressurization, the temperature in the core continued to rise, but a smaller increase rate could be observed for both, the core temperature and the CET (see Figure 3.3.8, t = 10400 – 11000 s).

Phase C: Actuation of ACC injections

At a primary pressure of 26 bar, the 4 hot leg ACCs passively injected water into the primary system. On one side the ACC injection led to condensation of steam in the hot legs, on the other side a certain amount of the injected water evaporated on the hot structures. The rest of the water reached the core via the upper plenum, contributed to core cooling and partially quenched the tube cladding, leading to additional steam production. Because the evaporation effect was dominant compared to the condensation effect, the ACC water finally caused a deceleration of the primary side pressure drop gradient. The feed-rate of the ACCs, which is determined by the primary side pressure gradient, was therefore relatively small in this phase (see Figure 3.3.8, t = 11000 – 11700 s).

The cooling effect of the ACC water in the core differed radially. In the peripheral regions, below the hot leg nozzles, the tube claddings were quenched (see Figure 3.3.8, TW M 20 ME 7). In the central region of the core, the ACC water caused a retardation in the temperature rise of the tube claddings. However, a further temperature rise could not be prevented (see Figure 3.3.8, TW M 9 ME 7). The CET follows with a certain delay the max. core temperature in the center regions.

Phase D: Secondary Side Bleed and Feed

The depressurization of the secondary side of all 4 steam generators by means of main steam relief valves (MSRVs) was carried out after a maximum cladding temperature of 550°C had been reached (about 25 minutes after starting primary-side depressurization).

By opening the MSRVs, the secondary pressure in all 4 steam generators decreased rapidly and reached the saturation pressure of the hottest point of the feed water system. Subsequent evaporation inside the feed water line led to a displacement of water towards the steam generator secondary side, followed by condensation in the primary-side steam generator U-tubes. This resulted in an increased pressure drop on the primary side, subsequently leading to increased ACC feed. A short while after the passive injection of water from the feed water system, a secondary-side pressure of 14 bar was reached and active injection with a mobile pump to two steam generators was initiated. Consequently, the condensation effect on the primary side and the rate of ACC feed were further intensified. The ACC water injected into the hot leg flowed into the upper plenum and into the core, leading to complete core flooding and thereby quenching of the core. Around 100 s after initiation of secondary-side depressurization, all fluid and cladding temperatures reached saturation levels. Due to the rather high ACC flow rates the time delay between CET (indicating saturation) and rewetting of the core was relatively small (in the order of 50 s).

3.3.4.3   Heat removal in relevant test phases

Phase A: Situation in the core <u>after onset of core uncovery</u> in the upper core regions (rising of rod cladding temperature at ME 7, t = 9800 s after SOT, see Figure 3.3.8) is characterized as follows:

> Residual heat removal from core via evaporation of ambient coolant, steam flow from core via hot leg into PRZ (return to saturation conditions)

> Blow-down of (saturated) steam via PRZ relief and safety valves (cycling) at quasi-constant primary pressure (p_{abs}) ~ 43 bar (maximum pressure of PKL)

> No ECC injection

> No water back flow from the hot legs into the RPV or into the core

> Continuously decreasing coolant inventory and swell level in the core.

> Rise of the cladding temperatures in the upper core region (e.g. M9, see Figure 3.3.8)

Phase B: Situation in the core <u>after primary side depressurization</u> (t > 10400 s after SOT)

> Residual heat removal from core via evaporation of ambient coolant, steam flow from core via hot leg into PRZ (return to saturation conditions)

> Rapidly decreasing primary pressure, continuous blow-down of (saturated) steam via PRZ safety valve and relief valves (fully opened)

> Flashing of the core inventory due to rapid pressure decrease (temporal cooling effect on the rod claddings, visible in the decrease of the gradient of the cladding temperatures)

> No ECC injection

> No water back flow from the hot legs into the RPV or into the core

> Continuously decreasing coolant inventory and swell level in the core (Figures 3.3.15 and 3.3.16)

> Continue of rising of rod cladding temperatures

Phase C: Situation in the core <u>following the actuation of the ACC injection</u> (t > 11000 s after SOT)

> Residual heat removal from core via evaporation of ambient coolant, partly by evaporation of injected ECC into the hot legs, steam flow from core via hot leg into PRZ (return to saturation conditions)

> Blow-down of (saturated) steam via PRZ safety and relief valves

> Only low ECC flow from hot leg ACC due to pressure supporting effect resulting from evaporation of ECC at hot structures (see Figure 3.3.8, middle)

> Partial re-establishment of cooling (wetting of rod claddings) in peripheral core regions due to low ECC back flow (Figure 3.3.8, bottom; Figure 3.3.11, top)

> Continue of rising of rod cladding temperatures in the central core region
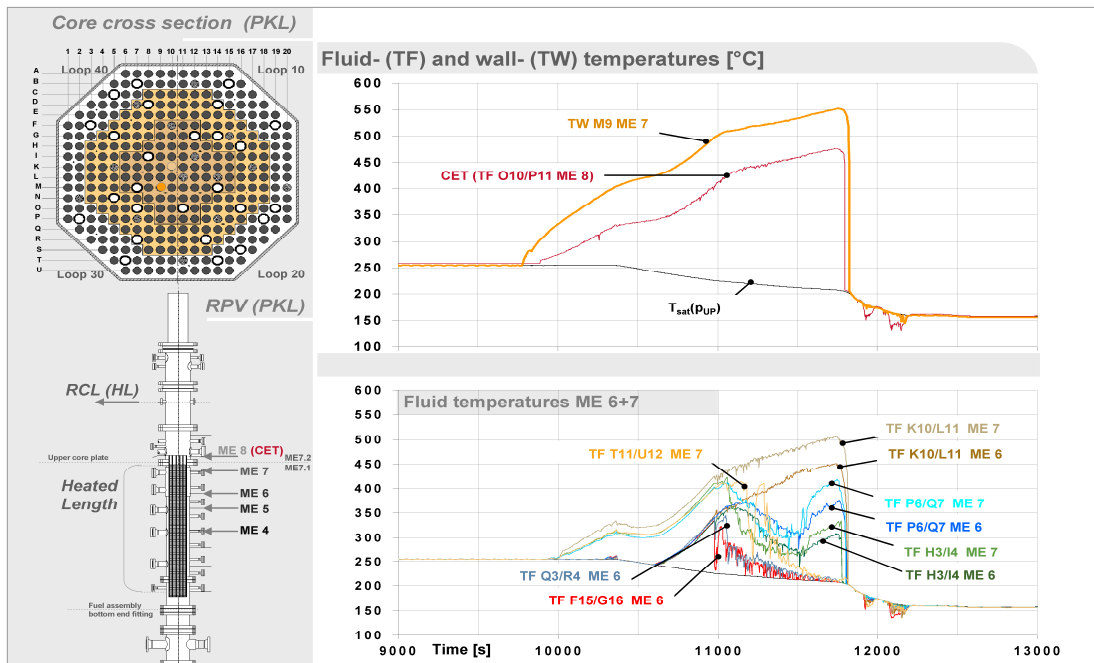
Figure 3.3.9 PKL SBO- Experiment
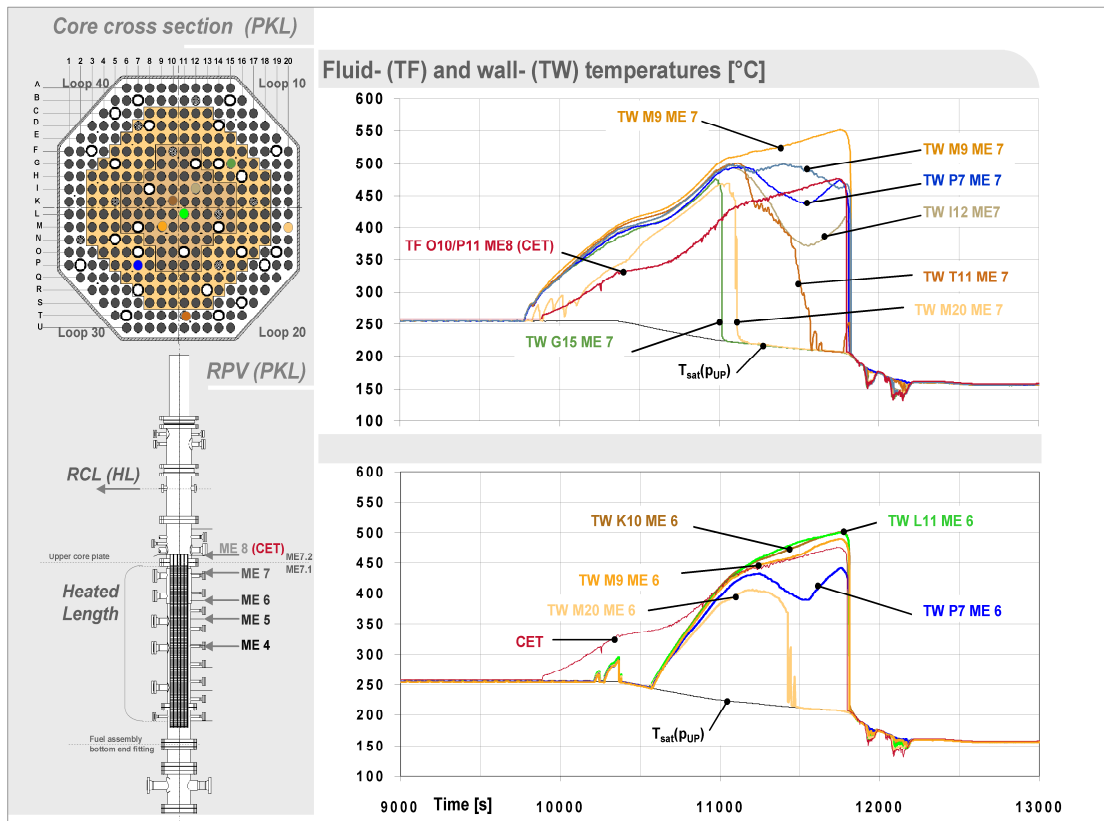
Figure 3.3.10 PKL SBO- Experiment
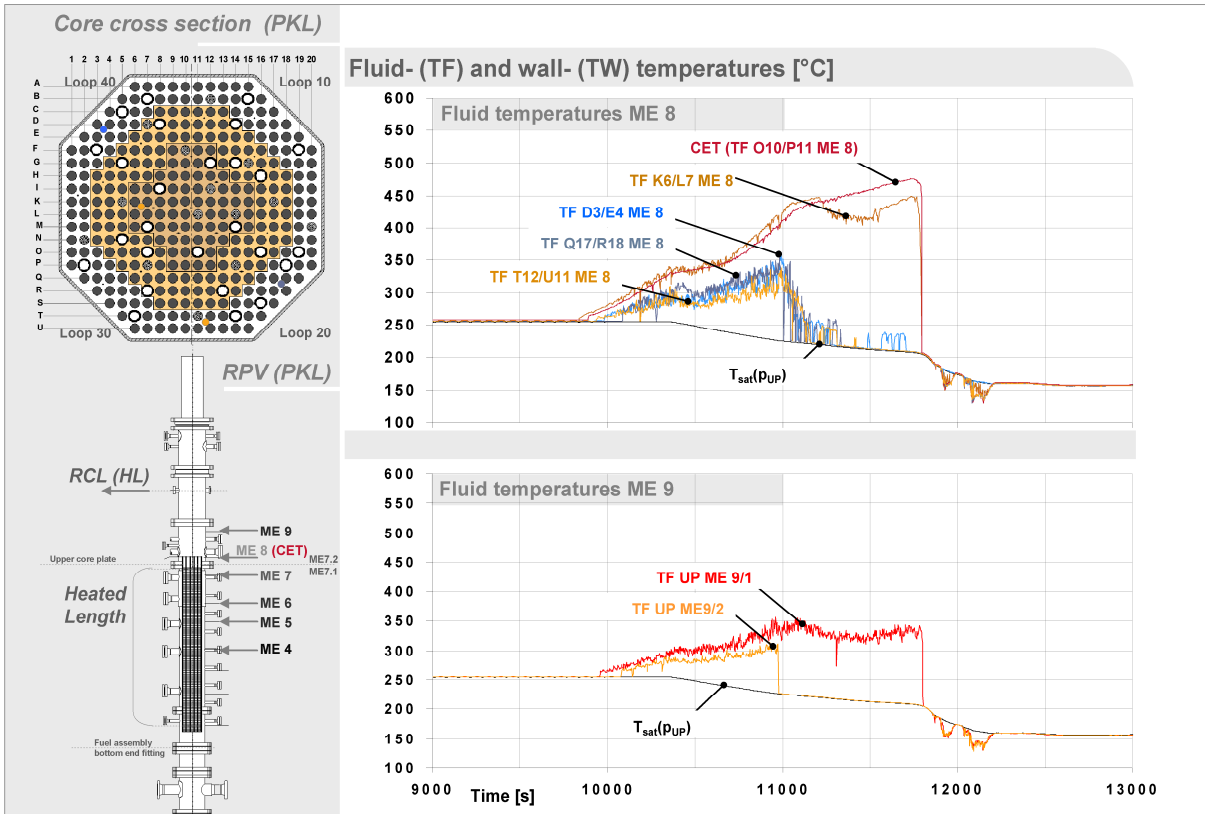
Figure 3.3.11 PKL SBO- Experiment
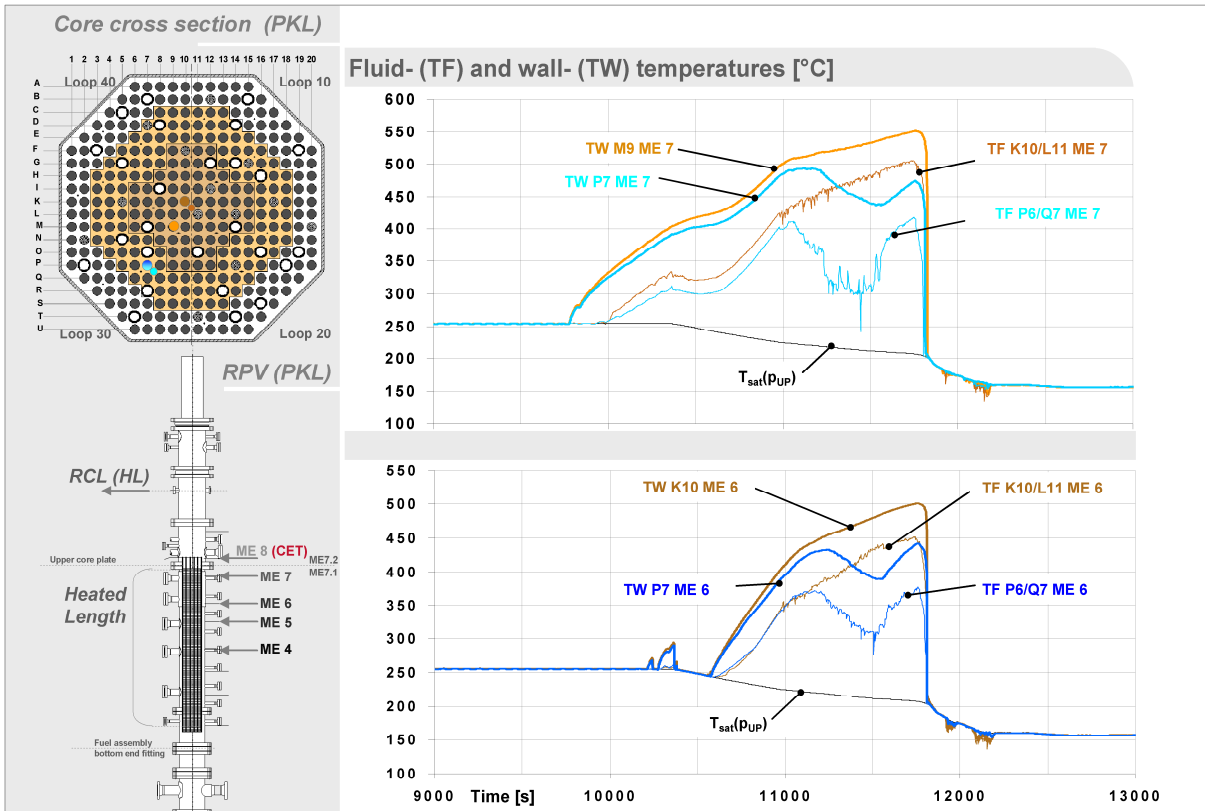
Figure 3.3.12 PKL SBO- Experiment
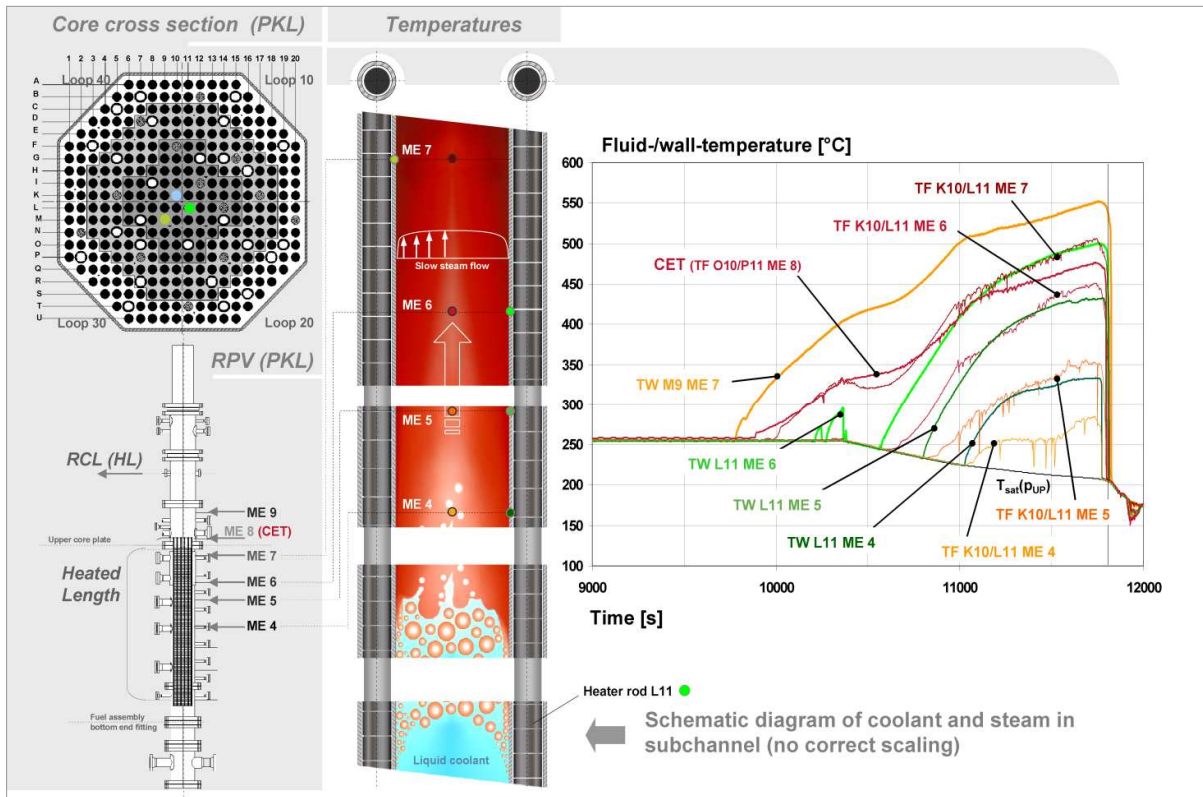
Figure 3.3.13 PKL SBO- Experiment
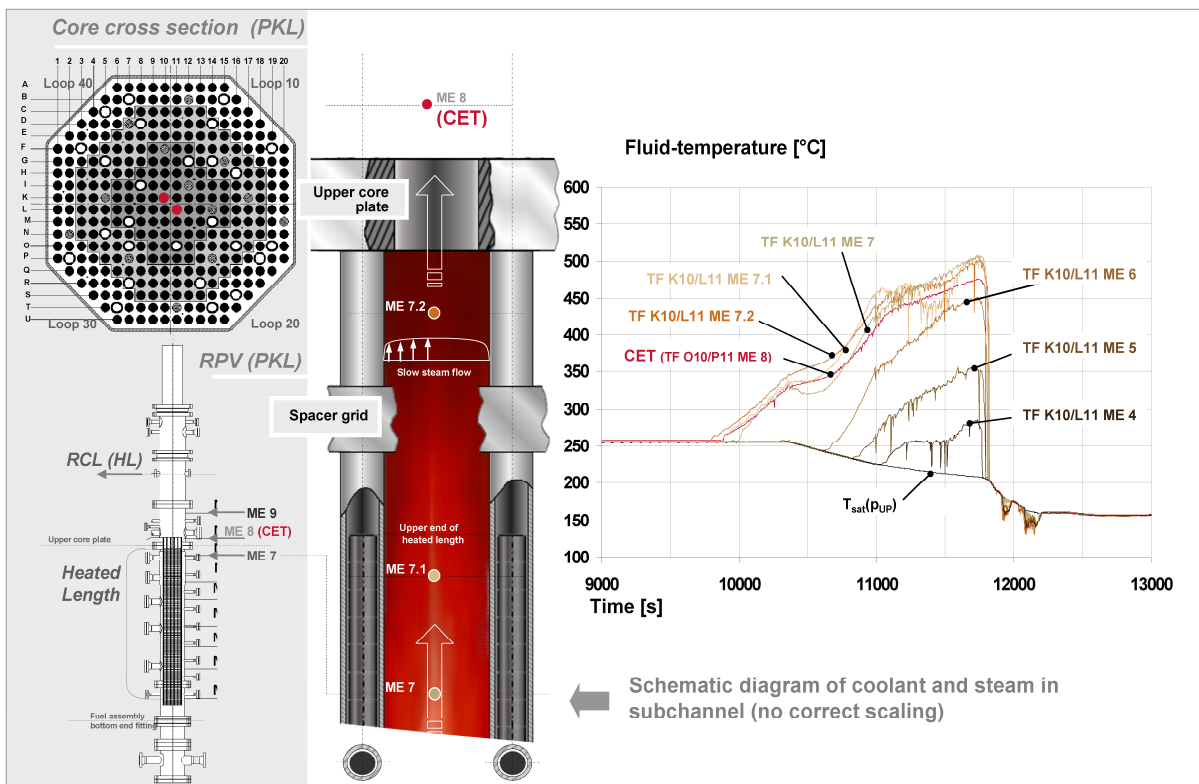
Figure 3.3.14 PKL SBO- Experiment
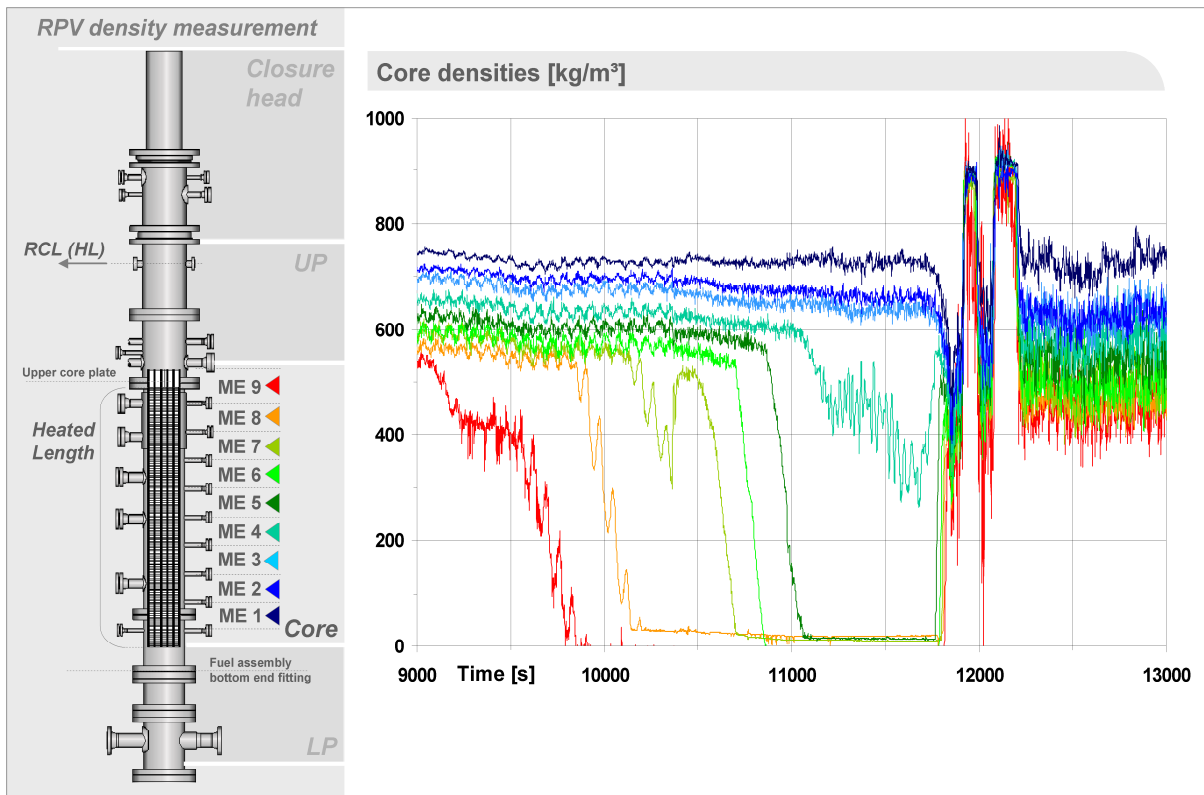
Figure 3.3.15 PKL SBO- Experiment
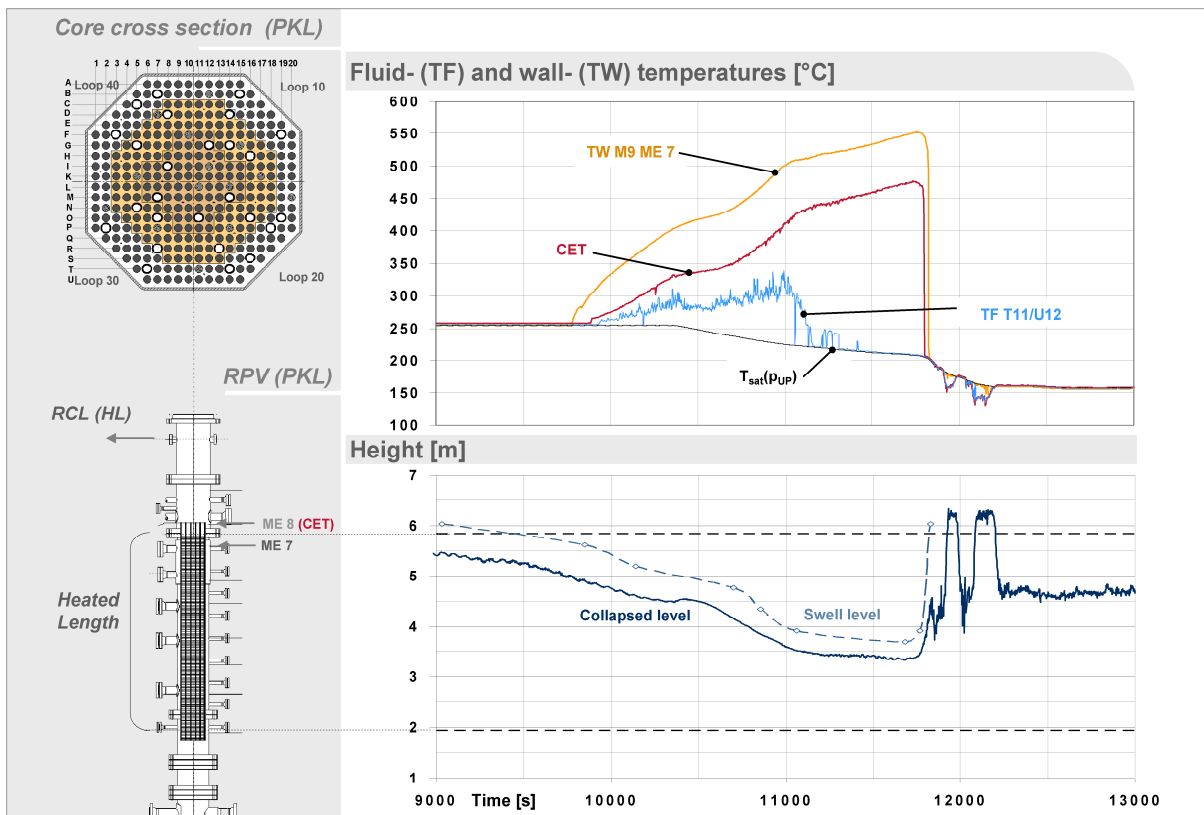
Figure 3.3.16 PKL SBO- Experiment

3.3.4.4 Results on significance of the CET

The point in time of the rise of the cladding temperatures (e.g. M9, ME7, see Figure 3.3.8) were not met by the CET. The CET starts to rise with a delay of about 100 s, but later-on the delay-time varies between 400 and 800 s. When the CET indicates insufficient core cooling, the maximum cladding temperature measured was about 50 K above CET. The delay between maximum cladding and fluid temperature in the adjacent sub-channel at the same elevation is even higher (more than 200 s, see Figure 3.3.12, top), which is caused by the deteriorating heat transfer.

During the following rise of the core temperatures until the initiation of the primary bleed procedure the temperature differential between CET and maximum cladding temperature increases slightly up to ~ 100 K. Apart from the now constant temperature differential between max cladding temperature and CET (~ 75 K) the evolution of the max. cladding temperature (rod M9, ME7) after primary depressurization (t > 10400 s after SOT), start of ACC injections (t > 11000 s) and the following pressure supporting effect (evaporation of ECC from ACC at UP and core structures) is reflected correctly in the CET.

Throughout the transient, the temperature differential measured between CET and maximum cladding temperatures never exceeded 100 K. The complete core quenching following the secondary side depressurization (restoration of secondary side heat sink, significant rise of hot leg ACC injection rates) is reliably indicated by the CET (with only a short delay of the max. cladding temperature, see Figure 3.3.9, top).

Cooling effects in the peripheral core regions induced by injected ECC (from ACCs) were visible in the appropriate fluid temperature measuring signals in the core sub-channels (ME 6 and ME 7; P6/Q7, H3/I4 ME7, see Figure 3.3.9, bottom). This pronounced heterogeneous radial temperature distribution is also observed above the upper core plate (see Figure 3.3.10, top). While the temperatures in the outer regions decrease to saturation values due to the even low ACC injection rates, the temperatures in the center regions remain on high levels (more than 250 K superheating) and with still increasing tendency. The radial temperature differences occur in the phases without water back flow from the hot legs due to the radial power profile and are still more pronounced after the onset of water back flow from the ACC injection. The delay in time for the indication of overheat by the TCs increases along the flow path of the steam from the core (CET, ME 8, see Figure 3.3.11) over the upper plenum (ME 9 see Figure 3.3.11) and the hot legs (ME 10, 11, not depicted in Figures). That is mainly a consequence of the heat storage capacity of the structures.

Concerning the significance of the CET, the main findings from the PKL test C5.2 can be summarized as follows:

- Steam leaving the heated part of the core has a significant lower temperature as the max. cladding temperature due to the rather poor heat transfer from the heater rod surface to the steam (rather low steam velocities in the order of 0.2 m/s)

- Another important effect is the heat storage capacity of the structures (unheated lengths of the heater rods, upper core plate, upper plenum internals, vessel walls) which are heated up by the steam leading to energy removal from the steam.

- Radial heterogeneity below and above the upper core plate is observed also in phases with no water back flow (due to radial power distribution). This effect is obviously more pronounced in phases with water backflow from the hot legs (ACC or reflux from SGs)

3.3.5   SB-LOCA transient

3.3.5.1 Background

The most important procedures which are automatically initiated in German PWRs in case of SB-LOCAs are the 100 K/h secondary cooldown and compensation of inventory losses by the high pressure injection system (HPIS). Failure of one or both of these procedures necessitate operator initiated AM-procedures to prevent core melt. The scenario under investigation in the PKL test D1.2 was a 40 cm^2 leakage at total failure both of the HPIS and of the 100 K/h cooldown. The AM-measure consisted of depressurization of the four secondaries assuming only one main steam valve to be available. The SG-secondaries were filled with water and feed water was available. A further system failure was postulated by the non-availability of 4 out of 8 ACCs. I.e. only hot leg feed was possible [4].

3.3.5.2 Test Procedure

Transient entrance in PKL was at an already reduced primary inventory at primary pressure of 40 bar. Calculations based on the mentioned leakage size predicted this pressure for equilibrium between leakage mass flow (pure steam) and the steam rate due to the residual heat. At this point of operation heat transfer to the secondary side was no longer existent as the isolated secondary side remained at 50 bar, leading to a low but permanent loss of inventory until beginning of core uncovery at about a quarter of the nominal primary inventory (see Figure 3.3.17). At a superheating of approx. 100 K at core outlet at 1610 s after SOT (approx. 2200 s after occurrence of the break in the PWR) the initiated AM-measure consisted of depressurization of the four secondaries assuming only one main steam valve to be available (secondary side B+F). The re-established secondary side heat sink caused the secondary pressure to drop from over 50 bar to below 40 bar, the value of the primary pressure. From then on (1710 s after SOT) the SGs began to work in reflux condenser mode of operation. Although the swell level in core further decreased, the reflux of condensate effectuated a slightly improved heat removal from the structures in the upper and peripheral core sections visible from the slightly decreased gradients in the TC readings from CET and upper cladding regions of central rods (M9 ME 7, see Figure 3.3.17) and from the dropping of peripheral fluid and wall temperatures (see Figure 3.3.17, subchannel F15/G16, rod M20). The primary pressure was dragged down by the secondary side but more central subchannel temperatures and the CET were still rising. The superheating at the core outlet reached some 250 K at 1970 s after SOT before the ACC injections quenched the entire heated length and restored core cooling (see Figure 3.3.18).
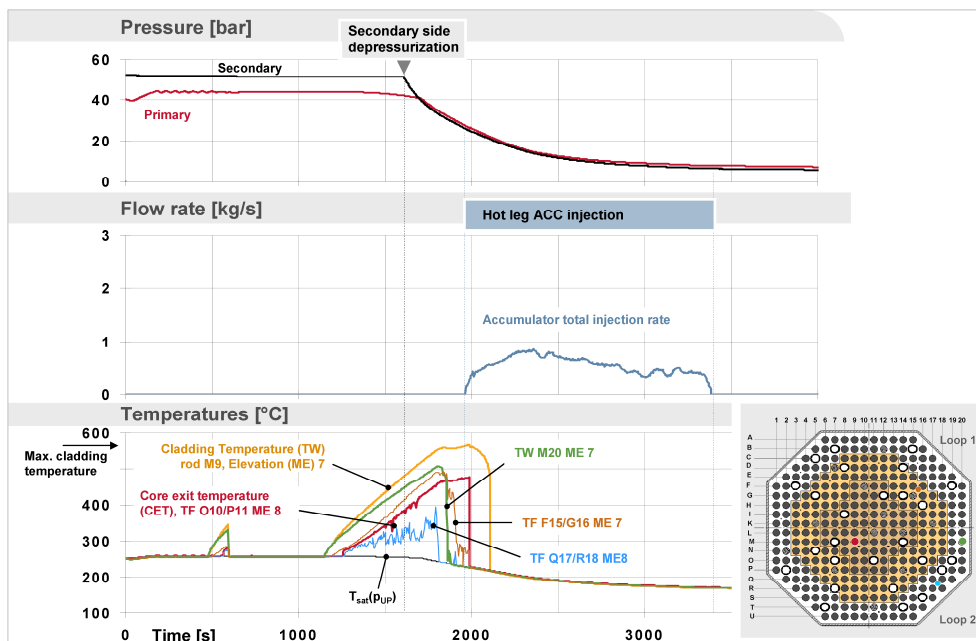
Figure 3.3.17 PKL SB-LOCA Experiment
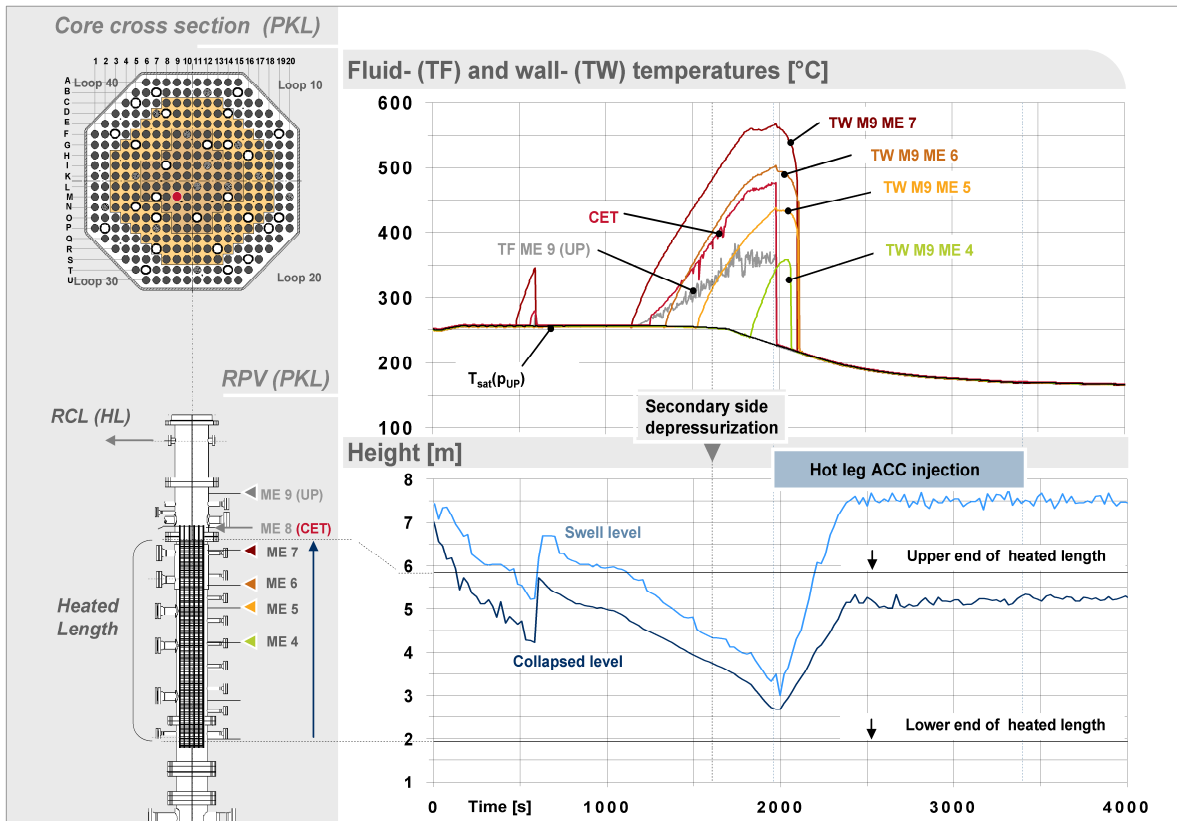
Figure 3.3.18 PKL SB-LOCA Experiment

3.3.5.3 Heat removal in relevant test phases

The situation in the core after core uncovery in the upper regions (rising of cladding temperature of rod M9 at ME 7, see Figure 3.3.17) is characterized as follows

> Residual heat removal from core via evaporation of ambient coolant, blow-down of steam via the break

> Continuously decreasing coolant inventory and swell level in the core, continuation of rise of core cladding temperatures following secondary side depressurization.

> Quench of entire heated length by ECC flow from ACCs for $t > 2000$ s after SOT and a maximum rod cladding temperature of $\sim 560\,°C$ ($T_{sat} = 225\,°C$). CET dropped earlier (from max. 477 °C for $t > 1984$ s) and more sharply.

3.3.5.4 Results on significance of the CET

Practically, the same conclusions apply as listed for the above mentioned test:

> The CET rises with a considerable delay of approx. 100 s and the delay-time increases as temperatures escalate to about 250 s.

> The evolution of the maximum cladding temperature is met with a temperature differential between max cladding temperature and CET not greater than 100 K.

> Final rewetting of the core (cladding temperature decrease to saturation) occurs more than 2 min after the indication of saturation conditions by CET (see Figure 3.3.17, bottom). The reason for the more pronounced delay is the lower ACC injection rate compared to the SBO experiment.

3.3.6 Loss of RHR test

3.3.6.1 Background

Test PKL III G1.1 was performed as a parameter study which focused on the dependence of different heat transfer mechanisms from primary to secondary side on the primary inventory in presence of nitrogen in the SG U-tubes; heat transfer mechanisms which are likely to occur in the course of a failure of the residual heat removal system (RHRS) during ¾-loop operation (primary circuit still closed) [5].

3.3.6.2 Test procedure

Designed as a parameter study for the investigation of heat transfer mechanisms emerging from loss of RHRS scenarios the following general boundary conditions applied:

> Single-loop operation, remaining 3 loops blocked by blank flanges in cold and hot legs close to RPV, dedicated SG initially filled with water on the secondary side, PRZ not in use (see Figure 3.3. 19)

> Simulation of cold shut-down conditions (i.e. primary inventory at ¾-loop level, N_2 above, CET $\sim 60\,°C$, p=1 bar)

> Core power set to 220 kW corresponding to 0,7 % of scaled full load core power after approx. 24 h after shut down of reactor, plus compensation for heat losses

> Prior to SOT: Removal of decay power via RHRS

> Temperature at core outlet approx. 60 °C

> Shut-down of RHRS at start of test

Multiple changes of primary coolant inventory (reduction/replenishment) with phases of steady-state operation returned a sequence of steady states (i.e. stable heat flux from primary to secondary at stable primary pressure) with intermediate changes of the primary coolant inventory.

Inventory was drained and replenished via lower plenum drain valve and a modified volume control system injecting into lower sections of downcomer tubes, respectively.

At start of test (SOT) the RHRS was shut down and inventory heat-up started. Prior to steam formation, inventory was drained from the RCS according to test specification. After steam formation started in the core (~ 500 s after SOT) the heat removal was taken over by the SG. Thereby, the removal of the entire 220 kW core power resulted in a steam flow velocity that effectuated CCFL in the SG-inlet chamber and U-tubes. Primary coolant inventory was successively displaced from RPV to the SG and accumulated in the U-tubes.

The effective reduction of core coolant inventory caused core uncovery and heat up in the upper core regions (at the upper end of the heated length). The heat up of the upper parts (ME 7) of the rod claddings was recorded by appropriate TC (fluid temperatures in central core axis and wall temperatures at rod claddings, see Figure 3.3.20) at 2000 s after SOT. Until 2190 s after SOT, the core heat up reached downwards as far as ME 6.

A stepwise reduction of core power down to ~ 150 kW (starting t = 2100 s after SOT, see Figure 3.3.20) then caused the successive re-displacement of coolant towards the RPV. The swell level then slowly proceeded upwards again, the rod cladding temperature (rod M9) at elevation ME 6 indicated re-establishment of cooling at 2580 s after SOT. At 3400 s after SOT the fluid and wall temperatures indicated a slow improvement of cooling along the entire heated length.

SG 1
p_{sec} = 1.0 bar

p_{prim} ~1.0 bar
$T_{Core,out}$ ~ 60 °C
P_{Core} = 200 kW (0.6 %)

COMBO

RHRS

Q

Coolant replenishment
(into both DC-tubes)

Lower plenum drain line

N₂, primary   Coolant, prim.

Air, secondary   Water, secondary

Plant configuration (G1.1):

> Single loop operation, other loops isolated

> Shut down conditions: ¾-loop operation, N_2 above

> RHRS in operation, p_{prim}. ~ 1bar, $T_{Core,out}$ ~ 60 °C

Test Procedure

> Start of test (SOT) with shut down of RHRS

⇨ Core heat up

⇨ Start of steam formation in the core

> Sequence of inventory changes (reduction/replenishment) to establish different heat transfer modes

> Phases of steady state operation at constant boundary conditions

Figure 3.3.19 PKL Test on loss of RHRS
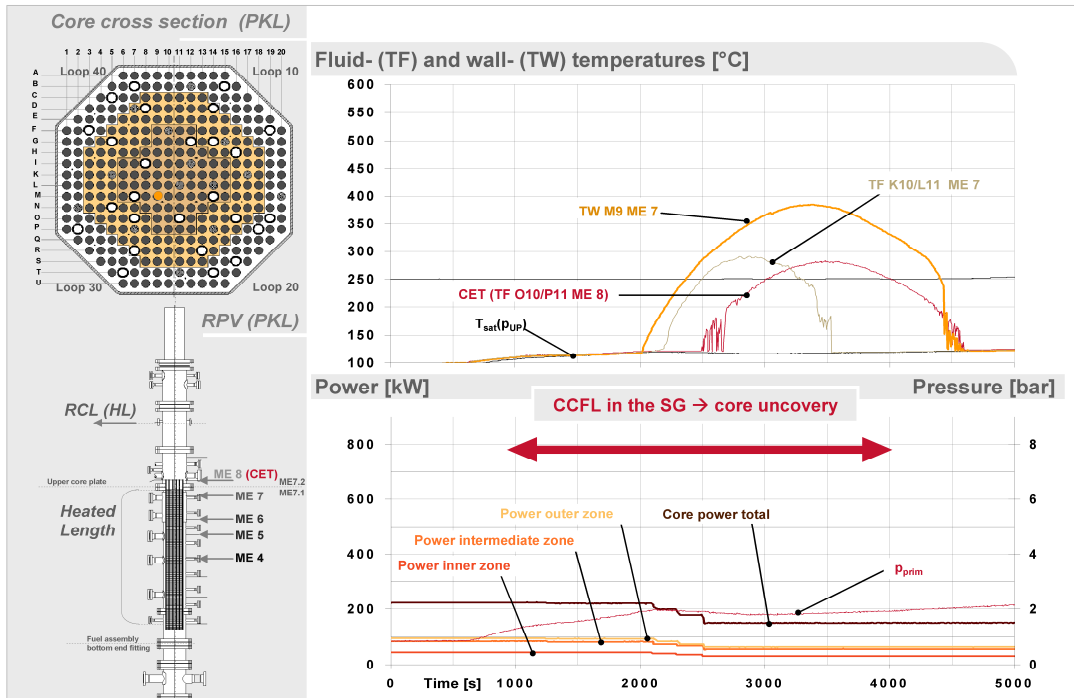
Figure 3.3.20 PKL Test on loss of RHRS

3.3.6.3   Heat removal in relevant test phases

The situation in the core after core uncovery in the upper regions (rising of rod cladding temperature at ME 7, see Figure 3.3.20) is characterized as follows:

> Residual power removed from the core by evaporation of ambient coolant, steam flow from the core to the SG U-tubes, RC-operation in the U-tubes, no or reduced reflux of coolant towards the RPV due to CCFL in the SG- inlet chambers

> No ECC injection

> Continuously decreasing swell level in the RPV at quasi-constant low primary pressure (p_{abs}) ~ 2 bar.

3.3.6.4   Results on significance of the CET

Due to the rapid evolution of core uncovery from cold shut-down conditions (approx. 2000 s after SOT), the initially cold structures (e.g. unheated lengths of rods, upper core plate) significantly contributed to a delayed rise of the CET and to a significant temperature difference between CET and maximum cladding temperature measured. Delay of Δt ~ 500 s with ΔT ~160 K (~160 k superheat at heater rod cladding e.g. rod M9, ME 7, see Figure 3.3.20).

The evolutions of the fluid temperatures measured between the heater rods in the sub-channels (e.g. TF, K10/L11, ME7, delay in heat up approx. 150 s) indicate a turnaround for t > 2880 s after SOT. The

evolving large temperature difference between rod surface and appropriate fluid temperature at the same elevation for t > 2880 s indicates water entrainment in the sub-channels (see Figure 3.3.20, TF K10/L11 ME7). Although saturated coolant was indicated by TCs at elevation ME 7, it did not reach the rod surface, the cladding temperature continued to rise until ~ 3380 s after SOT and the rewetting process, was only completed 4440 s after SOT.

In contrast to the temperatures in the sub-channels the delay of CET concerning the indication of core heat up is higher (about 500 s), however the rewetting of the core heater rods is well reflected by CET. The maximum difference between CET and measured cladding temperature was 160 K. The differences between measured temperatures in the sub-channels and CET are mainly due to the heat transfer to and from the structures in the upper part of the core region (unheated lengths of the rods, upper core plate) and due to water entrainment in the sub-channels.

3.3.7   Conclusions and applicability to PWR configuration

Differences between CET and maximum cladding temperature were observed in several PKL experiments mainly dealing with beyond-design-basis accidents and the employment of adequate AM measures. Three experiments representing relevant accident scenarios have been selected to analyze the differences between CET and maximum cladding temperature and to provide information on physical phenomena responsible for the CET performance.

The three tests are characterized by a significant primary inventory loss leading to a pronounced core uncovery for a longer period of time. As the existing boundary conditions (e.g. upward steam flow, water back-flow) are of high significance for the CET performance, the experiments or individual test phases within the experiments have been categorized as follows:

- Phases with no water back-flow from the top
    - o   With decreasing coolant inventory in the core at constant primary pressure
    - o   With decreasing coolant inventory in the core and depressurization in parallel (flashing)
- Phases with water backflow from the top, e.g.
    - o   From the hot leg ACC
    - o   From the SGs due to reflux condensation

The results from the described PKL tests concerning CET performance can be summarized as follows:

- Significant temperature differentials between CET and maximum cladding temperature (delay in start of superheating and difference in maximum measured temperature) were observed even in situations without water backflow.

    The following main reasons for this have been identified:
    - o   Rather poor heat transfer from the rod cladding to the ambient steam due to low steam flow velocities, to some extent a possible entrainment of water (made evident by comparison of wall and fluid temperatures in the core at the same elevations).
    - o   Impact of heat exchange with colder structures above the upper end of the heated lengths. Cold structures (e.g. unheated lengths of rods, upper core plate, core barrel) located in the steam flow path from the heated lengths towards CET measurement positions influence the maximum temperature differential measured between CET and maximum cladding temperatures.

- Higher differences occurred between the fluid temperatures in the upper plenum (or RPV outlet) and the maximum cladding temperature in the core because of the additional cooling effects of the structures in the upper plenum.

- A radial temperature profile (fluid and wall) in the core and above the core (CET) was observed in all the tests due to the radial power profile superposed by the effects of the core barrel and of the heat losses.

- Tests at low primary pressures (shut down conditions) also revealed pronounced differences/delay between CET and maximum cladding temperatures. A tendency is visible in the test results: The faster the evolution of the transient towards core uncovery, and the colder the structures in the UP the larger $\Delta T_{clad,max-CET}$.

- Despite the delay and the difference in the measured temperatures, the time evolution of the CET signal readings in the center section seem to reflect the change of the cooling conditions in the core and thus the tendency of the maximum cladding temperatures quite well.

The PKL test results and the identified phenomena relevant for the CET performance can be qualitatively extrapolated to the PWR. The thermal hydraulic conditions present in the different phases of the tests under investigation are typical for the relevant PWR accident scenarios.

The geometry of the core (i.e. rods, sub-channels, unheated lengths of rods) corresponds to the configuration of the reference PWR. The upper core plate in PKL (representing the fuel assembly top nozzle) was also adapted to the PWR design (thickness, diameter of flow channels, distance to end of heated lengths of the rods).

However, because of the diversity of influence parameters and the test facility design features (e.g. overall geometry, heat structures, uniform axial power profile, location of CET) the PKL test results cannot be directly extrapolated to PWR in quantitative terms.

Furthermore, the CET performance (i.e. the difference between CET and maximum cladding temperature) strongly depends on the accident scenario and the flow conditions in the core and around the CET measurements and may also vary between different PWR types (due to different design). E.g. in some PWR plants the CET is measured above the fuel assembly top nozzle and below the PWR upper core plate (as in PKL), partly installed in so-called finger-tubes (not realized in PKL) which provide protection against water backflow or entrainment but which would also lead to a further delay of the CET (additional heat transfer resistance).

Nevertheless, the clear boundary conditions present for different quasi-stationary heat transfer states in the PKL tests, in particular for the SBO experiment (phases of pool boiling without and with depressurization in parallel, no coolant backflow) contribute to a better understanding of the T/H phenomena associated with the issue in general on one hand and represent a good data base for the validation of codes and models on the other hand.

In Germany, the difference between CET and maximum cladding temperature is considered in the AM strategy: An early initiation of AM procedures on basis of other diverse criteria and initiated in a situation when the core cooling is still assured, is the preferred method to deal with corresponding accident scenarios. The CET is employed only as an ultimate criterion in case of a failure of previously conducted AM measures.

References

[1] H. Kremin, H. Limprecht, R. Güneysu, K. Umminger, Description of the PKL III Test Facility, Report FANP NT31/01/e30, Erlangen, July 2001

[2] K. Umminger, B. Brand, W. Kastner, PKL Test Faciliy of Framatome ANP - 25 Years Experimental Accident Investigation of Pressurized Water Reactors, VGB PowerTech, Januar 2002

[3]   K. Umminger, W. Kastner, P. Weber, "Effectiveness of Emergency Procedures under BDBA-Conditions-Experimental Investigations in an Integral Test Facility (PKL)," The 4th International Conference on Nuclear Engineering (ICONE-4), March 10-14, 1996, New Orleans, USA, Proc. Vol. 3, pp. 311 - 319

[4]   T. Mull, M. Perst, K. Umminger, "Effectiveness of Accident Management Procedures under Small Break LOCA Conditions," The 5th International Conference on Nuclear Engineering (ICONE-5), May 26-30, 1997, Nice, France, Paper 2192, pp. 1-8

[5]   K. Umminger, B. Schoen, T. Mull, "PKL Experiments on Loss of Residual Heat Removal under Shutdown Conditions in PWRs," 2006 International Congress on Advances in Nuclear Power Plants (ICAPP '06), Reno, USA, June 04-08, 2006.

Abbreviations and acronyms

ACC	Accumulator
AM	Accident Management
CCFL	Counter Current Flow Limitation
CET	Core Exit Temperature
ECCS	Emergency core cooling system
HPSI	High pressure safety injection
LB	Large Break
LOCA	Loss of coolant accident
LPSI	Low pressure safety injection
ME	Elevation of measurement
MSRV	Main steam relief valve
MST	Measurement point
NC	Natural circulation
OECD	Organization for Economic Cooperation and Development
PKL	Test facility, (German acronym for "Primärkreislauf", primary circuit)
PRZ	Pressurizer
PWR	Pressurized water reactor
RC	Reflux-condenser
RCL	Reactor coolant line
RCP	Reactor coolant pump
RCS	Reactor cooling system
RHRS	Residual heat removal system)
RPV	Reactor pressure vessel

SB	Small Break
SG	Steam generator
SOT	Start of test
TC	Thermocouple

3.4   THE ROSA/LSTF EXPERIMENTS

3.4.1 Introduction

Test 6-1 [1, 2] of the OECD/NEA ROSA Project using the LSTF [3], shown in Figure 3.4.1, simulated a vessel head small break loss-of-coolant accident (SBLOCA) with a break size equivalent to 1.9% cold leg break under an assumption of total failure of the high pressure injection (HPI) system. A large temperature time delay of about 230 s for the CET readings to reach 623 K (criterion to start an accident management - AM- operator action) was observed in the test. This situation appeared under no reflux water fall-back conditions. A large temperature difference from the maximum core temperature was observed too in the test.

As a member of the WGAMA CET task group that was set up based on the Test 6-1 results and historical discussions since LOFT tests [6, 7], JAEA decided to provide twelve other LSTF tests [4] to thoroughly study CET performances in the LSTF experiments. The additional tests include ten SBLOCA tests with or without AM actions and two abnormal transients each with extremely high or low pressure conditions by considering some diversity and similarity of the test results. The ten SBLOCA tests were conducted with a break at five different locations (see Figure 3.4.1-2) and break sizes ranging from 0.1 to 10% equivalent to cold leg break (CLB). Two abnormal transient tests simulate station blackout scenario and loss of residual heat removal (RHR) system under mid-loop operation. Two tests among these twelve tests showed no CET heat-up because of significant water fall-back, while seven tests showed CET heat-up under limited fall-back water effects. Two abnormal transient tests suggested alternative criterion for the CET superheat detection during their specific boil-off conditions under significantly high or low primary pressures. Through the data analyses for the in-total thirteen LSTF experiments, reasons of the time delay and temperature discrepancy from the core heat-up were clarified by considering especially on the average
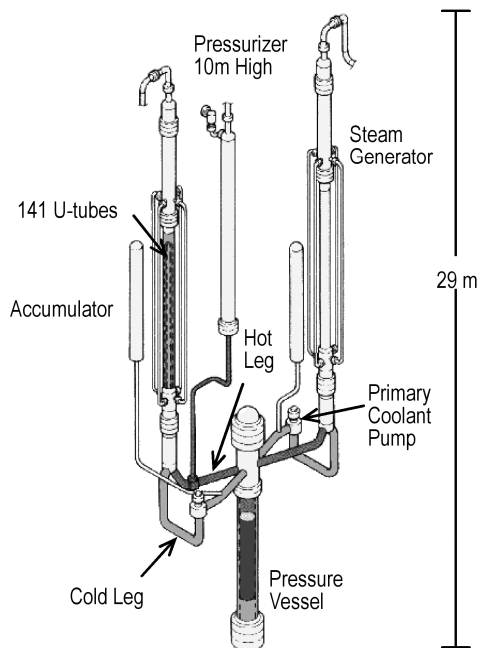
Figure 3.4.1-1 ROSA/LSTF facility
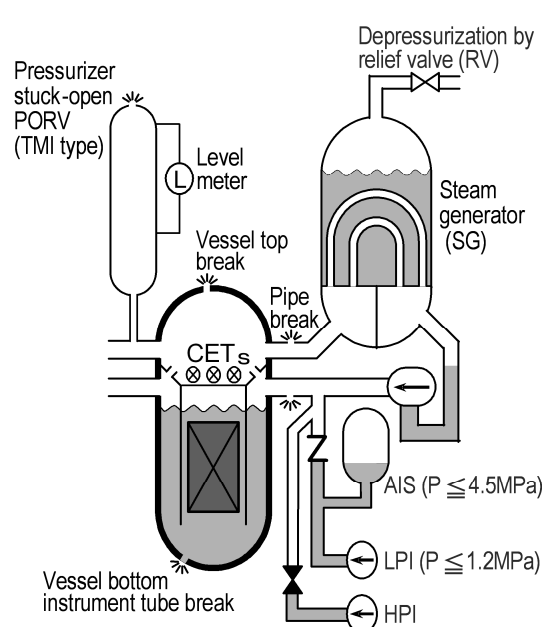
Figure 3.4.1-2 Break locations for PWR SBLOCA tests

steam velocity at the core exit and cooling effects of structural materials such as the upper core plate (UCP) and core barrel on hot steam uprising flow from the heat-up core [5].

This section summarizes the findings based on ROSA/LSTF experiments; Section 3.3.2: the description of the LSTF and CETs with test conditions. Section 3.3.3: the CET performance in Test 6-1 [1, 2], Section 3.3.4: results of additional 12 tests [4, 5], Section 3.3.5: summary of general CET performances [5], Section 3.3.6: brief discussion on applicability of the LSTF results to PWR.

3.4.2 FACILITY DESCRIPTION AND TEST CONDITIONS

3.4.2.1 ROSA/LSTF facility and CETs

The LSTF shown in Figure 3.4.1-1 is a full-height and full-pressure PWR simulator referring a Westinghouse- type 4-loop 3423 MWt PWR, Tsuruga Unit-2 of the Japan Atomic Power Company (JAPC), with a 1/48-volumetric scaling in two-loop system as shown in Table 3.4.2-1.

Table 3.4.2-1 Major design characteristics of LSTF and 4-loop PWR

Items	Unit	LSTF	PWR	Ratio
Pressure	MPa	16	16	1 / 1
HL Temperature	K	598	598	1 / 1
Maximum Core Power	MWt	10	3423	1 / 342
Primary Fluid Volume	m^3	8.1	347	1 / 43
Number of Fuel Rods	-	1008	50952	1 / 50.5
Number of Fuel Rod Bundles	-	24	193	1 / 8.0
Rod Array in Bundle	-	7×7	17×17	-
Number of CRGTs	-	8[*1]	53	1 / 6.6
Number of CETs	-	20	50	1 / 2.5
HL Inner Diameter (d)	m	0.207	0.7369	1 / 3.6
UP Inner Diameter (D)	m	0.514	3.759	1 / 7.3
HL Height above UCP Top (h)	m	1.355	0.8255	1 / 0.61
UP Aspect Ratio (D/h)	-	0.379	4.554	1 / 12
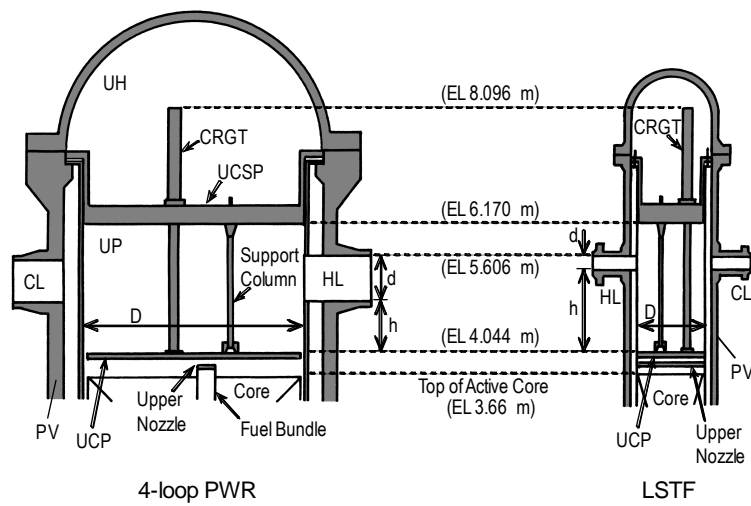
Figure 3.4.2-1 Comparison of upper PV configuration between LSTF and 4-loop PWR

Figure 3.4.2-1 compares upper PV configuration between LSTF and the reference PWR. The LSTF is furnished with PV internal structures such as the core with 1008 electric heater rods (7×7 rod array in one bundle), 8 slender control rod guide tubes (CRGTs), UCP and surrounding core barrel, which neatly simulate multi flow paths in the core and core exit region. The LSTF upper plenum (UP) configuration is atypical of the reference PWR with respect to the UP diameter (D) and the hot leg height (h) above the UCP. The LSTF UP aspect ratio (D/h) is 1/12 of that in the reference PWR (Table 3.4.2-1), which should be taken into account in the discussion on influences of reflux fall-back water on the CET temperature responses.

Figure 3.4.2-2 shows detail of structures at the LSTF core exit region above the core heating elevation (EL 3660 mm). There are complicated flow paths around non-heating parts such as the top portion of electric heater rods, No.9 spacer, end box (upper nozzle) and UCP within the core barrel. Most of these structures are made of stainless steel, which become heat sink to hot steam flow.

The LSTF core assembly consists of 16 square bundles with 7x7 rod array and 8 peripheral bundles. Eight high power bundles (bundle numbers B13 through B20) have a radial peaking factor of 1.51, four middle power bundles (B21 through B24) have that of 1.0 and twelve low power bundles (B01 through B12) have that of 0.66, respectively. The outer diameter, pitch and arrangement of the heater rods are the same as those in the reference PWR. Since the shake-down of LSTF in 1985, the core assembly has been replaced three times.

Figures 3.4.2-3 (a) and (b) show horizontal cross- section of the current fourth core assembly with 1008 heater rods including six instrumented rods, which was used for three
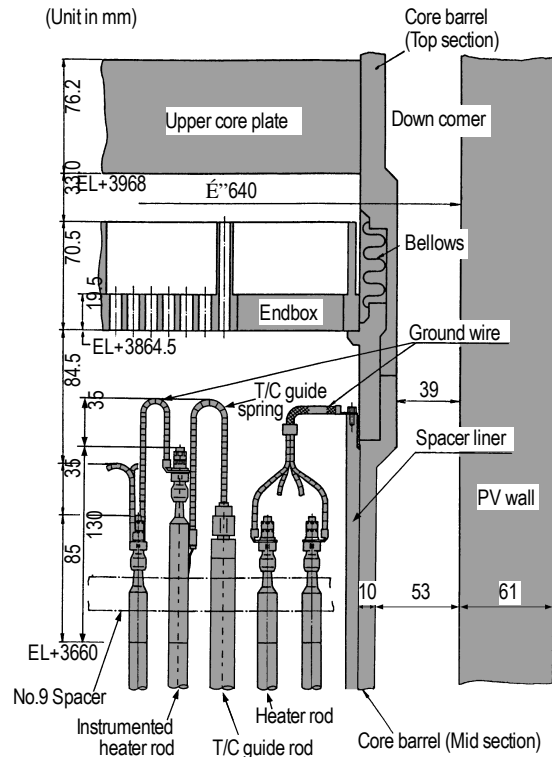
Figure 3.4.2-2 Detail of structures and core rod assembly in core exit region of LSTF
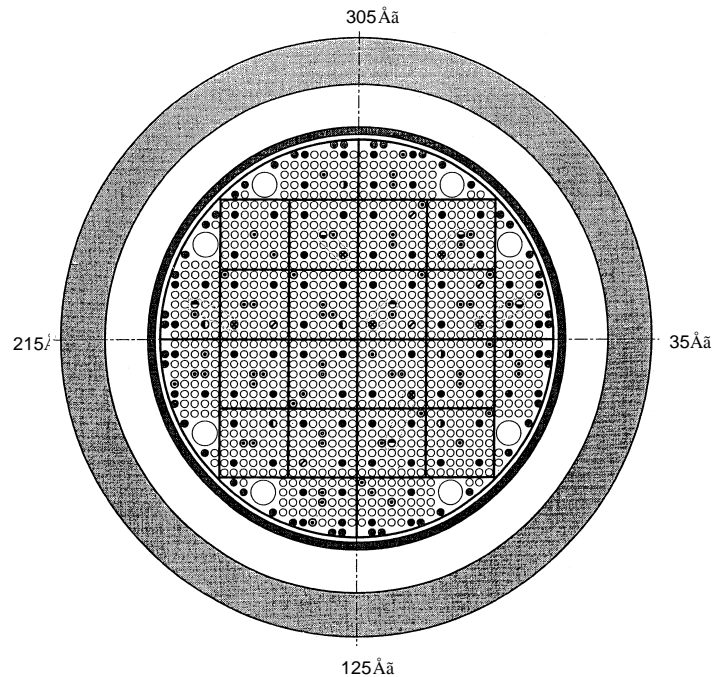
Figure 3.4.2-3 (a) Horizontal cross-section of LSTF fourth core assembly
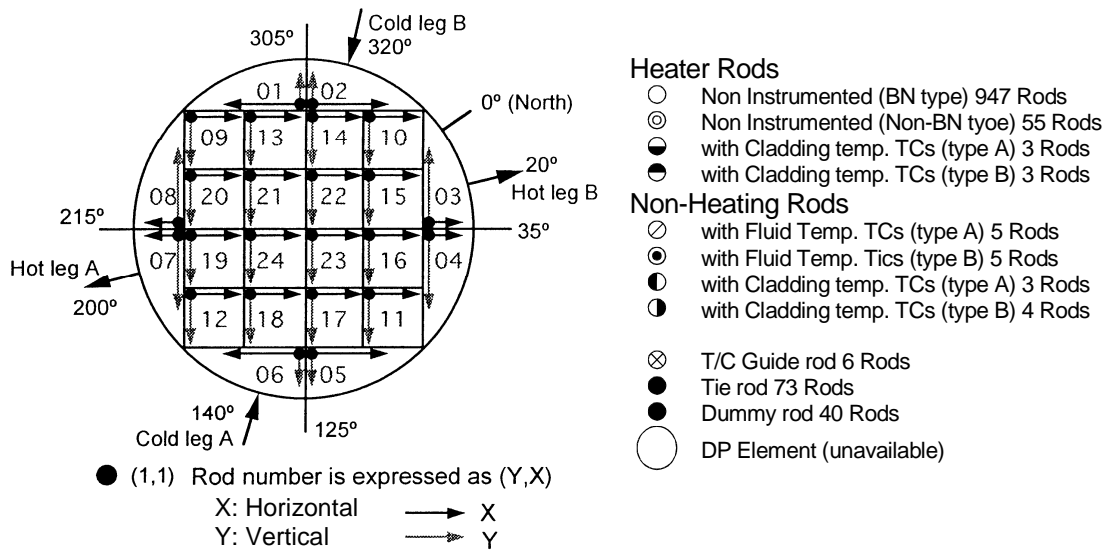
Figure 3.4.2-3 (b) Arrangement of 7x7 rod bundles and instrumented rods in LSTF fourth core

SBLOCA tests of SB-PV-03 [11], SB-PV-07 and SB-PV-08. The first core assembly with

surface temperature measurements for 53 heater

rods was used until Aug. 1988 for five SBLOCA tests of AT-SB-03 [8], SB-CL-01,

SB-CL-09 [9], SB-PV-01 [8] and SB-PV-02 [8], and one abnormal transient test TR-LF-03. The second core assembly was used between Dec. 1988 and July 1993 with 1008 heater rods including 54 instrumented rods for two SBLOCA tests of SB-CL-24 [10] and SB-HL-05, and one abnormal transient test of TR-RH-06. Table 3.4.2-2 summarizes major conditions of 13 LSTF experiments dealt with in this chapter.

There are 20 CETs in LSTF and their locations are shown by Figure 3.4.2-4 (a) along with the 24 flow path holes of the UCP, 8 CRGTs and 10 support columns. The CRGTs and flow path holes are located above the rod bundles. Each CET is located at 13 mm above the UCP top surface. Four CETs shown in Figure 3.4.2-4 (b) are installed outside of the CRGT-basements above the rod bundles of B10, B12, B22 and B24.

Table 3.4.2-2 Major test conditions for OECD ROSA Project Test 6-1 and additional 12 tests

Test ID	Type of Test	Break Location	Size (%)*1	Operator/AM Action	Start of Action	Set Point	Init. P. (MPa)	Test Year
Test 6-1[1]	SBLOCA	PV Top	1.9	SGRV	CET-T	623 K	15	2005
SB-PV-07	SBLOCA	PV Top	1.0	HPI	CET-T	623 K	15	2005
SB-PV-02	SBLOCA	PV Top	0.5	HPI	HL-T	T_S+10K	15	1987
SB-PV-08	SBLOCA	PV Top	0.1	SGRV	CET-T	623 K	15	2005
SB-CL-09	SBLOCA	Cold Leg	10.0	-	-	-	15	1986
SB-CL-01	SBLOCA	Cold Leg	2.5	HPI	Time	1200 s	15	1985
SB-CL-24	SBLOCA	Cold Leg	0.5	SGRV/PORV	Time	600 s	15	1990
SB-HL-05	SBLOCA	Hot Leg	0.5	PORV	HL-T	T_S+5 K	15	1989
SB-PV-01	SBLOCA	PV Bottom	0.5	HPI	HL-T	T_S+10K	15	1986
SB-PV-03	SBLOCA	PV Bottom	0.2	SGRV/PORV	Time	SI+600s	15	2002
AT-SB-03	SBLOCA	TMI-type	0.45	HPI	Time	6600 s	15	1985
TR-LF-03	TMLB' Transient			-	-	-	15	1988
TR-RH-06	Mid-loop / Loss-of-RHR			AFW Supply	Core-T	523 K	0.11	1993

*1 Break size equivalent to 1/48-scaled cold leg area at the reference PWR

Sixteen other CETs are installed at the top edge (exit side) of UCP flow path holes as shown in Figure 3.4.2-4 (c). Eighteen Thermocouples are placed at the bottom edge (inlet side) of UCP flow path holes in pair with CETs. Figure 3.4.2-5 shows nine axial power steps of all heater rods with nine thermocouple locations (P.1 through P.9). Thermocouples of 0.5 mm diameter are imbedded in the heater rod sheath to measure surface temperature while those for the fluid temperature measurements are installed outside of non-heating rods at the same elevations as the rod temperature measurements (Figure 3.4.2-6).

3.4.2.2 Test conditions

Table 3.4.2-2 compares test conditions of all the thirteen LSTF experiments including Test 6-1 of the OECD/NEA ROSA Project. Initial test conditions and control logics for the scram, primary pump coast-down, SG isolation, SG pressure regulation are common for all of the SBLOCA tests. Initial primary pressure of all the tests was about 15 MPa except for TR-RH-06 test at 0.11 MPa. Several test conditions peculiar to each experiment are presented below especially for break conditions, operator actions and selected indicator for operator or AM actions during core heat-up.

(1) Break conditions

Break locations are i) PV upper head (UH), ii) PV bottom (lower plenum), iii) cold leg (CL), iv) hot leg (HL) and v) pressurizer top (TMI-type break with stuck-open power- operated relief valve (PORV)). The break size ranges from 10% (31.9 mm inner diameter (ID)) to 0.1% (3.2 mm ID) of the scaled cold leg area.
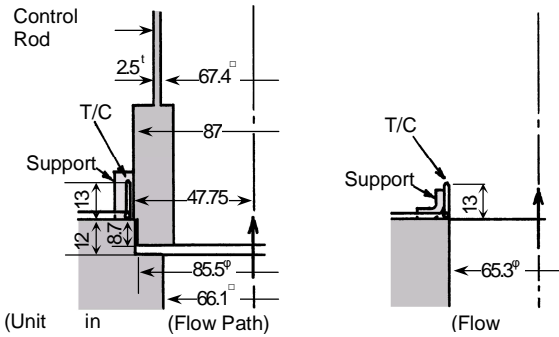
Figure 3.4.2-4 (b) Detail of CET at CRGT

Figure 3.4.2-4 (c) Detail of CET at flow
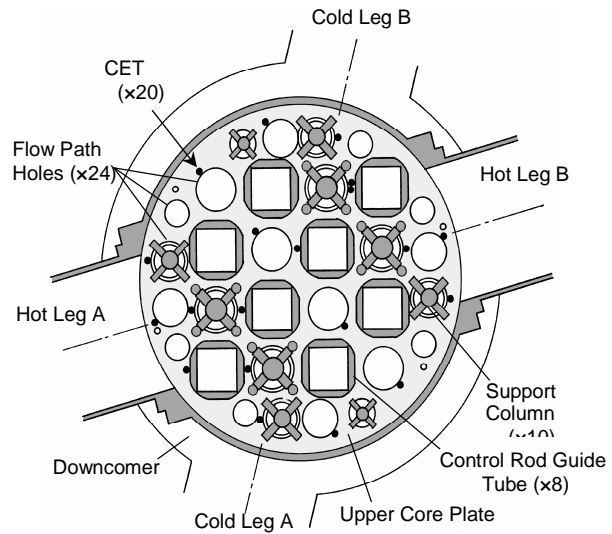
Figure 3.4.2-4 (a) Location of core exit thermocouples (CETs) and arrangement of internal structures on UCP of LSTF
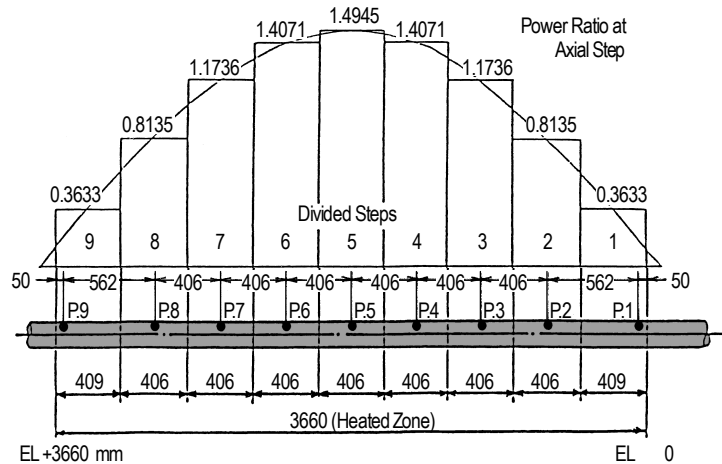
Figure 3.4.2-5 Axial power steps of heater rods with thermocouple locations of LSTF

Thin-edged break orifice in a branch pipe was used for most of SBLOCA tests except for SB-HL-05 and SB-CL-24 that used an orifice mounted flush with the horizontal leg inner surface. Two abnormal transient tests simulated coolant discharge through a valve or an opening; a pressurizer safety valve (SV) under high pressure conditions for TR-LF-03, and a manhole simulated with 58.4 mm ID orifice at the pressurizer for TR-RH-06 that simulated a loss-of-RHR during mid-loop operation under atmospheric pressure condition.

(2) Core power decay curves

Three types of core power decay curves were applied for Test 6-1 and 11 tests [4] while a constant power of 0.38 MW was applied to TR-RH-06 test. The JAERI-power curve which simulates 1/48-scaled PWR decay power after the scram with a conservative delayed fission power and fuel rod stored heat release was

TC direction

Figure 3.4.2-6 Location of thermocouples for fluid

applied to six tests (SB-CL-01, SB-CL-09, SB-CL-24, SB-PV-01, SB-PV-02 & SB-HL-05) within a power limit of 10 MW that corresponds to 14% of the 1/48-scaled PWR rated power. On the other hand, the new power curve which simulates a 1/48-scaled heat transfer rate at the reference PWR core in a range of 10 MW based on a best estimate analysis of SBLOCA conditions, was applied to five tests (Test 6-1, SB-PV-07, SB-PV-08, SB-PV-03 & TR-LF-03). A core power curve for AT-SB-03 test was specific for TMI-type LOCA simulation.

(3) AM action starting conditions

Table 3.4.2-2 includes conditions to start simulation of AM actions. The CET temperature (designated as CET-T) of 623 K was employed in SB-PV-07 and SB-PV-08 as in Test 6-1 while the steam superheat in HL (designated as HL-T) was used in SB-PV-02, SB-PV-01and SB-HL-05. For three tests of SB-CL-01, SB-CL-24 and SB-PV-03, a delay time of 10-20 minutes from the break or safety injection (SI) signal was applied. In SB-CL-09, operator action was not planned because of the fast primary depressurization and early AIS actuation. In SB-CL-24 and SB-PV-03, the second or third AM actions were conducted to promote primary system cooling by opening PORVs when the primary pressure turned to increase under loss of secondary coolant (SB-CL-24) or when the primary depressurization was significantly degraded by non-condensable gas inflow from the AIS tanks (SB-PV-03). In AT-SB-03 as TMI-type, HPI was manually initiated 6600s after the break. In TR-RH-06 test, auxiliary feedwater (AFW) was manually started after a significant core heat-up (Core-T).

3.4.3 CET performance in OECD/NEA ROSA project test 6-1

CET performance in ROSA project test 6-1 (SB-PV-09 in JAEA) [1, 2] is summarized first. A CRGT-focused steam flow was observed in this test in addition to cooling effects of cold structures around core exit.
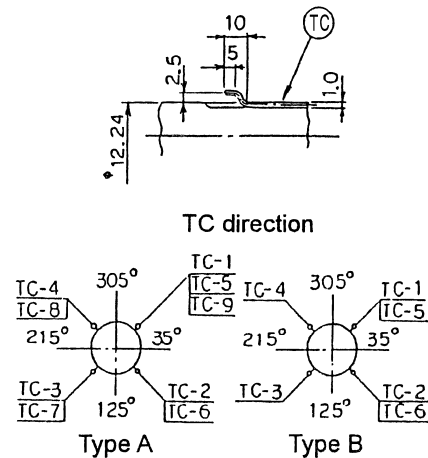
3.4.3.1 CET performance to detect core heat-up under no reflux fall-back water

(1) Primary and secondary pressure responses with major events

The primary pressure rapidly decreased after the break as shown in Figure 3.4.3-1and became lower than the SG secondary pressure at about 700s when steam discharge started at the break. This resulted in the termination of reflux condensation in the SG U-tubes during the core boil-off and AM action at 1074 s. The AM action was to initiate AIS via rapid depressurization of the SG secondary sides, but was ineffective because of the lower primary pressure than the secondary pressures. The core coolant mass started to recover after 1400 s due to the AIS coolant injection after about 1300 s.
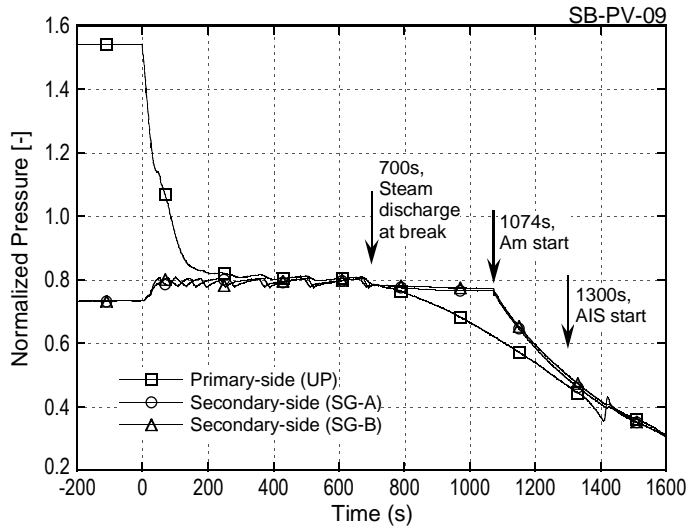
Figure 3.4.3-1 Primary and secondary pressures in 1.9% PV top break test (Test 6-1)

(2) Core heat-up behaviors

The core heat-up started at 840 s because of typical boil-off as shown in Figure 3.4.3-2 that indicates collapsed water levels in core, UP and downcomer (DC). Typical heater rod surface temperatures are shown in Figure 3.4.3-3 with the primary saturation temperature (T_S) for a heater rod in a high-power bundle (B17) at elevations of P.9 (Top), P.7, P.5 (middle) and P.3. The maximum rod temperature at P.7 reached the limit to start an automatic core power decrease at 1204s to protect core from overheating. The core power was

Figure 3.4.3-2 Collapsed water level in vessel in Test 6-1

stepwise decreased to 50% at 1215 s and 10% at 1220 s resulting in the gradual core temperature decrease. Most of the core was quenched by 1400 s except for the core top region that was finally quenched by 1550 s. No core power reduction could have resulted in slightly higher primary pressure, in AIS actuation postponed beyond 1300 s, in smaller AIS injection rates and in later core level recovery. The maximum rod temperature may have exceeded 1200 K as suggested by a broken line in Figure 3.4.3-3 in case of no core protection procedure.

(3) CET temperature responses during core heat-up

All the CET temperatures during the core heat-up period are shown in Figures 3.4.3-4 (1) and (2). The maximum value appeared at the central region above the middle-power bundle B21 with large fluctuations probably because of unstable steam flows at different temperatures. The low steam temperatures appeared at peripheral regions in the core suggesting inflow of low-temperature steam from low-power bundles and cold structures such as the core barrel and non-heating rods.

The CET detected earliest superheating at 910 s more than an uncertainty range of temperature measurement. The AM action was initiated at 1074 s when two CET temperatures reached the criterion of 623 K. The CET temperatures at the exit of high power bundles with no CRGT (B14, B15, B18 & B19) showed intermediate values between those in the central bundles and peripheral bundles.

Figure 3.4.3-5 shows maximum, average and minimum superheating of all the CETs. Temperature range between the max. and min. values may be due to the radial power profile, three-dimensional (3D) steam flows in the upper core and core exit regions under cooling

effects of colder structures such

as the UCP. All of the CETs were quenched by 1576 s.

(4) Relation between average superheating at CETs and core top region

The peak rod temperature and its location in the core changes with the core water level, and it is difficult to
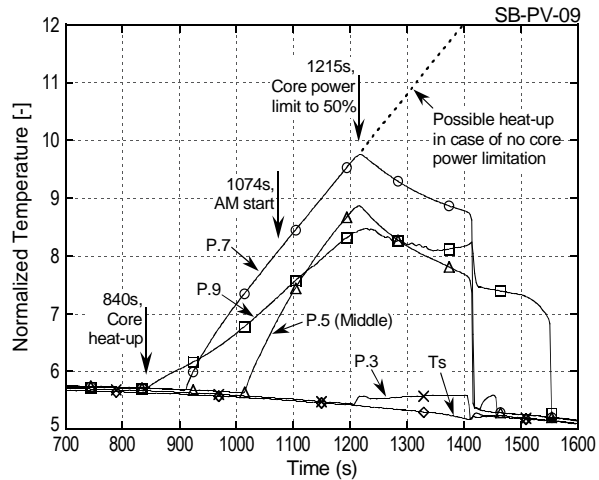
Figure 3.4.3-3 Typical high power rod temperatures (B17) during core heat-up in Test 6-1
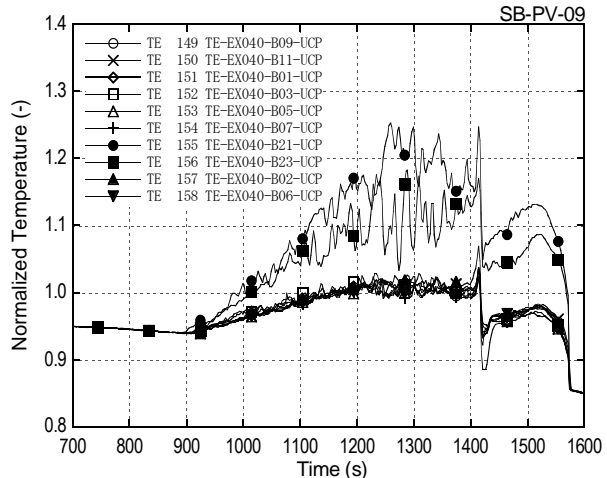
(1) Central and peripheral regions (TE149-TE158)
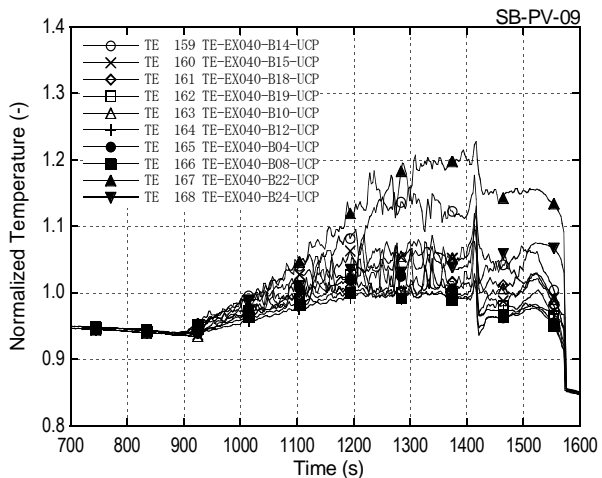
(2) Central and other regions (TE159-TE168)

Figure 3.4.3-4 CET responses during core heat-up in Test 6-1

identify the peak rod temperature and its location by using the CET temperature. On the other hand, the top portion of the core generally shows the earliest superheat than the other core regions and they are nearest to the CETs. Thus, a relation between the average superheats (DT=T-T$_S$ [K]) of CET temperatures [DT$_{AVE}$ (UCP Outlet)] and core top region temperatures [DT$_{AVE}$ (P9)] shown in Figure 3.4.3-6 is obtained for the core heat-up time period of 800-1300 s. A good relation is suggested to exist between DT$_{AVE}$ (UCP Outlet) and DT$_{AVE}$ (P9). A linear correlation; DT$_{AVE}$ (P9)=2.75×DT$_{AVE}$(UCP Outlet), is indicated too except for initial heat-up period. Similar correlation is derived for other tests and discussed in the following Sections 3.3.4 and 3.3.5.

(5) Time delay from core heat-up compared with other SBLOCA tests

A time delay of CETs to detect the criterion temperature was about 230 s after the start of core heat-up (840 s), which consists of an initial time delay of about 70 s until the CET heat-up start, and about 160 s up to the

Figure 3.4.3-5 CET superheats (Max, Ave, Min) in Test 6-1
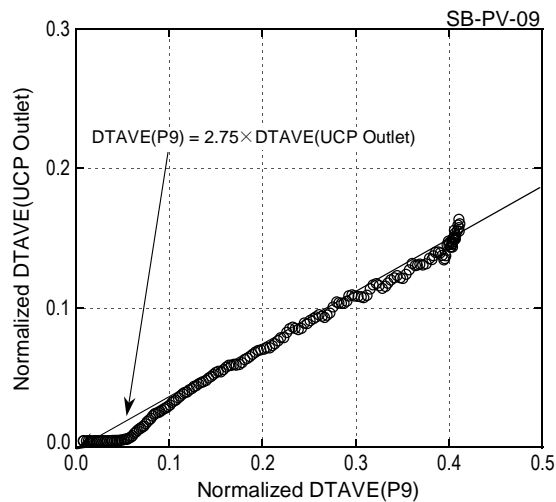
Figure 3.4.3-6 Average superheats at core top region vs. CETs

criterion temperature of 623 K. The initial time delay was compared with that in the 20 former LSTF tests [7] in Figure 3.4.3-7 that indicates a relation between the initiation timing of inadequate core cooling (ICC) (t_{ICC}) and the earliest ICC detection timing by CETs (t_{CET}). All the data are well correlated by the relation; $t_{ICC}=a \times (t_{CET})^b$, where a=0.7603 and b=1.027. The result of Test 6-1 (t_{ICC}=840 s and t_{CET}=910 s) is shown by a thick cross mark, indicating a good correspondence to the former LSTF test results. This means that it generally takes a certain time delay for CETs to detect early stage of core heat-up for LSTF SBLOCA tests irrespective of the location and size of break (5.0-0.5% CLB equivalent). It is confirmed that the initial time delay of 70 s in Test 6-1 is equivalent to those of the 20 former LSTF SBLOCA experiments. The second time delay of 160 s was influenced by a break condition specific to the PV top break as shown below.

Figure 3.4.3-7 Comparison of times at core heat-up start
and its detection by CETs between Test 6-1
and 20 other LSTF LOCA tests (Ref.7)

3.4.3.2 Steam flow chimney effect through control rod guide tubes

Figure 3.4.3-8 compares steam superheat measured at 7 elevations in the core along two simulated fuel rods in high-power bundles with CRGT (B20, rod No.=(6,6)) and without CRGT (B15, rod No.=(2,6)) on top of them [2]; B20(6,6) close to middle-power bundle (B21) and B15(2,6) close to low-power bundle (B03). Steam superheats measured at the inlet and outlet

Figure 3.4.3-8 Evolution of steam and rod surface superheat profiles in two high power bundles with and without CRGT in Test 6-1

(CET) of the UCP above the B15 bundle are also compared. The superheat in rod surface temperature of high-power rod B17(4,4) at 1200s is added for comparison. Due to the limited number of temperature measurements in the fourth core assembly used for Test 6-1, the steam and rod surface temperatures are of different rods with the same linear heat rate.

The steam temperatures in the upper core region (P.8 and P.9) of B15 bundle were always far lower than those in B20 bundle. At 1200 s, the steam temperature difference at P.9 was about 180 K. On the other hand, the steam temperature at P.9 in B20 bundle was a little higher than the rod surface temperature in B17 bundle suggesting that the uprising steam is not readily cooled once heated by the high-temperature rod surface in lower elevation (e.g. rod temperature at P.7). On the other hand, the distorted steam temperature profile in B15 bundle may be ascribed to the outflow of high temperature steam to adjacent bundles with CRGT and inflow of colder steam from peripheral bundles. The highest steam temperature was detected at P.9 in B20 bundle and thus this hot steam should have entered the CRGT above B20 bundle. The CET above B15 bundle detected the low temperature steam. Such a chimney effect that a large portion of steam enters CRGTs without CETs inside and goes towards the PV top break prevailed in Test 6-1, causing the long time delay for the CETs to detect high-temperature steam. It should be noted that the difference of upper core steam temperatures around B20(6,6) and B15(2,6) rods also includes effects of 3D steam flow from the adjacent bundles at lower power level, though the extent of influence may depend on the location of rod with the temperature measurement in each bundle. This point is discussed further in Section 3.4.4(2) for 2.5% CLB LOCA test results shown in Figure 3.4.4-12.

In addition, an average steam velocity at the UCP flow paths was estimated as 0.30-0.19 m/s for Test 6-1 by using an average coolant mass decreasing rate in the PV lower regions during each 50 s in the time period of 800-1200 s ([1], see Table 3.4.5-1). The hotter steam flow in the high power bundles may have focused into the CRGTs at higher steam velocity than this average value, and cooler steam flow in the peripheral low power bundles would have lower steam velocity than this average value. As a general response, the core barrel temperature was significantly lower than steam temperatures in the peripheral low power bundles. The core barrel wall was then gradually heated up by both the relatively high-temperature steam and thermal radiation from the heating rods. The other cold structures in the core such as dummy rods at the core periphery were also heated by hot steam. These structures should have a significant cooling effect especially in the peripheral region during the boil-off process.

3.4.4 Typical CET performance in additional 12 tests

The CET performance in additional twelve ROSA/LSTF experiments [4] is summarized including their diversity and similarity. Some tests include influences of fall-back water with a limited or significant effect on CET performance.

3.4.4.1 CET performance in PV top break LOCA tests

The CET responses in three PV top break LOCA tests with break sizes of 1.0% (SB-PV-07), 0.5% (SB-PV-02, [8]) and 0.1% (SB-PV-08) are compared with that in 1.9% break (Test 6-1, [1,2]). As the break size decreased, the time duration of cycle opening of SG relief valve increased, though the basic trend of core uncovery because of core boil-off was unchanged. CET response relative to the core temperature during the core boil-off was similar among the four cases, including the steam flow chimney effect into CRGTs in the top part of core. However, the effectiveness of the chimney effect became weak as the break size is decreased and negligible in the case of 0.1% break. Instead, the reflux fall-back water becomes significant to the local CET responses and core cooling when break size becomes small; especially less than 1%.

(1) 1.0% PV top break tests without reflux fall-back water

The smaller break size of 1% in SB-PV-07 than 1.9% in Test 6-1 caused a later boil-off start at 1610 s than 840 s in Test 6-1 as shown in Figures 3.4.4-1 and 3.4.4-2. In the 1% top break case, the primary pressure became lower than SG secondary pressure at about 1800 s and reflux cooling remained till about 1850 s. The influence of the reflux fall-back water on CETs was insignificant as shown in Figure 3.4.4-3. The liquid level in the core dropped to the lower region until a little after the HPI actuation at 1926 s.

Typical core heat-up behavior at three elevations (P.9, P.7 & P.5) is shown in Figure 3.4.4-1 and CET temperatures in the center and peripheral regions during core heat-up period are shown in Figure 3.4.4-3. The core and CET heat-up behaviors are compared in Figure 3.4.4-4 in a form of superheat (DT=T-T$_S$ [K]) distribution between DT$_{MAX}$ and DT$_{MIN}$. The core superheat is shown by DT$_{MAX}$, DT$_{AVE}$ and DT$_{MIN}$ at the core top (P.9), and DT$_{MAX}$ at P.8 and P.7 with an envelope of the maximum core temperature. Operator action to start HPI was done at 1926 s by detecting two CET temperatures exceeded 623 K (see Figure 3.4.4-3). Temperature difference between the hottest core (789 K) and CET (623 K) at 1926 s was 166 K. The peak cladding temperature (PCT) was detected as 880.5 K at 2080 s at P.7 of high-power rod B17 (4,4).
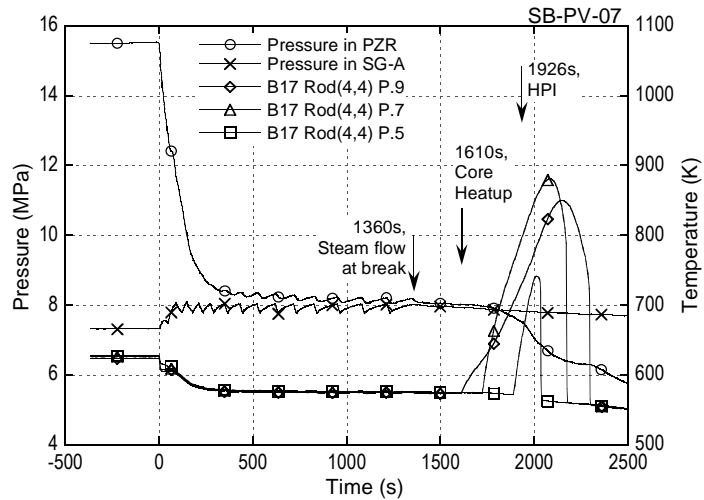
Figure 3.4.4-1 Pressure and typical rod temperatures in 1% PV top break test
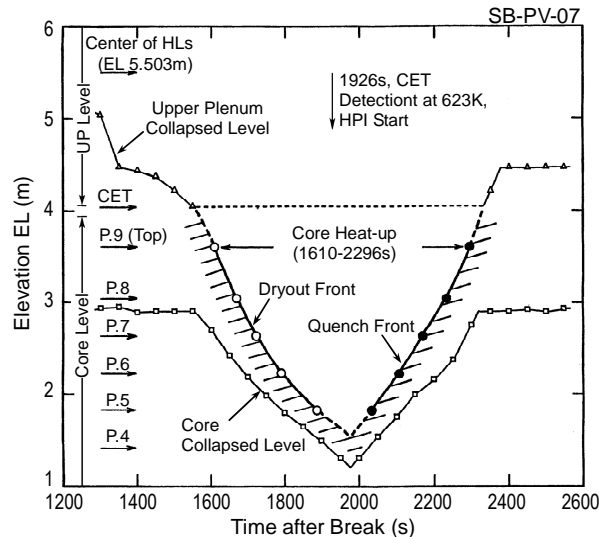
Figure 3.4.4-2 Core heat-up and quench behavior in 1% PV top break test
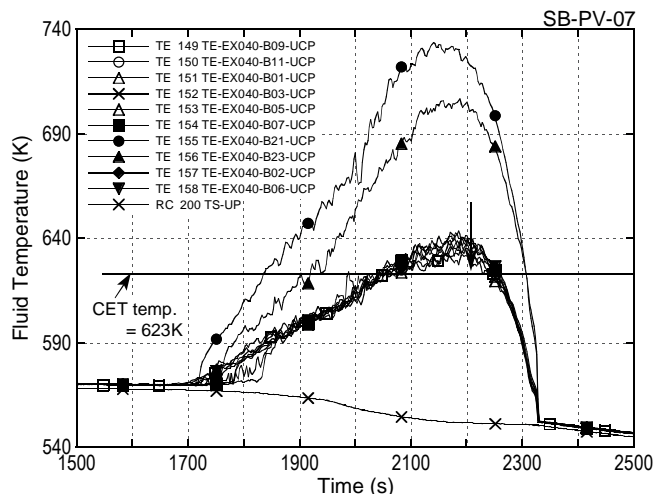
Figure 3.4.4-3 Rep. CET temps. in 1% PV top break test

Similar discrepancy in steam superheats between two high power rods of B20 with CRGT and B15 without CRGT appeared in the 1% top break test (not shown) as in the 1.9% break case shown in Figure 3.4.3-8 suggesting a similar 3D core steam flow with the chimney effect into CRGTs. Temperature difference at P.9 between B20 and B15 rods was 122.5 K at 2000 s and 152.7 K at 2100 s, and was lower than about 180 K in the 1.9% break case probably because of lower core power.

(2) 0.5 and 0.1% PV top break tests with reflux fall-back water

In 0.5% top break test (SB-PV-02), the core heat-up started at 3532 s at high pressure conditions with cycle opening of relief valves in one of two SGs (SG-A). The reflux water which contributed to local core cooling in the HL-A side increased when SGRV opened as suggested by fluid density increase at HL-A bottom in Figure 3.4.4-5.

Figure 3.4.4-6 shows distribution of superheat at the CETs and that of upper core at P.9 and P.8 in the 0.5% PV top break case, similar to Figure 3.4.4-4. The CET temperatures did not reach 623 K due to early HPI actuation at 3930 s. Earlier and higher CET superheat (DT$_{MAX}$) appeared in the HL-B side after 3704 s while no superheat (DT$_{MIN}$=0 K) appeared at CETs and core rods at HL-A side, suggesting the local cooling effects of fall-back water. The steam flow chimney effect into CRGTs was suggested to occur by steam superheat difference between high power bundles with or without CRGT, but was far less than
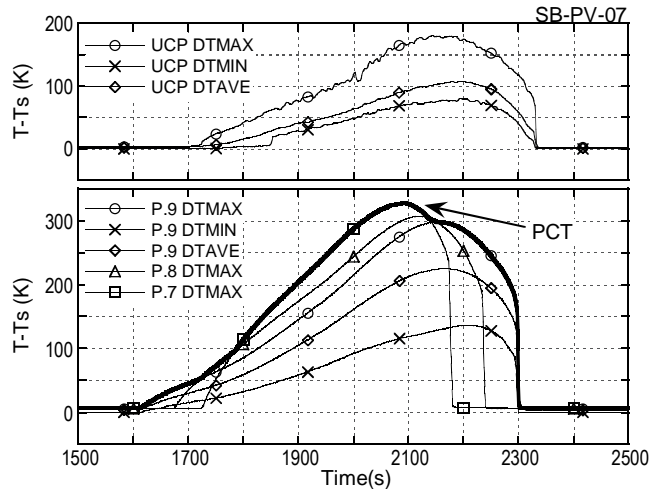
Figure 3.4.4-4 Distribution of superheats at CETs and upper core region during boil-off in 1% PV top break
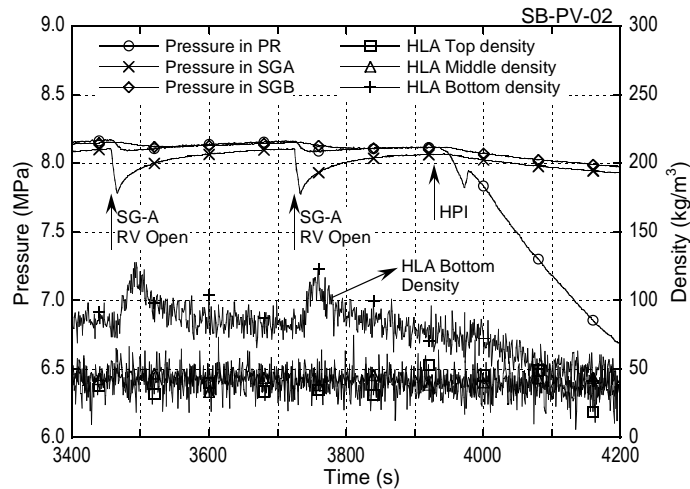
Figure 3.4.4-5 Pressures and hot leg fluid densities affected by SG pressure regulation in 0.5% PV top break test
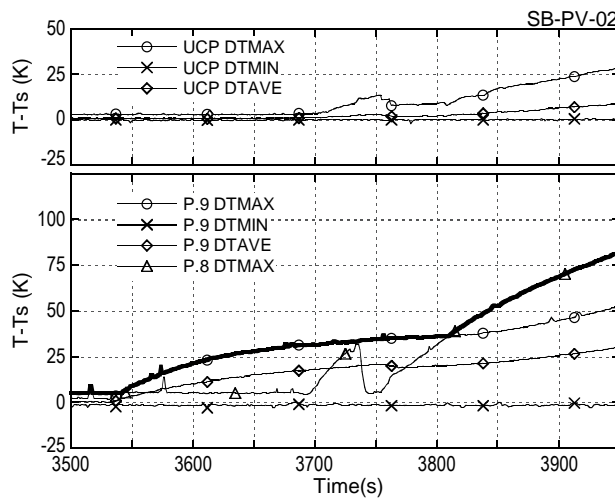
Figure 3.4.4-6 Superheats at CETs and upper core region in 0.5% PV top break test with limited fall-back water

those in 1.0% break test shown above [2].

Figure 3.4.4-7 shows distribution of superheat at CETs and upper core
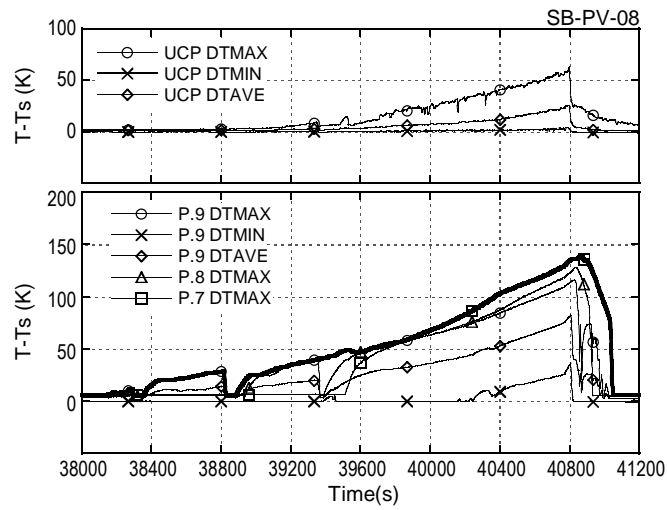
Figure 3.4.4-7 Superheats at CETs and upper core region in
0.1% PV top break test with limited fall-back water

region in the 0.1% PV top break case (SB-PV-08). Similar to the 0.5% break case, the primary pressure was controlled by the cycle opening of relief valves of SG-A and reflux water temporarily came down to UCP and core. The reflux water cooled the core, not only the CETs in the 0.1% break case during the long term transient. The CETs were significantly influenced by the fall-back water, showing later and smaller heat-up. The steam flow chimney effect into CRGTs on high power rod superheat was not observed in this 0.1% break case.

3.4.4.2 Effects of break size on CET performance in cold leg break LOCA tests

The CET responses in three cold leg break (CLB) LOCA tests with break sizes of 10% (SB-CL-09, [9]), 2.5% (SB-CL-01) and 0.5% (SB-CL-24, [10]) are summarized. Typical phenomenon in the CLB LOCA is the two core heat-ups during loop-seal clearing (LSC) and core boil-off.

(1) Fast blowdown and no CET indication for core heat-up in 10% CLB test

The 10% CLB LOCA test (SB-CL-09) [9] showed the fast primary depressurization as shown in Figure 3.4.4-8. The core heat-up shown in Figures 3.4.4-8 and 3.4.4-9 started at 67 s at the core middle elevation (P.5) during the LSC and the resulted high core temperature caused core power trip at 111 s; a little after the primary pressure became lower than the SG secondary side pressure at about 100 s. The PCT of 930 K was detected at P.6 of high power rod in this test. No CETs showed heat-up during the core heat-up period as shown in Figure 3.4.4-9 because of significant fall-back water from hot legs under downward core flow condition during the LSC. Figure 3.4.4-10 shows typical propagation of dryout and quench fronts of several rods. The influences of fall-back water appear clearly as top-down quench in the low-power peripheral region in the core. The 10% CLB LOCA does not need AM action based on the CET heat-up because of the very rapid transient, but indicates the influence of remaining coolant at UCP on CET responses.
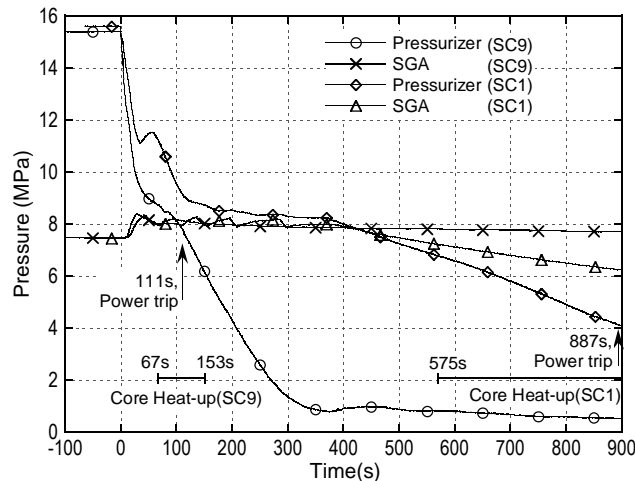
Figure 3.4.4-8 Primary and secondary pressures in 10
and 2.5% CLB tests

(2) CET responses for core heat-up in 2.5% CLB test (SB-CL-01)

The primary pressure in 2.5% CLB test (SB-CL-01) shown in Figure 3.4.4-8 became lower than the secondary pressures after 440 s causing no reflux fall-back water during the core heat-up period after 575 s. The LSC at 360 s had less influence on core heat-up except though there was a temporary and small core level depression and rod temperature increase at the upper core region. During the boil-off, the dryout region extended to P.4 below the core middle height. The highest cladding temperature was 923 K for core protection at 887 s observed at P.7 of high power rod, though the accumulator started at 850 s which finally cooled the whole core by 1086 s.

Figure 3.4.4-11 compares distribution of superheats at CETs and upper core region. The CET heat-up started at 629 s and the earliest CET temperature reached 623 K at 790 s when the maximum rod temperature was 805 K showing a temperature difference of 182 K. The latest CET heat-up was observed in the peripheral region at about 770 s. The average superheat of CETs (UCP DT_{AVE}) was well related to that of core top (P.9 DT_{AVE}) as shown in Section 3.4.5(3-3).

Axial steam superheats in high power bundles with CRGT (around B20(6,6) rod) or without CRGT (around B15(2,6) rod) are compared in Figure 3.4.4-12, similar to Figure 3.4.3-7 for Test 6-1 in Section 3.4.5(2). During the core boil-off,
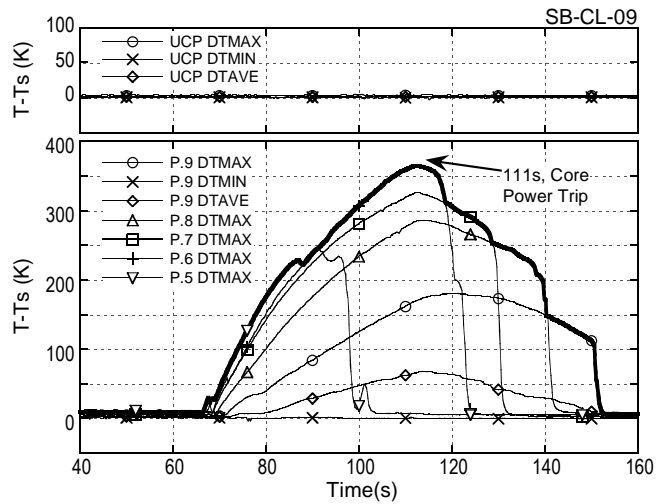
Figure 3.4.4-9 Distribution of superheats in upper half core and no CET heat-up in 10% CLB test
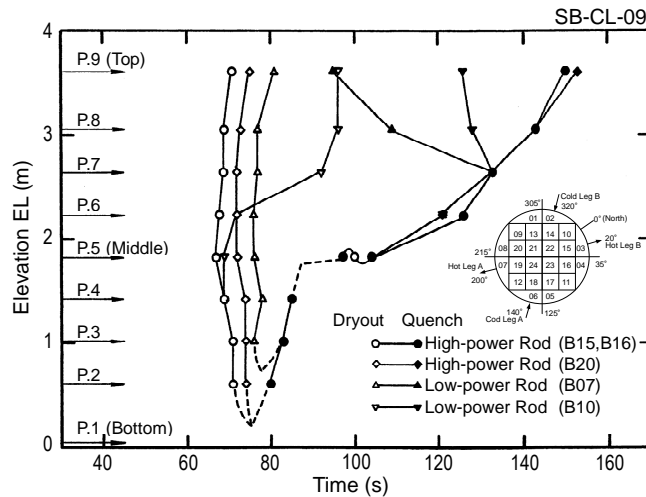
Figure 3.4.4-10 Variety of rod heat-up and quench behavior in 10% CLB test
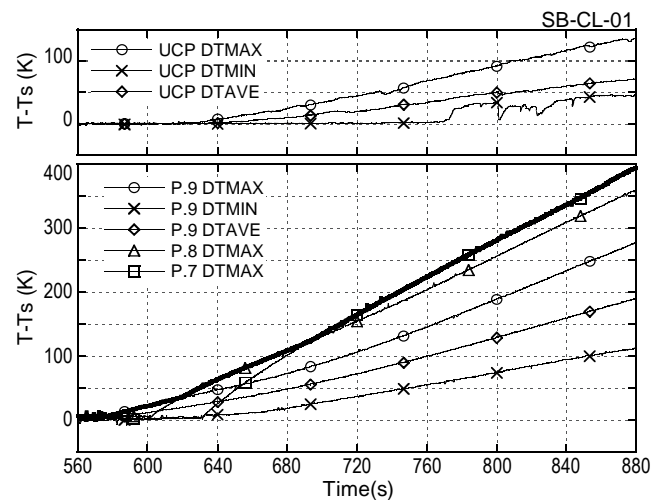
Figure 3.4.4-11 Distribution of superheats at CETs and upper core region during core boil-off in 2.5% CLB test

94

temperature difference appeared between these bundles, but the difference was far smaller than that observed in Test 6-1 probably because the chimney effect through the CRGTs is negligible in the CLB LOCA.
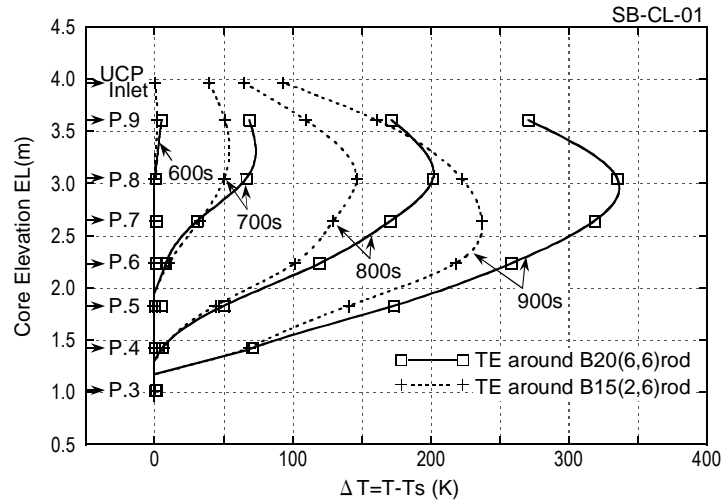
Figure 3.4.4-12 Comparison of steam heat-up behavior in two high power bundles in 2.5% CLB test

However, this result is important that 3D steam flow that causes such temperature distribution in high power bundles surely exists in the core under significant influences of steam cooling by the peripheral low power bundles and low-temperature structures.

(3) Core heat-up detection in 0.5% CLB test (SB-CL-24) with three AM actions

This test is characterized by a small size CLB with early AM action (600 s) to depressurize the SG secondary sides to achieve primary cooling at a rate of -100 K/h and also by repeated LSCs prior to the initiation of major core boil-off. Each LSC caused temporary and limited heat-up at the upper core region while no heat-up was detected by the CETs during each short period of time. The primary loop was pressurized in later phase of the test due to loss of secondary coolant as shown in Figure 3.4.4-13.

Intermittent opening of RV at two SGs as the first AM action, and rapid primary depressurization as the second and third AM actions were taken in the later phase of transient (5000- 8000 s) as shown in Figure 3.4.4-13. The core heat-up (5929-7675 s) took place because of core boil-off as shown in Figure 3.4.4-14, followed by the second and third AM actions for the primary depressurization. There was reflux water fall-back on the CETs during the core heat-up period because the SG secondary pressures were lower than the primary pressure. The core power was finally limited after 7109 s for protection of heater rods from
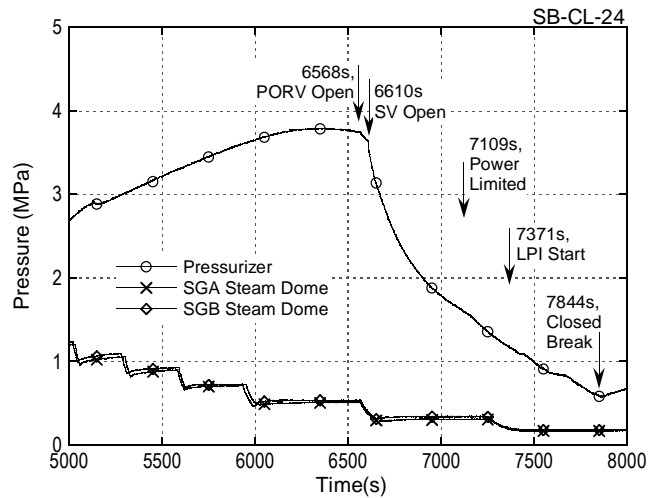
Figure 3.4.4-13 Primary and secondary pressures during boil-off in 0.5% CLB test
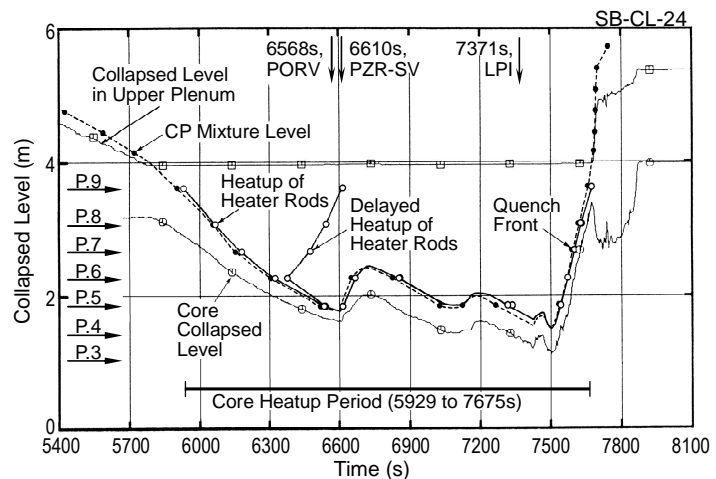
Figure 3.4.4-14 Core heat-up and quench behavior in 0.5% CLB test
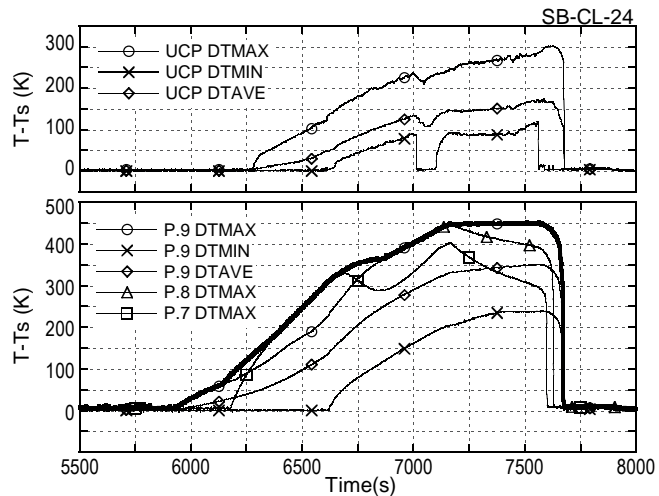
Figure 3.4.4-15 Distribution of superheats at CETs and upper core region in 0.5% CLB test

96

further heat-up. The LPI was started at 7371 s for core cooling.

A significant delay appeared in the core heat-up at both hot leg sides by the effect of reflux water fall-back until the second AM action. The delay in the CET temperature increase happened too above the affected core regions. On the other hand, the rapid primary depressurization by the second and third AM actions at the pressurizer caused significant steam generation with a temporary level increase in the core. As a result, uprising steam flow in the core and upper plenum almost stopped the fall-back water onto CETs and core, enhancing the temperature increase in the CETs as shown in Figure 3.4.4-15. The average CET superheat (UCP DT_{AVE}) was well related to the average rod superheat at core top (P.9 DT_{AVE}) irrespective of the local fall-back water effects on both CETs and core top (see Figure 3.4.4-21).

3.4.4.3 Significant fall-back water effects on CETs during SG depressurization action and improved responses after PORV opening in 0.2% PV bottom break test

Core boil-off started after a long transient and significant influences of reflux fall-back water on CET responses appeared in the 0.2% PV bottom break LOCA test (SB-PV-03). The SG depressurization was initiated at 945 s to cool the primary system at a rate of -55 K/h. The primary depressurization, however, was degraded after 7190 s as shown in Figure 3.4.4-16 because non-condensable (nitrogen) gas from accumulator tanks accumulated in the SG U-tubes. The core heat-up due to boil-off started at 8573 s and the core power was lowered to 10% of decay power at 9200 s to limit the further heat-up as also shown in Figure 3.4.4-16. Whole core was quenched until 9680 s by the LPI actuated at 9280 s. The dryout front of heater rods in high-power bundles (B13 and B17) shown in Figure 3.4.4-17 indicates the earliest heat-up straightly corresponding to the core mixture level transient while that of other rods in peripheral low-power bundles (B03 and B08 located below the hot leg nozzles) showed significantly delayed heat-up indicating the influences of reflux fall-back water. It should be noted that such locally-cooled rods generated saturated steam that rose up contributing to maintain steam in saturated condition at the CETs. All the heater rods started heat-up after the third AM action to fully open the PORV at 9060 s, which was partly related to the CET response.

Figure 3.4. 4-18 shows all CET temperatures during the core heat-up period. The CET temperature started to rise after upward superheated steam flow was established by the PORV full-open. Thus, the CET performance to detect core heat-up was significantly limited by the reflux fall-back water during the SG depressurization action, and was clearly improved by sudden increase in the uprising steam flow induced by the PORV open action as the third AM action.

Figure 3.4. 4-18 shows all CET temperatures during the core heat-up period. The CET temperature started to rise after upward superheated steam flow was established by the PORV full-open. Thus, the CET performance to detect core heat-up was significantly limited by the reflux fall-back water during the SG depressurization action, and was clearly improved by sudden increase in the uprising steam flow induced by the PORV open action as the third AM action.

3.4.4.4 Break location effects on CET performance

Three LOCA tests with different break locations but with the same break sizes of 0.5% CLB equivalent are compared; hot leg break (SB-HL-05, SH5), PV bottom break (SB-PV-01, SP1) and TMI-type (AT-SB-03, SB3). These three tests cover both highest and lowest break locations in the primary system as extreme boundary conditions, considering that the break location controls primary coolant discharge rate and thus depressurization rate in SBLOCAs under gravity control.

Figure 3.4.4-19 compares the primary pressures of three tests with major event timing. The earliest core heat-up in SB-PV-01 started at 1498 s due to large mass discharge rate mostly by subcooled water from the lower plenum until about 2000 s. The last heat-up occurred at 5517 s in AT-SB-03 because steam apt to
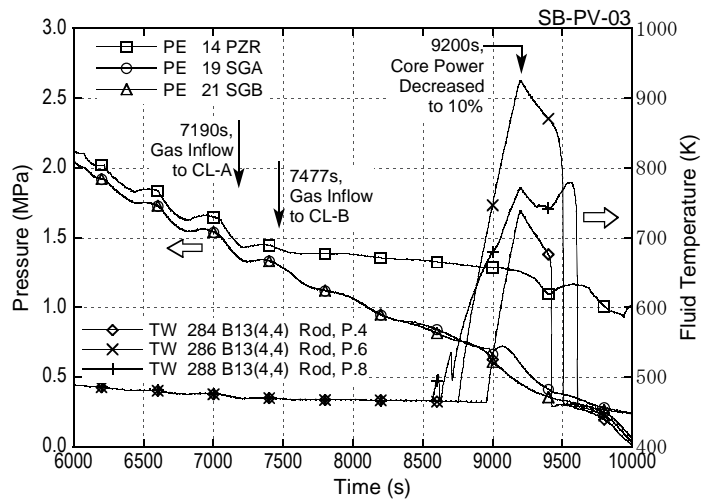
Figure 3.4.4-16 Degraded primary depressurization under AIS gas inflow and rod temperatures in 0.2% PV bottom break test
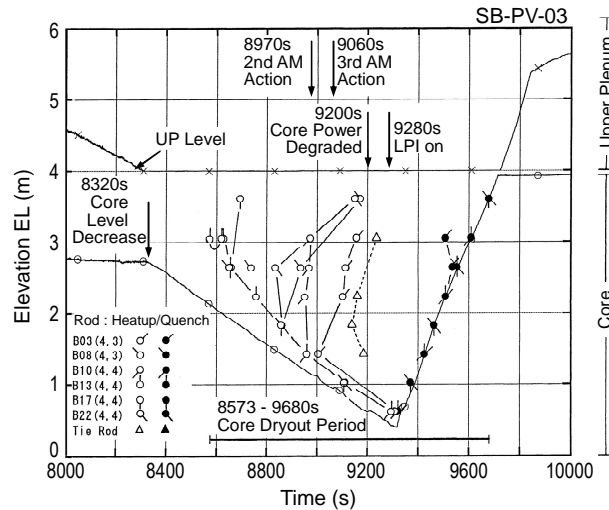
Figure 3.4.4-17 Local core cooling by fall-back water in 0.2% PV bottom break test
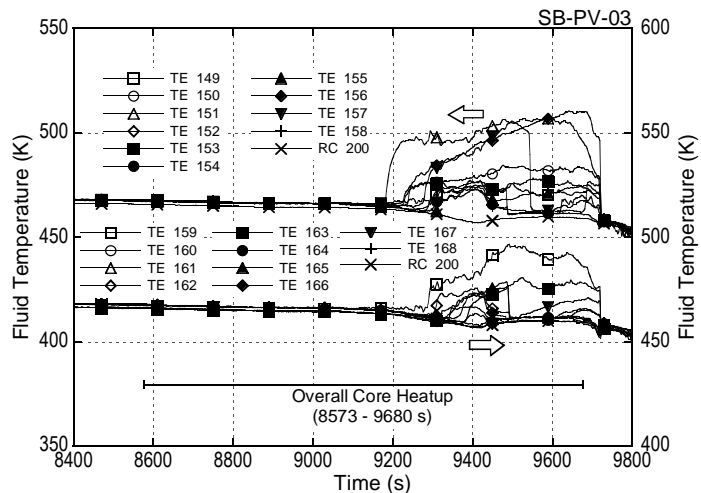
Figure 3.4.4-18 No CET heat-up by fall-back water until PORV open in 0.2% PV bottom break test
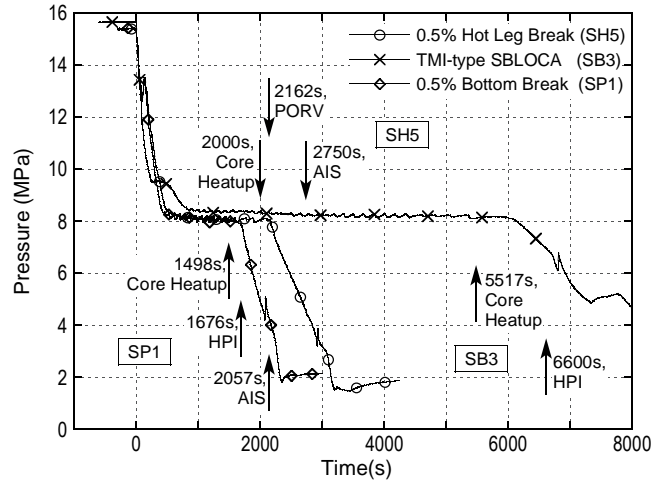
Figure 3.4.4-19 Primary pressures in 0.5% HLB, PV bottom break and TMI-type LOCA tests
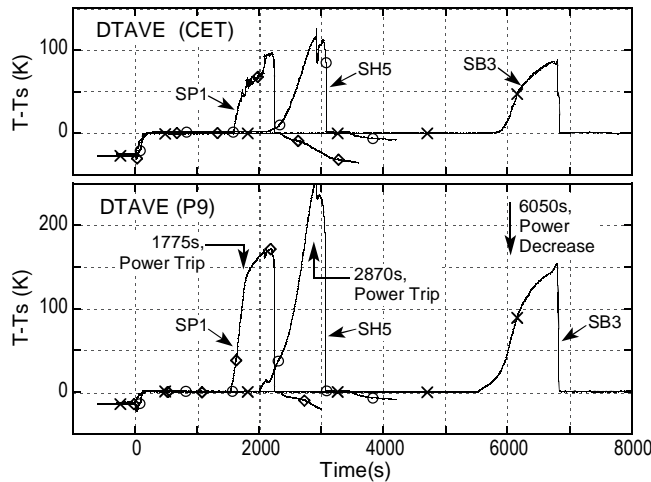
Figure 3.4.4-20 Average superheats at CETs and core top region in 0.5% HLB, PV bottom break and TMI-type tests

99

be discharged, leaving coolant in the primary loop. The core heat-up in SB-HL-05 occurred at 2000 s as an intermediate case where water discharge turned into steam discharge at about 1500 s. An operator action to fully open the PORV was initiated at 2162 s in SB-HL-05 by using the hot leg superheat (T_S + 5 K) as an indicator. The primary pressure rapidly decreased afterwards. Though the core heat-up timing is different in these three tests as above, the core heat-up occurred at similar primary coolant mass inventories [8].
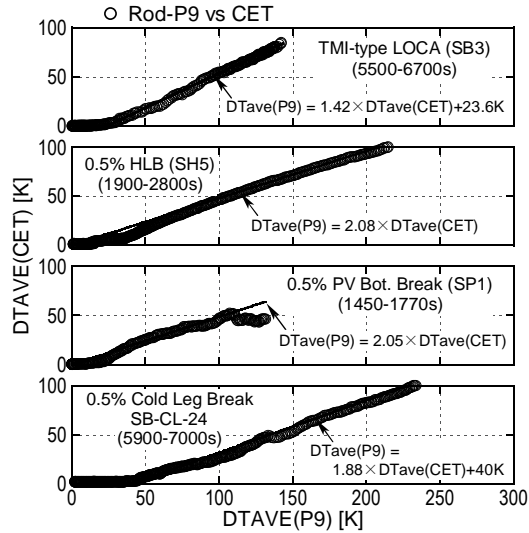
Figure 3.4.4-21 Comparison of relations between average super- heat at CET and core top rod in 0.5% HLB, CLB, PV bottom break and TMI-type

The CETs in each test detected superheat during each core heat-up period as shown in Figure 3.4.4-20 that compares average superheats at CETs ($DT_{AVE}(CET)$) and core top region ($DT_{AVE}(P9)$) in three tests. The core heat-up in each test was limited by terminating or limiting core power and the core was cooled afterwards by HPI or AIS. Figure 3.4.4-21 shows relations between the average superheat at CETs and core top region for these three tests in comparison with that in 0.5% CLB test (SB-CL-24). These showed that CETs successfully detected steam superheating, though with a certain time delay and CETs temperature difference under limited influences of reflux fall-back water. Similar CET
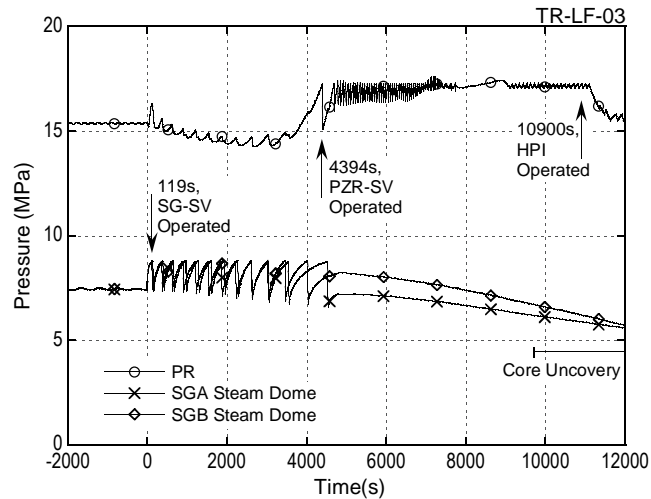
Figure 3.4.4-22 Primary and secondary pressures in station blackout scenario transient test

responses were derived irrespective of their break locations. In the 0.5% PV bottom break test (SP1), however, the CET temperature difference from the heating-up core increased at high-temperature region when steam generation became almost zero because of the whole core uncovery.

3.4.4.5 CET performance in two transient tests under extremely high or low pressure conditions

(1) Station blackout (TMLB') scenario test (TR-LF-03)

The primary system was initially cooled by cycle opening of SG safety valve (SV) but started pressurization at about 3600 s as shown in Figure 3.4.4-22 when the SG secondary coolant was almost lost. The cycle opening of pressurizer (PZR) SV after 4394 s caused gradual loss of primary coolant mass, leading to core heat-up at 9657 s due to boil-off. The CETs detected superheat at 9780 s with a time delay

of 123 s after core heat-up start with a temperature distribution as shown in Figure 3.4.4-23. The saturation temperature (T_S = 626 K) is higher than 623 K at such high pressure. The average superheating of CETs was well related to that of core top region in this test too, as shown in Figure 3.4.5-1, and a difference between these two superheats in this test is the least among the compared eleven LSTF tests. The CET superheat (DT=T-T_S) should thus be useful for core heat-up detection.

(2) Loss-of-RHR during mid-loop operation (TR-RH-06)

This test was started at primary pressure of 0.11 MPa, water level at HL middle height, HL coolant temperature at about 333 K and constant core power of 0.38 MW (0.5% of 1/48-scaled PWR rated power to simulate 1.5 day after the reactor shut-down). The primary pressure started to increase at 1250 s after boiling start in the core resulting in steam discharge through an open manhole at PZR, and finally core heat-up started at 9045 s at 0.15 MPa (T_S=384 K) as shown in Figure 3.4.4-24.

The earliest CET heat-up started at about 9800 s as shown in Figure 3.4.4-25, which was 755 s after the core heat-up start, and the last one was 390 s later than the earliest one. The CET temperature increase rate was significantly lower than that of core top region under the extremely low saturation temperature condition. The CET temperature did not reach the criterion of 623 K. AFW and HPI were thus respectively initiated at 9830 s and 10340 s based on monitored core temperature. This result may suggest that the superheat of CET (DT) is suitable for the core heat-up detection instead of a certain constant value such as 623 K. The significant delay of CET heat-up resulted due to reflux fall-back water during the gradual primary pressurization process (subcooled water existed only in the HL-B bottom) and also by the significantly higher steam velocity at the core exit as shown in Table 3.4.5-1.

3.4.5 General CET performance in LSTF experiments

CET performances observed in the thirteen LSTF tests are summarized below being related to an average volumetric flux of steam flow at the core exit, fall-back water effects and delay of time and temperature increase from core heat-up.

(1) Rather stagnant steam flow during core boil-off in most of SBLOCA tests

Steam is generated below mixture level in the core under influences of core decay power, local cooling of rods by fall-back water above mixture level, stored heat release from metal structures and flashing under depressurization. An average steam velocity (V_G [m/s]) at the UCP with flow area of 0.08558 m^2 during core boil-off of each test was estimated in Table 3.4.5-1 considering above factors for all the experiments to study the uprising steam condition except for the 10% CLB test in which downward flow is dominant. The obtained results reveal that the steam velocity was very small; typically around 10 to 30 cm/s and less than 0.6 m/s in most of LSTF tests except for the case of Loss-of-RHR (TR-RH-06) test with the velocity more than 1.5 m/s under atmospheric pressure.
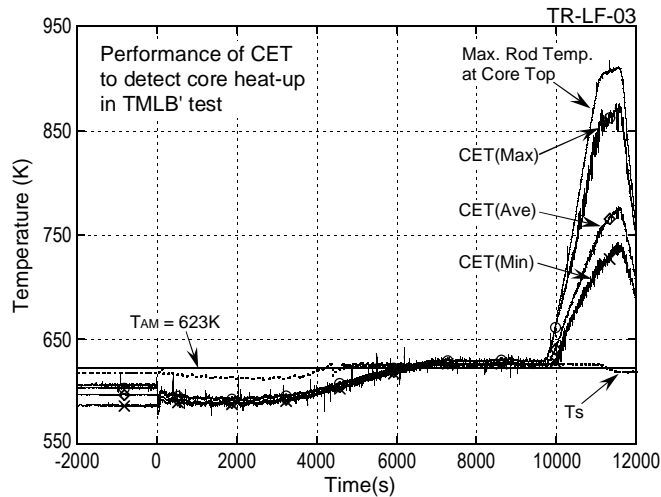
Figure 3.4.-23 CET temperature distribution and maximum core top region temperature in station blackout scenario test
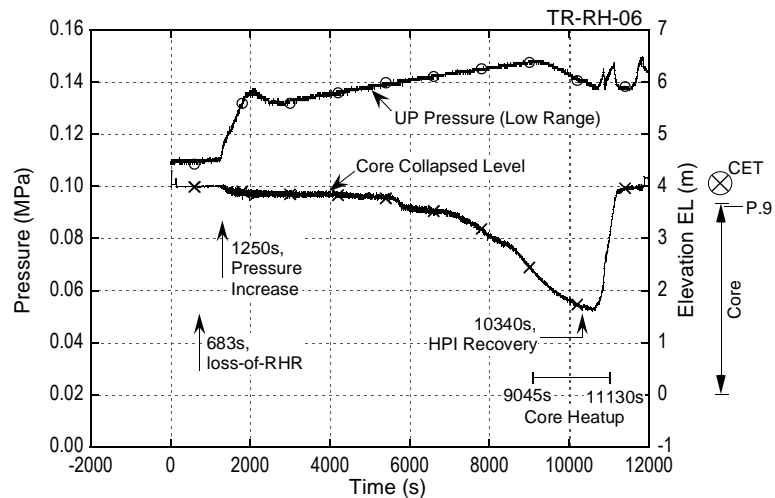
Figure 3.4.4-24 Primary pressure and core collapsed water level in loss-of-RHR transient test
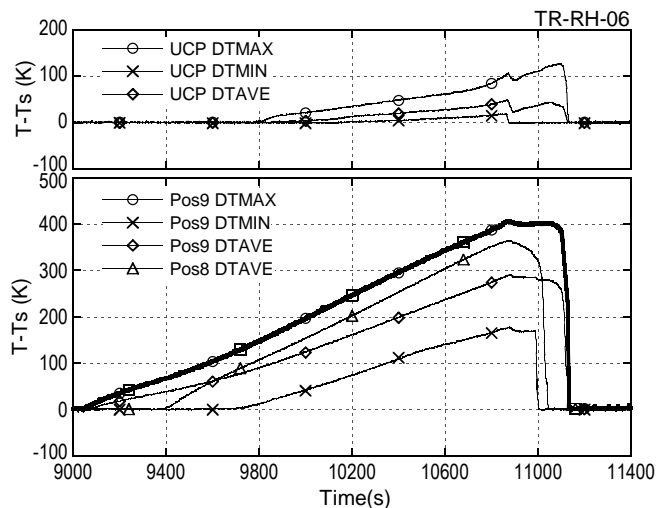
Figure 3.4.4-25 Distribution of superheats at CETs and upper core region in loss-of-RHR transient test

102

Under such low-velocity conditions, 3D steam flow would be apt to emerge in the core and around the core exit even with small driving force. Several factors that may cause such 3D steam flow include (a) radial power profile, (b) cooling effect by low-temperature structures [5] and (c) CRGT-chimney effect for PV top break LOCA. The steam temperature distribution in the core and the core exit under influences of such 3D steam flows is clearly observed in both CLB LOCA and PV top break LOCA tests respectively shown typically in Figures 3.4.4-12 and 3.4.3-7.

Table 3.4.5-1 Average steam velocity at core exit during core boil-off in ROSA/LSTF tests

Test ID	Time (s)		Primary Pressure (MPa)	Total Power Q_T (MW)	Core Mix. Level EL (m)	Av. Steam Flow Rate W_G (kg/s)	Steam Velocity[1] V_G (m/s)	Case[2]
	Heat-up Period	Δt						
Test 6-1(1)	800-1200	50	7.6-5.4	1.59-1.46	3.66-1.05	0.92-0.32	0.30-0.19	C
SB-PV-07	1600-1950	50	7.9-7.4	1.37-1.28	3.68-1.61	0.74-0.43	0.20-0.13	C
SB-PV-02	3500-3900	100	8.1	1.06-1.02	3.66-2.81	0.73-0.65	0.20-0.18	B
SB-PV-08	38000-40600	200	8.0	0.55-0.54	3.66-2.07	0.38-0.30	0.10-0.08	B
SB-CL-01	600-900	100	6.6-4.3	1.57-1.46	3.05-1.05	0.76-0.22	0.28-0.11	A
SB-CL-24	6000-7100	100	3.8-1.5	0.88-0.82	3.58-1.83	0.51-0.28	0.39-0.23	A/B/C
SB-HL-05	2000-2700	100	8.1-4.2	1.21-1.13	3.61-1.09	0.82-0.55	0.29-0.22	A/B/C
SB-PV-01	1500-1660	20	8.2-8.1	1.30-1.27	3.05-0.00	0.72-0.03	0.22-0.01	B
SB-PV-03	8600-9200	200	1.3	0.80-0.79	2.89-0.81	0.35-0.24	0.62-0.44	B
AT-SB-03	5500-6700	400	8.0-6.6	0.94-0.23	3.66-1.05	0.61-0.06	0.17-0.02	A/B
TR-LF-03	9500-11000	500	17.2-17.3	0.95-0.92	3.66-0.80	0.87-0.14	0.08-0.01	A
TR-RH-06	9000-10500	500	0.14	0.38	3.66-1.98	0.16-0.11	2.35-1.59	A

[1]   Average steam velocity at upper core plate flow path (A=0.08558 m^2)

[2]   Case A: W_G is determined by core power under mixture water level during a time period of Δt (s).

Case B: Mean value of W_G and a steam flow rate determined by Q_T under fall-back cooling.

Case C: W_G is determined by average coolant mass decreasing rate in core, lower plenum and downcomer during a time period of Δt (s) in case of fast depressurization conditions.

Case A/B/C uses three cases corresponding to each time period in one test.

(2) Effects of fall-back water on CET performance during core heat-up

Table 3.4.5-2 summarizes conditions of fall-back water for all the tests. No or almost no fall-back water condition designates "No" for three tests; Test 6-1, SB-PV-07 and TR-LF-03. Significant fall-back water condition designates "Yes" for two tests; SB-CL-09 during LSC process and SB-PV-03 under SG depressurization. The SB-PV-03 test, however, showed superheat detection by CETs when uprising steam flow was induced after the PORV was opened as an operator action. Limited effects of reflux fall-back water designate "Ltd". In the "Ltd" cases, reflux coolant from hot leg(s) was effective only in a short time during core heat-up process or in a local domain of UCP or core allowing the superheat detection by remaining CETs. The CET superheat detection behavior related to the core top heat-up presented in Figure 3.4.5-1 is summarized for the cases of "No" and "Limited (Ltd)".

Table 3.4.5-2 Summary of CET performance on delay of time and temperature from core heat-up in ROSA/LSTF tests

Test ID	Fall-back Ef.*1	Time of Events (s)				$a \times B^b/A$ (-)[7]	C_1 in Eq(2)	C_2 in Eq(2)	T (K) at Time C	
		A: Core Heat-up	B: CET Heat-up	B - A	C: CET at 623 K				T_{max}*2 in Core	T_{max}*2 - T_{CET}
Test 6-1[1]	No	840	910	70	1074	0.99	2.75	-	-	190
SB-PV-07	No	1610	1722	112	1926	0.99	1.98	28.1	789	166
SB-PV-02	Ltd	3532	3704	172	(4180)	1.00	1.47	16.9	(658)*2	(58)
SB-PV-08	Ltd	38140	39125	985	40760	1.04	1.96	28.9	694	71
SB-CL-09	Yes	67	-	-	-	-	-	-	(930)*2	(364)
SB-CL-01	Ltd	575	629	54	790	0.99	2.15	26.0	805	182
SB-CL-24	Ltd	5929	6280	351	6536	1.02	1.88	40	781	158
SB-HL-05	Ltd	2000	2110	110	2606	0.99	2.08	-	749	126

SB-PV-01	Ltd	1498	1586	88	1612	0.98	2.05	-	732	109
SB-PV-03	Yes	8573	(9182)	(609)	-	-	-	-	(925)*2	(437)
AT-SB-03	Ltd	5517	5850	333	5996	1.02	1.42	23.6	698	75
TR-LF-03	No	9657	9780	123	-	0.99	1.58	-	(902)*2	(60)
TR-RH-06	Ltd	9045	9800	755	-	1.06	3.85	120	(926)*2	(449)

*1 Fall-back water effects on CET responses are noted by Yes, No or Limited (Ltd) in time or local domain.

*2 T_{max} in bracket is a maximum core temperature when CET did not reach 623 K.

(3) Similarity and diversity of CET performance during SBLOCAs and transients

(3-1) No CET heat-up under significant fall-back water in two cases

No CET heat-up was observed in two LOCA tests simulating 10% CLB (SB-CL-09) and 0.2% PV bottom break (SB-PV-03) under SG depressurization action. In these tests, fall-back water significantly limited the CET heat-up as well as local core cooling. In SB-PV-03, the CETs became to detect superheat at 9182 s (609 s after the core heat-up start) after the uprising steam flow was induced in the core due to PORV opening at 9060 s.

(3-2) General CET responses for time delay from core heat-up

Table 3.4.5-2 shows times of core heat-up start (A, t_{ICC} [s]), CET heat-up start (B, t_{CET} [s]), CET heat-up to 623 K (C) and a time delay of (B-A) for each test. The delay time seems to depend on break size and varies from the shortest of 54 s in the 2.5% CLB LOCA test to the longest of 985 s in 0.1% PV top break LOCA test. These times of A and B, however, are well correlated by the following equation [7] as,

$$t_{ICC} = a \times (t_{CET})^b ,\qquad\qquad\qquad (1)$$

where a=0.7603 and b=1.027, within an uncertainty of ± 6%, except for 10% CLB LOCA test and 0.2% PV bottom break LOCA test (see Table 3.4.5-2 & Figure 3.4.3-7).

A time delay of (C-A) in each test also shows diversity from the shortest of 114 s in 0.5% PV bottom break LOCA test to the longest of 2620 s in 0.1% PV top break LOCA test. It was found that the CET heat-up rate depends not only on the break size but also on the core heat-up rate which was affected by the water level decreasing rate and the time to start core heat-up (A). In the 0.5% PV bottom break LOCA test, the core uncovery region extended to middle elevation only in 34 s after the core boil-off start because of the water discharge from the lower plenum.

(3-3) General temperature discrepancy between CETs and core

As shown in Section 3.4.3.1 (4), superheats of the average CET temperature ($DT_{AVE}(CET)$) and average core top region temperature ($DT_{AVE}(P9)$) are generally related in a linear relation for most of the tests except for the 10% CLB LOCA test and 0.2% PV bottom break LOCA test (see Figure 3.4.5-1 & Table 3.4.5-2) as,

$$DT_{AVE}(P9) = C_1 \times DT_{AVE}(CET) + C_2 , \qquad\qquad (2)$$

where C_1 varies from 1.4 to 2.8 (1.93 in average) for ten tests except for TR-RH-06 test with C_1 of 3.85 under extremely low pressure condition, and C_2 varies from 0 to 40 K for ten tests except for TR-RH-06 test in which C_2 is as large as 120 K. Similar relation exists for most of the tests irrespective of significantly different heat-up timing or time delay of (B-A) including a few tests with limited fall-back water effects. These relations indicate that the temperature discrepancy of the CETs from the core top region generally increases with time, if the core heat-up region extends toward the middle of core with higher linear heat rate.

A large temperature discrepancy was observed between the maximum temperatures (T_{max}) of CETs and whole core as shown in Table 3.4.5-2. When the CET was heated up to 623 K, the maximum rod temperature was 70-190 K higher than it for eight tests. The peak cladding temperatures (PCT) in three tests (two tests with no CET heat-up and TR-RH-06 test under extremely low pressure condition) were significantly higher by about 360-450 K than CET temperatures when PCT reached limiting temperature of 923 K for protection.

(3-4) Need of CET superheat indication for AM action in case of extremely high or low pressure boil-off conditions

Steam superheating in place of constant CET threshold temperature would be preferable in abnormal transient with extremely high or low pressure boil-off. In the station blackout test, CETs prior to heat-up were at a saturation temperature higher than the AM setpoint temperature of 623 K. On the other hand, in the loss-of-RHR test, the initial saturation temperature was far lower than 623 K and the CET temperature increasing rate was significantly lower than that of core top region, resulting in no arrival of CET temperature to 623 K during the test period. In these cases, CET superheat indication would be helpful
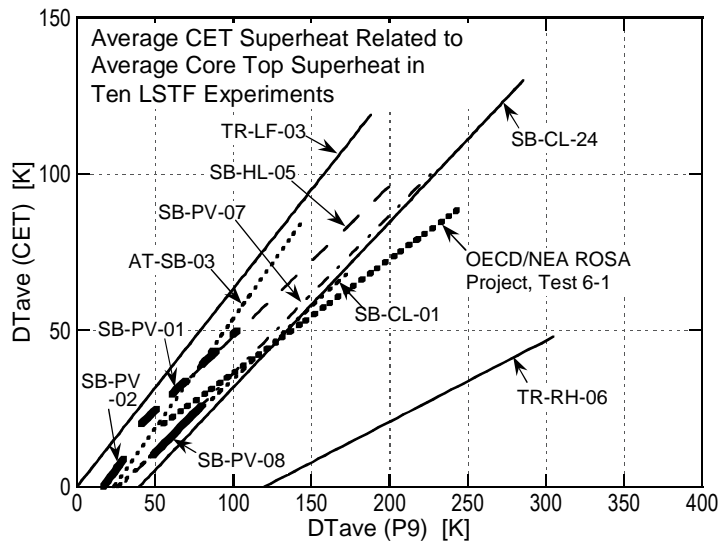
Figure 3.4.5-1 Comparison of relations between average superheats of CETs and core top region in Test 6-1 and 10

for operators instead of the absolute CET temperature.

(4) Reasons for time delay and temperature discrepancy from heating-up core

Following conditions are clarified that may cause for CETs time delay to detect superheat and temperature discrepancy from the heating-up core for the 13 LSTF tests [2, 5].

    (a) In smaller break size cases, time delay from core heat-up will be longer as the average steam velocity decreases with decay heat due to the later initiation of core boil-off.

    (b) Cold metal structures at the core exit (such as UCP, upper nozzles and core barrel in the peripheral region) as well as low temperature rods at the core top decrease steam temperature as steam rises from heating-up core.

    (c) In a special case of PV top break LOCA, hot steam preferentially flows into CRGTs due to their chimney effects, which increase a delay in CET heat-up because of its measuring location around CRGTs.

    (d) In loss-of-RHR transient under atmospheric pressure, high speed steam flow causes low steam superheat leaving large temperature discrepancy between core top region and steam at the CETs.

    (e) The CET temperatures depend on fall-back water conditions and radial power profiles in the core.

3.4.6 Applicability of LSTF/CET performance to PWR conditions

The applicability of the LSTF test results to the reference PWR is briefly discussed concerning the following four points.

(1) Volumetrically-scaled steam generation in core as a basic factor

Thermal hydraulic factors such as the core power and PV coolant inventory in the LSTF are well volumetrically scaled as well as the scaled break size to simulate real-time transient. The steam generation rate in the core during boil-off in the reference PWR is thus well simulated in the LSTF experiments, though the metal stored heat per unit fluid volume, mostly of pressure vessel, is relatively large compared with that for PWR. Since the flow area of the core and UCP in the LSTF are both volumetrically scaled to those of the reference PWR, average steam velocity at these regions during core boil-off should be equivalent to that of the reference PWR.

(2) Steam cooling effect by colder structures around core exit

The reference PWR is furnished with internal structures at and above the active core region, which include the UCP, upper nozzle (End-box), No.9 spacer, gas plenum region of each fuel rod and core barrel in the core peripheral region. These structures are almost simulated in the LSTF by the same elevation (see Figures 3.4.2-1 and 3.4.2-2) and 1/48-scaled total flow areas. Instead of the gas plenum of each fuel rod, the LSTF heater rods have non-heating part above the top of heating region. Steam flow area in each structure per one fuel rod is almost equivalent to those of the reference PWR. Since there is no core bypass region (baffle structure) around the core in the LSTF, the scaled metal capacity around the core shroud would be smaller than in PWR. The cooling effects of colder structures on superheated steam flow in the LSTF would thus be qualitatively comparable to those for the reference PWR.

(3) CET installation conditions at the core exit

The installation of CETs is plant-specific. Reference [6] on LOFT experiments, for example, describes that CETs are mounted in a variety of ways in commercial PWRs; some are housed in guide tubes, some are in the fluid stream, some are located up to several inches above the top of the fuel rods etc. It is, therefore, difficult to perfectly cover all of the different conditions in the LSTF experiments. The CET location in the LSTF facility roughly simulates that in the reference 4-loop PWR. The number of CET in the reference

PWR is 50 (about 1 CET per 4 fuel bundles with 17x17 rod array), while it is 20 in LSTF (almost 1 CET per 1 bundle with 7x7 rod array). In addition, core exit structures such as the upper core plate (UCP), upper nozzle, No.9 spacer also roughly simulate those in the reference PWR. These CET installation and core exit structures in LSTF may give similar CET responses for core heat-up detection especially for no reflux fall-back water cases.

(4) Applicability of LSTF/CET performance under fall-back water conditions

The aspect ratio of UP (D/h in Table 3.4.2-1) of LSTF is 1/12 of that of the reference PWR. This distortion may influence CET responses when SG reflux (fall-back) flow exists during core boil-off. In general, CETs under the influence of reflux coolant may indicate saturation temperature at certain area under hot leg with SG for reflux cooling while the CETs at the central core region or far from such hot legs may detect superheat due to free from coolant splashing. Though there is no systematic information on the area size subject to splashing water, it is expected that the dry region around the core exit and on the UCP would be far larger in the reference PWR because of the large diameter of the core.

3.4.7 Summary

CET performances were studied based on the thirteen ROSA/LSTF experiments [1, 2, 4, 5] including OECD/NEA ROSA Project Test 6-1. Major results are summarized below.

(1) General CET responses (time delay and temperature discrepancy relative to heating-up core)

The CET temperature behavior during core boil-off seems to show wide diversity because of such conditions as radial power profile, 3D flow of steam at different temperatures around core exit, cooling by cold structures and fall-back water. General relations, however, were found in the CET performances in most of the examined LSTF tests for the time delay and temperature discrepancy relative to the heating-up core, even for some tests with limited fall-back water effects.

(1-1) The relation between the time to start core heat-up (t_{ICC} [s]) and the time to start CET heat-up (t_{CET} [s]) is expressed in the following equation within an uncertainty of $\pm 6\%$ as,

$$t_{ICC} = a \times (t_{CET})^b, \tag{1}$$

where a=0.7603 and b=1.027 (see Table 3.4.5-2 & Figure 3.4.3-7).

(1-2) The relation on the temperature discrepancy is expressed by means of average temperature increase above saturation temperature ($DT=T-T_S$ [K]) at the CETs ($DT_{AVE}(CET)$) and core top region ($DT_{AVE}(P9)$) in the following equation as,

$$DT_{AVE}(P9) = C_1 \times DT_{AVE}(CET) + C_2 \tag{2}$$

where C_1 varies from 1.4 to 2.8 and C_2 from 0 to 40 K (see Table 3.4.5-2 & Figure 3.4.5-1). In the extremely low primary pressure case (TR-RH-06), C_1 and C_2 indicated exceptionally large value of 3.9 and 120 K, respectively. The temperature discrepancy in the maximum temperatures between the CETs and the core increased when the core water level dropped into the lower region, taking a rather long time.

(2) Steam flow conditions at core exit influential to CET response

Average steam velocity at UCP during core boil-off was found to be very small; typically around 10 to 30 cm/s and less than 0.6 m/s, in most of LSTF tests except for the extremely low pressure case (TR-RH-06) and 10% CL break LOCA test (SB-CL-09) with significant downward coolant fall-back at the core top. The 3D steam flow may be generated in the core and core exit even with small driving force. Several factors that may cause such 3D steam flow include (a) radial power profile, (b) cooling effect by low-temperature structures and (c) CRGT-chimney effect for PV top break LOCA, (d) the longer delay time with the smaller break size in small-break LOCAs even in the PV top break case, because of lower core power and slower level drop in the core during core boil-off, (e) high speed steam flow in a loss-of-RHR transient under atmospheric pressure, which causes low steam superheat leaving large temperature discrepancy between core top and steam at the CETs.

(3) Exceptional but important cases

(3-1)　　Steam superheating (DT=T-T$_S$ [K]) would be preferable in extremely high or low pressure boil-off such as the station blackout and loss-of-RHR during mid-loop operation where saturation temperature is higher/lower than the constant criterion value to start AM action. The CET superheat indication should then be helpful to operators to notice the core heat-up.

(3-2)　　No CET heat-up was observed in the two LOCA tests simulating (i) 10% CL break (SB-CL-09) and (ii) 0.2% PV bottom break (SB-PV-03) under SG depressurization action. Fall-back water significantly limited the CET heat-up as well as local core cooling. In the latter case, the core temperature excursion started even after the SG depressurization operation as an AM measures. The CETs then became to detect the core superheating when the uprising steam flow was significantly enhanced in the core by opening the PORV at the pressurizer.

(4) Applicability of LSTF/CET performance to PWR conditions

The LSTF/CET responses to detect core heat-up under no SG reflux cooling effects may be applicable to PWR once the following conditions are taken into account well such as the 3D steam flows depending on core power profile, CET location relative to the CRGTs and effects of cool structures including fuel rods around core exit. Applicability of the CET performance under fall-back water conditions including the detection/non-detection of superheated steam by a part of CETs under limited fall-back water conditions should then be carefully estimated, considering the effects of atypical upper plenum configuration of the LSTF.

References

[1]   OECD/NEA ROSA Project Supplemental Report for Test 6-1 (SB-PV-09 in JAEA) - Performance of Core Exit Temperatures for Accident Management Action in LSTF 1.9% Top Break LOCA Test - , JAEA-Research 2007-9001 (Proprietary report, to be opened in April 2012).

[2]   M. SUZUKI, et al., "Performance of Core Exit Thermocouple for PWR Accident Management Action in Vessel Top Break LOCA Simulation Experiment at OECD/NEA ROSA Project," Proceedings of ICONE16*,* Orlando, Florida, USA, May 11-15, ICONE16- 48754, 11p, (2008) in CD-ROM.

[3]   The ROSA-V Group, ROSA-V Large Scale Test Facility (LSTF) System Description for the Third and Fourth Simulated Fuel Assemblies, JAERI-Tech 2003-037, (2003).

[4]   M.SUZUKI, et al., "CET Performance at ROSA/LSTF Tests - Twelve Tests with Core Heat-up -," JAEA-Research 2009-011, (2009).

[5]   M.SUZUKI, et al., "Reliability of Core Exit Thermocouple (CET) for Accident Management Action during SBLOCA and Abnormal Transient Tests at ROSA/LSTF," (to be presented in Proceedings of NURETH13, Kanazawa City, Ishikawa Prefecture, Japan, Sept. 2009 – Oct. 2).

[6]   J. P. Adams, et al., Detection of Inadequate Core Cooling with Core Exit Thermocouples: LOFT PWR Experience, NUREG/CR-3386, (1983).

[7]   M. SUZUKI, "Characteristic Responses of Core Exit Thermocouples during Inadequate Core Cooling in Small Break LOCA Experiments Conducted at LSTF of ROSA-IV Program," Proceedings of ICONE2*,* San Francisco, California, USA, March 21-24, ICONE2, Vol.1, pp.63-68, (1993).

[8]   M. SUZUKI, "Break Location Effects on PWR Small Break LOCA Phenomena – Inadequate Core Cooling in Lower Plenum Break Test at LSTF," JAERI-M 88-271, (1989).

[9]   M.SUZUKI, et al., "A Study on ROSA/LSTF SB-CL-09 Test Simulating PWR 10% Cold Leg Break LOCA – Loop-seal Clearing and 3D Core Heat-up Phenomena", JAERI- Research 2008-087, (2008).

[10] M.SUZUKI, et al., "ROSA/LSTF Experiment Report for RUN SB-CL-24, Repeated Core Heatup Phenomena during 0.5% Cold Leg Break LOCA," JAERI-Tech 2000-016, (2000).

[11] M.SUZUKI, et al., "Experimental Study on Secondary Depressurization Action for PWR Vessel Bottom Small Break LOCA with HPI failure and Gas Inflow (ROSA-V/LSTF Test SB-PV-03)," JAERI-Research 2005-014, (2005).

3.5   PSB – VVER 0.7% SBLOCA: RELAP5 MOD 3.3 AND CATHARE2 V15 POST TEST ANALYSIS WITH SPECIAL EMPHASIS ON CET PERFORMANCE

3.5.1 Introduction

The present document provides experimental data of one SBLOCA experiment which has been performed during the EC-funded project TACIS-30303 "Accident Management Technology in VVER 1000" 20003-2006 [1]. The whole experimental campaign consists of 15 experiments with relevance to accident management. Four experiments show a significant drop of the level in the reactor core and heat up of the core simulator, and one of these experiments, Test 4, a small break loss of coolant accident, has been selected.

The scope of this section is a.) to show the delay between the temperature increase of the heater rods, and the measurement of superheated vapor at the core exit during the experiment, and b.) to show the performance of the codes Relap5 and Cathare2 in predicting the delay.

The analyst did not aim to model the above mentioned phenomena while setting up the nodalisation. The post test calculation tries to predict the overall behavior of the facility. No special attention has been placed on the core region (modeled with one stack of volumes) and the upper plenum thermocouples. Although it can be expected that accuracy of the prediction of the phenomena could be improved considerably, the presented modeling approach might be closer to the current best practice in safety analysis calculations, and gives an impression to what extend the phenomena is considered in the development of EOPs.

3.5.2 Description of PSB-VVER

The PSB-VVER is a full height integral test facility (see Figure 3.5.1), power and volume are scaled 1:300. The facility has four loops (each one is constituted by a hot leg, a steam generator, a loop seal, a main circulation pump and a cold leg); a pressurizer, connected via the surge line to the hot leg of loop 4; the ECCS is provided by an active pump, that simulates high and low pressure injection systems, and four hydro-accumulators. All system components are insulated from the environment with glass wool to limit the heat losses.

The main parts of the VVER vessel are reproduced in the facility by separate pipes: one for the downcomer, one for the core model and upper plenum, and one for the core bypass. A horizontal pipe connects the downcomer to the lower plenum. Another bypass links the downcomer to the upper plenum.

The core model contains 168 Fuel Rod Simulators with a uniform power profile (axial as well as radial) and a central unheated rod. The active bundle is of electrical type and has a hexagonal cross section. Also the bypass section is heated over the same elevation range of the core, to simulate the heating that water receives in the channels, within the reactor core, in which the coolant flows from the lower plenum to the upper plenum, bypassing the assemblies.

The primary side of the steam generator consists of a hot and a cold collector and of 34 tubes coiled in 10 complete turns with 51 mm difference from inlet and outlet height. The length of one tube is the same like the one of the reference plant. The distributor of feed water is a ring with several holes placed above the steam generator tubes. Figure 3.5.1 shows an isometric view of the PSB-VVER facility, Table 3.5.1 compares main parameter of PSB-VVER and the VVER1000.
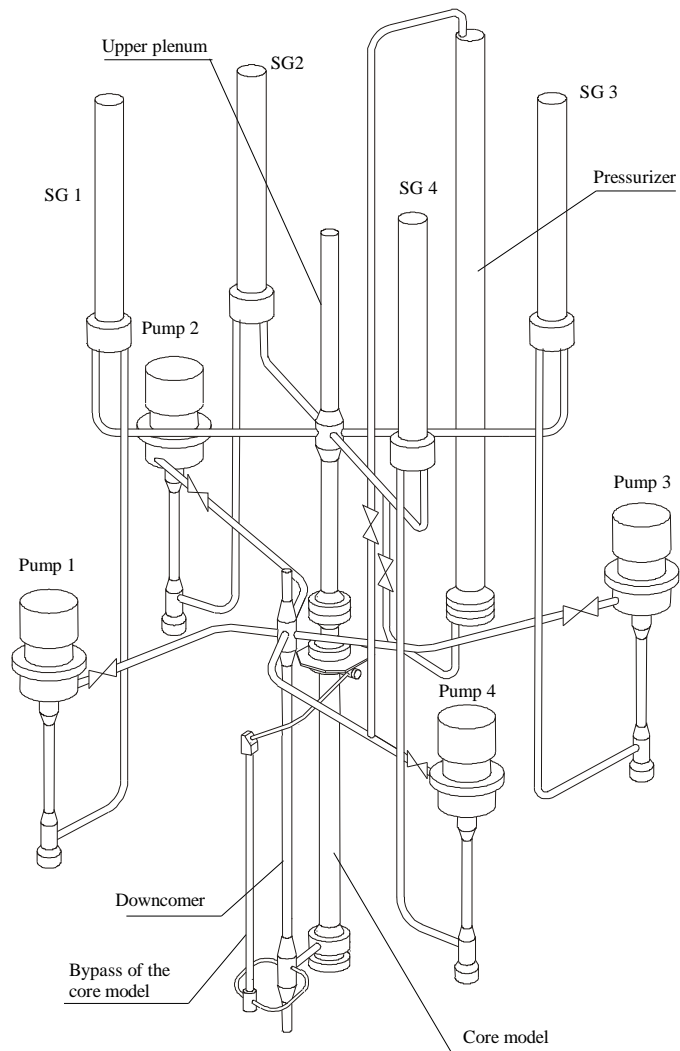
Figure 3.5.1 PSB-VVER test facility

3.5.3 Location of measurements relevant for CET performance

Of importance are thermocouples in the core region and in the upper plenum. In the core region, see "heated section" from elevation 1915 to elevation 5445 in Figure 3.5.2, the heater rod surface temperature is measured. Thirty heater rods are instrumented with a total of about one hundred thermocouples. Figure 3.5.5 shows a cross section of the bundle and which heater rods are instrumented. Figure 3.5.6 (three parts) shows the elevation of the installed thermocouples. The thermocouples are installed inside the heater rods and not on the surface (see Figure 3.5.3). Fluid temperatures of the heated section are not measured.

Table 3.5.1 Comparison of key parameters of the PSB-VVER facility and the VVER

#	Name	VVER-1000	PSB-VVER
1.	Scale	1	1:300
2.	Number of loops	4	4
3.	Heat losses, %	0.063	1.8
4.	Heat power, MW	3000	10
5.	Primary circuit volume, m^3	370	1.23
6.	Primary circuit pressure, MPa	15.7	15.7
7.	Secondary circuit pressure, MPa	6.3	6.3
8.	Coolant temperature, °C	290/320	290/320
9.	Core length, m	3.53	3.53
10.	Number of fuel rods	50856	169
11.	Core volume, m^3	14.8	$4.9*10^{-2}$
12.	Upper plenum volume, m^3	61.2	$20.0*10^{-2}$
13.	Downcomer volume, m^3	34.0	$11.0*10^{-2}$
14.	Hot leg volume (4 pieces), m^3	22.8	$8.0*10^{-2}$
15.	Cold leg volume (4 pieces), m^3	60.0	$24.0*10^{-2}$
16.	Number of steam generators	4	4
17.	Heat exchanging surface, m^2	6115	18.2
18.	Water volume in SG for primary circuit, m^3	21.0	$6.8*10^{-2}$
19.	PRZ volume, m^3	79	$26.3*10^{-2}$
20.	Number of hydroaccumulators	4	4
21.	Number of pumps	4	4
22.	Volume of hydroaccumulators, m^3	240	$80*10^{-2}$

23.	Water volume in ACCU, m^3	200	66.6*10^{-2}

Two fluid temperature measurement devices are at elevations of interest: T04 a Pt – thermometer, at elevation 5840 (end of heated length 5445), downstream the upper lead grid, and T04b, a Ch-Co thermocouple at elevation 7185 (downstream of the connection of the core bypass simulation line). For details see Figures 3.5.3 and 3.5.4. There is no information on the about the angular position of the temperature measurements, the penetration depths, and how the devices are installed (upward, downward).

Table 3.5.2 - Fluid temperature measurements in the reactor model

Measurement identifier	Location	Elevation, mm	Transducer
YC01T04	Heated section outlet	5840	Pt - thermometer
YC01T04 b)	Upward section	7185	Ch-Co thermocouple
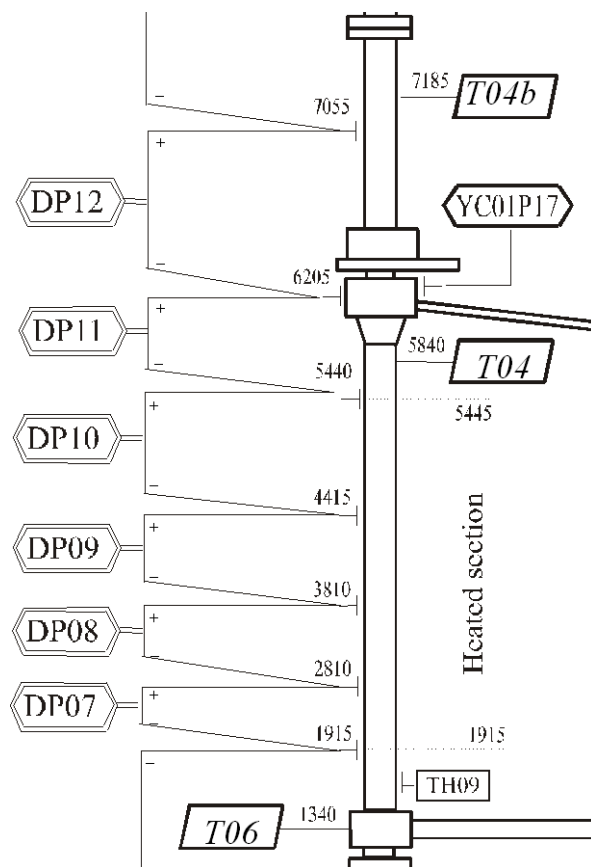
Figure 3.5.2: Upper plenum fluid temperature measurements at 5840 (YC01T04) and 7185 (YC01T04 b).

1 - Cladding
2 - MgO insulator
3 - Nichrome heating element
4 - Copper conductor
5 - Proofing compound
6 - Ceramic bushing
7 - Upper conductor
8 - Inner cladding
9 - Cable thermocouple
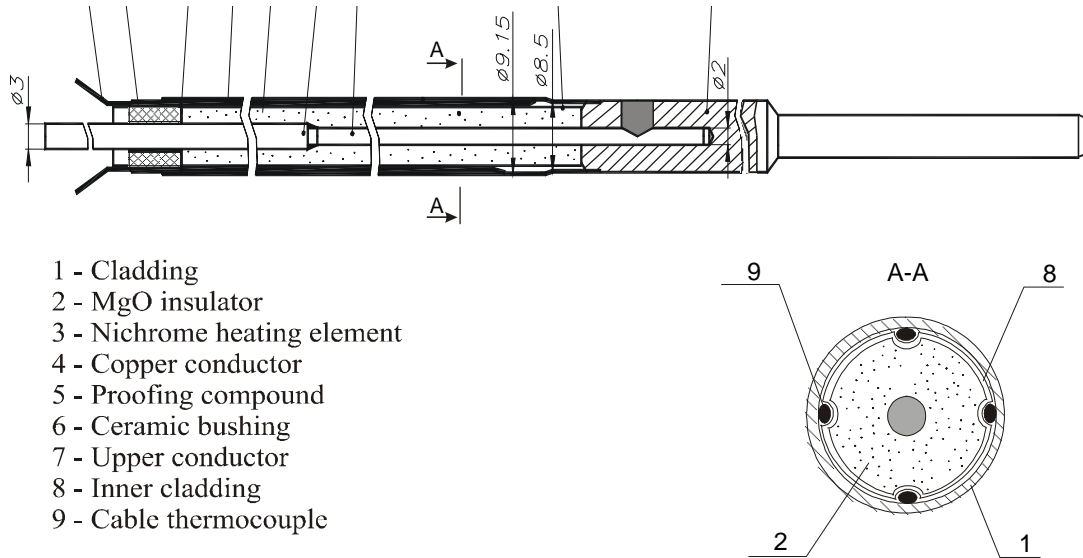
Figure 3.5.3   Thermocouple mounting on the heater rod cladding

Figure 3.5.4 Core simulator model

1 – coolant feed branch pipe;
2 – fuel assembly housing;
3 – FRS bundle;
4 – upper current lead grid;
5 – instrumented fuel rod;
6 – insulating grid;
7 – air supply branch pipe to the lower
     current leads cooling chamber;
8 – displacer;
9 – spacer grid;
10 – pressure tap nozzle;
11 – upper current lead.
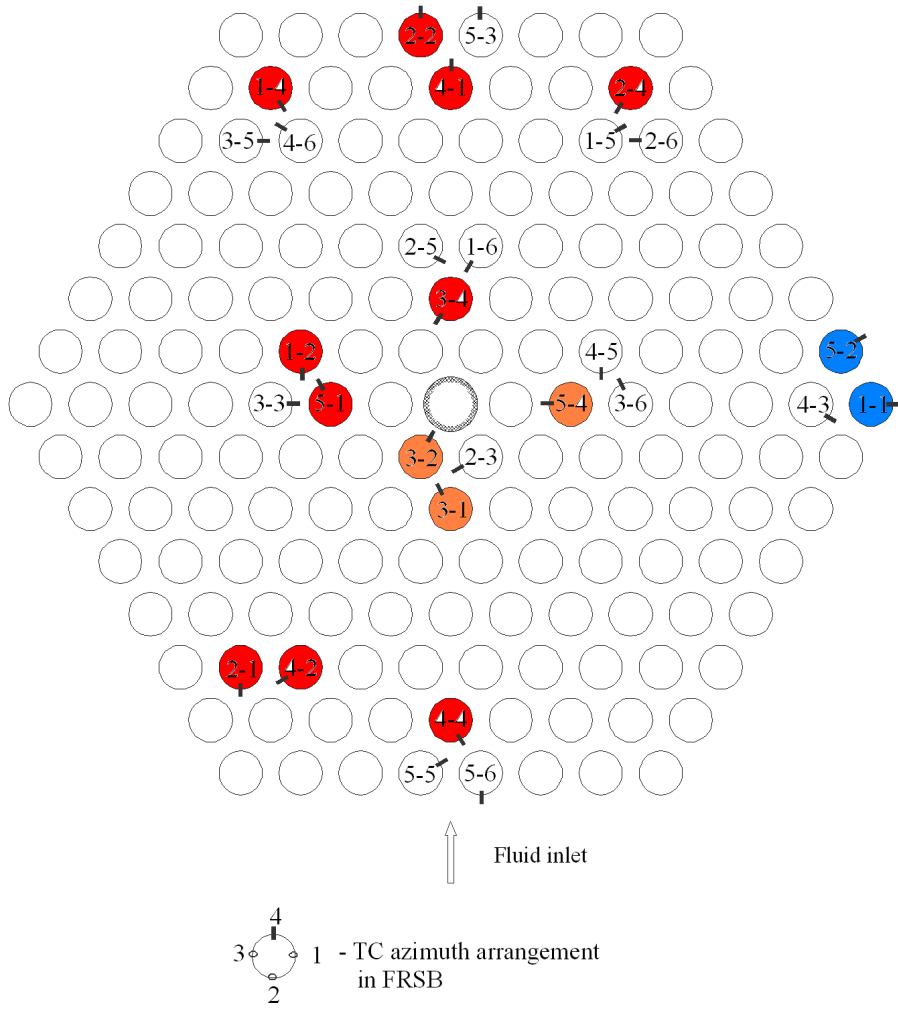
Figure 3.5.5 Arrangement of instrumented FRS in the 1.5 MW FRSB (top view)
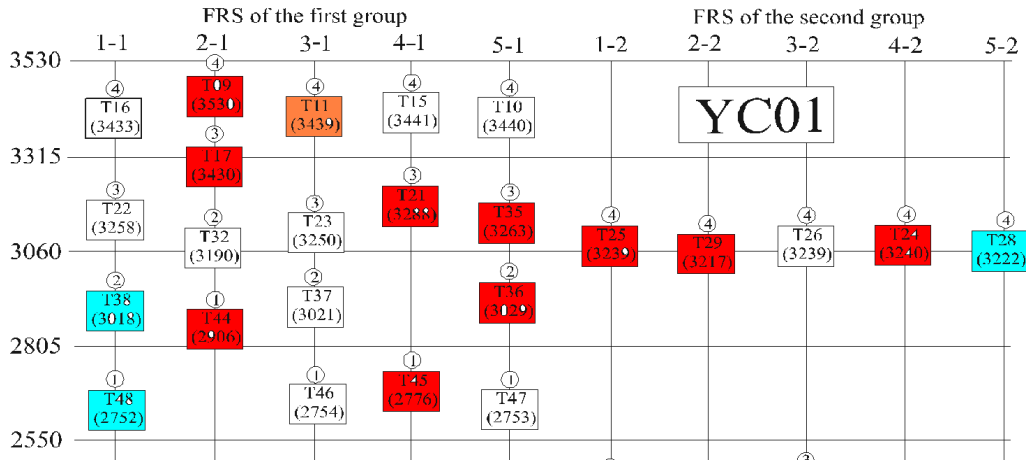
Figure 3.5.6(a)   Arrangement of top instrumented FRS in the 1.5 MW FRSB (top elevation)
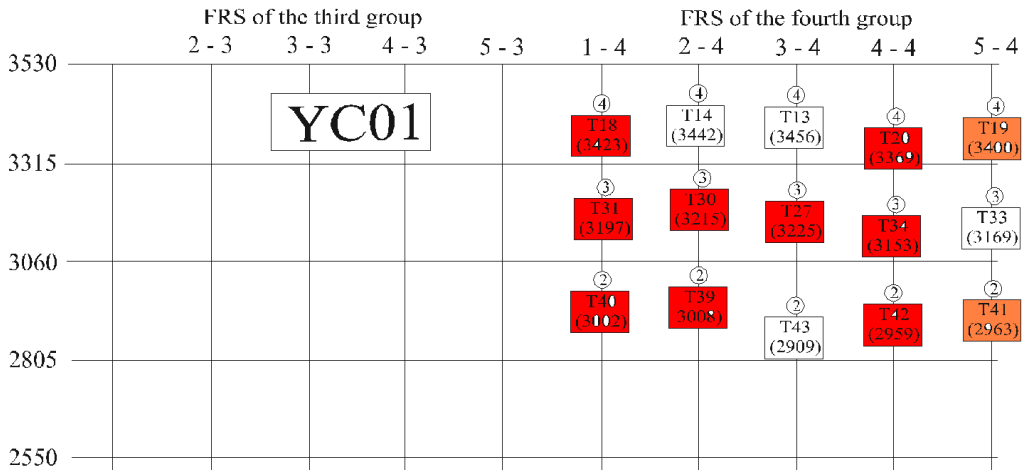
Figure 3.5.6(b)   Arrangement of top instrumented FRS in the 1.5 MW FRSB (top elevation)

3.5.4 Description of the experiment – 70mm equivalent break between MCP and RPV of CL4

The test simulated a SBLOCA with break area 0.7% of the CL area (70mm equivalent diameter) with delayed AM procedures. The break was located in CL of loop #4 between MCP and DC. All high pressure injection systems were assumed to fail, but accumulators and two trains of the low pressure injection system were available. The pressurizer was connected to loop #4. At a cladding temperature (maximum of all thermocouples) of 450 °C it was assumed that the operator would depressurize the secondary side by full opening of SRV.

The test was stopped when the facility stabilized and the PS pressure was below the set point of the LPIS.

The experiment was started by opening the break simulation valve. This led to a sharp decrease of the primary side pressure. At 47s the primary pressure fell below 13.7 MPa and the scram signal was generated – core and core bypass power was reduced accordingly. The primary side pressure continued to decrease. At 780 s a first dryout occurred, which was quenched by loop seal clearing. The liquid level of the primary system dropped below the break at about 800s, which slowed down the loss of mass from the primary. Accumulator injection starts at 1374 s. Two accumulators inject into the upper plenum section, two into the downcomer section. Although the accumulators become effective only after the secondary system depressurization (see Figure 3.5. 11), an influence on the upper plenum fluid temperature cannot be excluded.

From dryout to detection of superheated vapor:

The loss of primary system inventory continued, until at 2877 s a second dry out occurred in the upper part of the core. Only the top group of thermocouples (2.5 m and above of the beginning of the heated section) showed dryout, and a left-right asymmetry can be seen (please refer to Figure 3.5. 5 and 6: white circles with numbers are heater rods, which are not instrumented at the top of the core, and therefore do not show dryout. Red circle heater rod thermocouples indicate a dryout, with peak temperatures above 350 °C, orange circles heater rods with dryout but peak temperatures less than 350 °C, and blue circles show heater rods with thermocouples at the top, which do not indicate dryout). At 3430 s, the Pt-thermometer which is positioned 40cm above the end of the heated section, downstream the lead grid, showed temperatures above saturation temperatures. At 3470 s the thermocouple located 1.5 m downstream of the end of the heated section started to indicate superheated vapor. The temperature measurements came back to saturation temperature when the secondary side depressurization became effective. The time delay between heater rod thermocouple temperature increase and core exit fluid thermocouple temperature increase is therefore about 500 s. The highest cladding temperature reading is 225 °C above the saturation temperature (240 °C), at the same time CET – equivalent reading temperature reading is only 30 °C above saturation temperature.

Table 3.5.3 Main events

No	Event	Exp	R5	C2
1	Opening of break	0	0	0
2	Scram	52	37	46
3	First dryout	780	-	820
4	Loop seal clearing, break covered by steam	800	775	825
5	Primary pressure lower than secondary pressure	815	797	880
6	Begin of Accumulator injection	1374	1230	1304
7	Second dryout (temperature excursion heater rods)	2877	2465	3265
8	Superheated steam at core outlet	3425	2650	3265
9	Begin of AM measures (secondary system depressurization by full opening of SRV)	3419	3162	3540
10	Start of LPIS injection	3674	3350	3550

Primary system pressure (upper plenum)
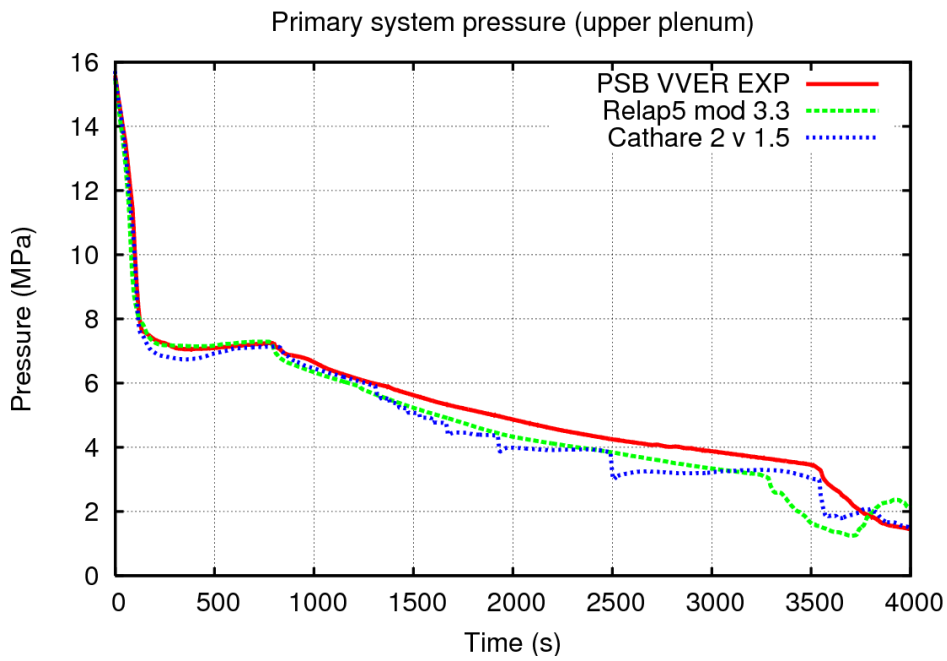
Figure 3.5.7 Primary system pressure (PSB-VVER, R5, C2)

EXP Cladding temperature various positions 2.5 - 3.5 m
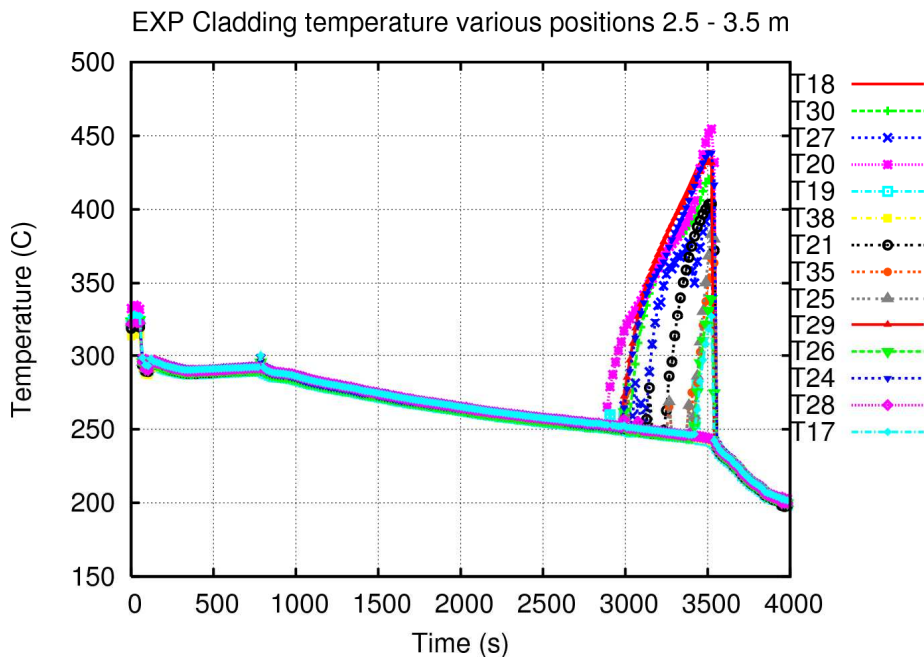
Figure 3.5.8   Temperature upper part of core simulator rods (PSB-VVER)
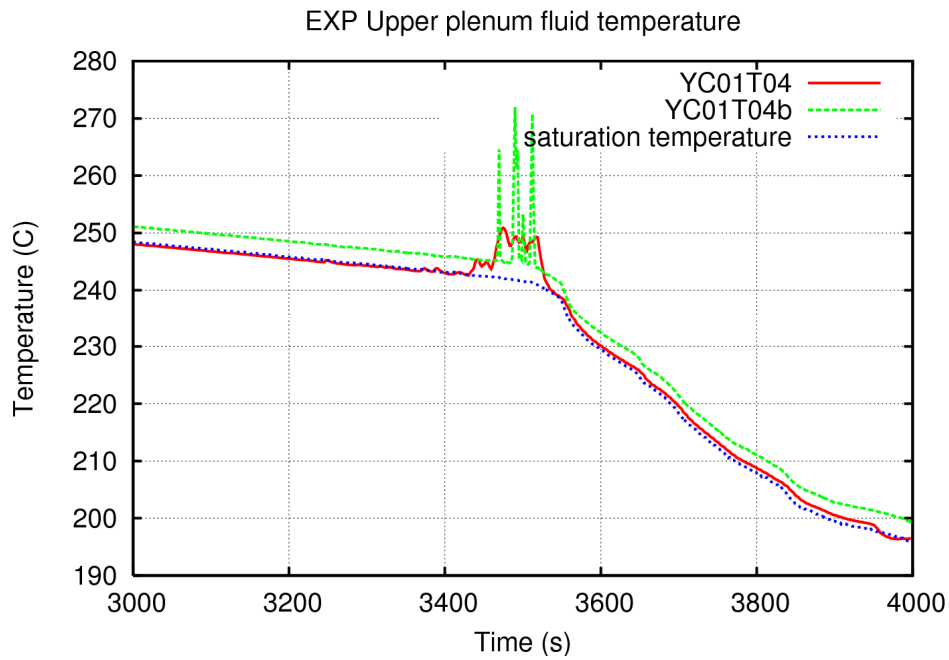
Figure 3.5.9   Temperature above the core (PSB-VVER)
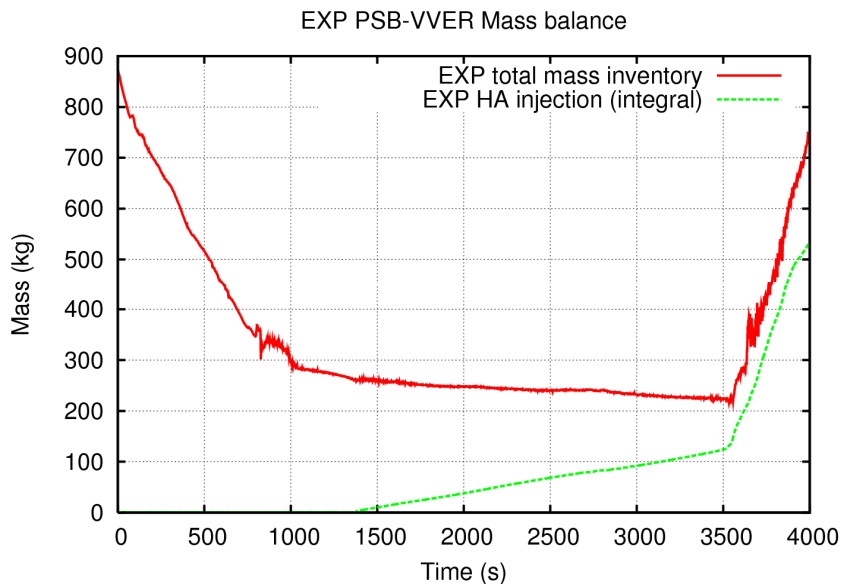
Figure 3.5.10   Mass inventory and accumulator injection (PSB-VVER)

3.5.5 Post-test calculation results

Both nodalisations, the Relap5 and Cathare2 nodalisation of the facility, are very detailed and complex, and aim to reproduce the overall system behavior. Neither of the nodalisations aims for a specific purpose (i.e. LBLOCA analysis with a simplified secondary side), both of them should be able to reproduce almost every experiment with reasonable accuracy. This means, that all components of the facility are modeled. Figure 3.5.11 shows the modeling approach for the reactor core simulator of the facility. The section is modeled in both codes with one stack of volumes. All structures are modeled, as well as the rod lead grid at the end of the heated section in both nodalisations. The rod surface temperatures that are presented have been taken for both nodalisations from the last two top nodes of the active structure, the fluid temperature has been taken for the Cathare2 nodalisation from the volume V5UP1, for the Relap5 nodalisation from the volume 120-01 (bottom subvolume).

Table 3 compares the main events of the experiment and for the two codes. Figure 3.5.7 shows that the primary pressure trend is well predicted by both codes. The loop seal clearing is, again, well predicted by both codes.

The second dryout, see Figure 3.5.12, is, regarding the shape, well predicted by relap, but starts about 300 s earlier than in the experiment. Cathare2, on the other hand, predicts a second dryout, which is then quenched, and a third dryout, which matches well the second dryout from the experiment. The reason for this can be found in the accumulator injection – while the experiment, as well as Relap5, show a slow, but continuous injection of the accumulators, Cathare2 predicts a step-wise injection (see also the steps in the Cathare2 primary side pressure, Figure 3.5.7.

From dryout to detection of superheated vapor:

Figures 3.5.13 and 3.5.14 show the relation between fuel rod simulator heat up, and core exit fluid temperature, as seen by the codes. Figure 3.5.14, Cathare2 calculation, shows clearly that the one-dimensional modeling approach, with flow in one direction, predicts a difference in heater rod and core exit temperature, but not a time delay between the two. Core heatup takes place when the local heat flux exceeds the critical heat flux, which, since both codes use for CHF-prediction the Groeneveld Look-up table method, in principle could also happen with an equilibrium quality of less than one, but this does not seem to be the case at least for Cathare2. Relap5 on the other hand (see Figure 3.5.13), seems to predict core heatup prior to superheated vapor at the volume above the core. But looking more closely one can see that the heatup takes place first in the second to top node. Since the heat structure is uniformly heated, this means that the continuous accumulator flow provides liquid from above, which is able to suppress the heat up at the top node for another 200 s. Together with the top node heat-up, the vapor temperature rises.
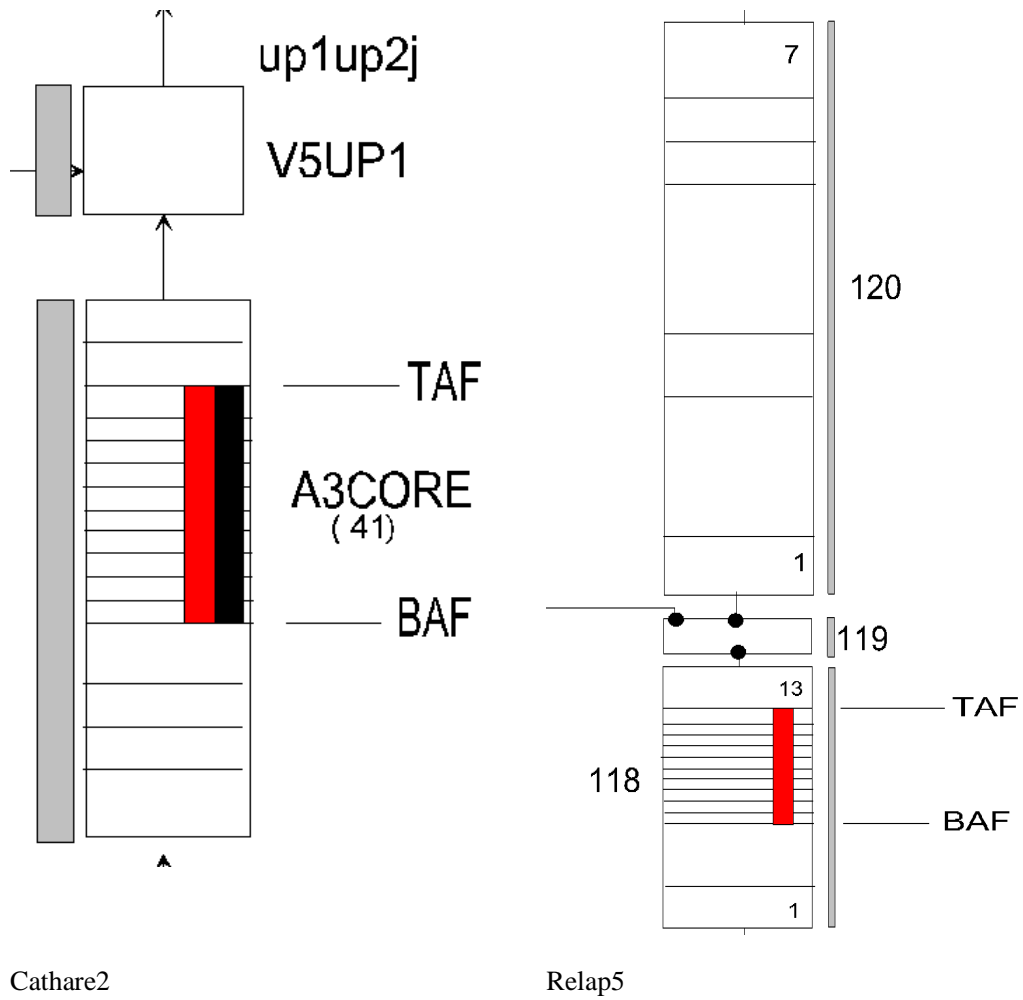
Cathare2   Relap5

Figure 3.5.11   Nodalisation of the core region, Cathare2 and Relap5
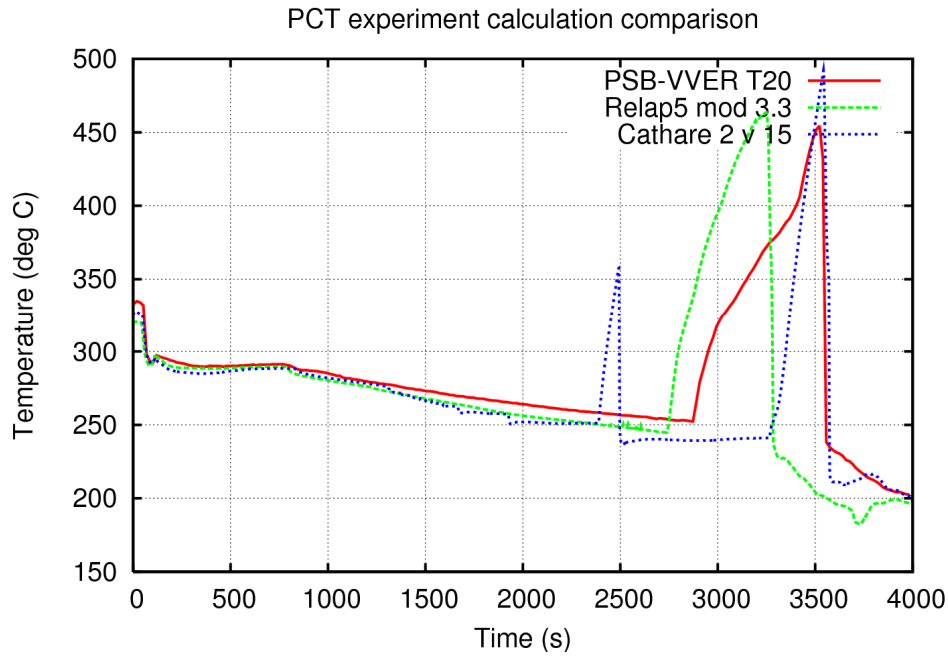
Figure 3.5.12   PCT comparison between PSB-VVER, Relap5, and Cathare2
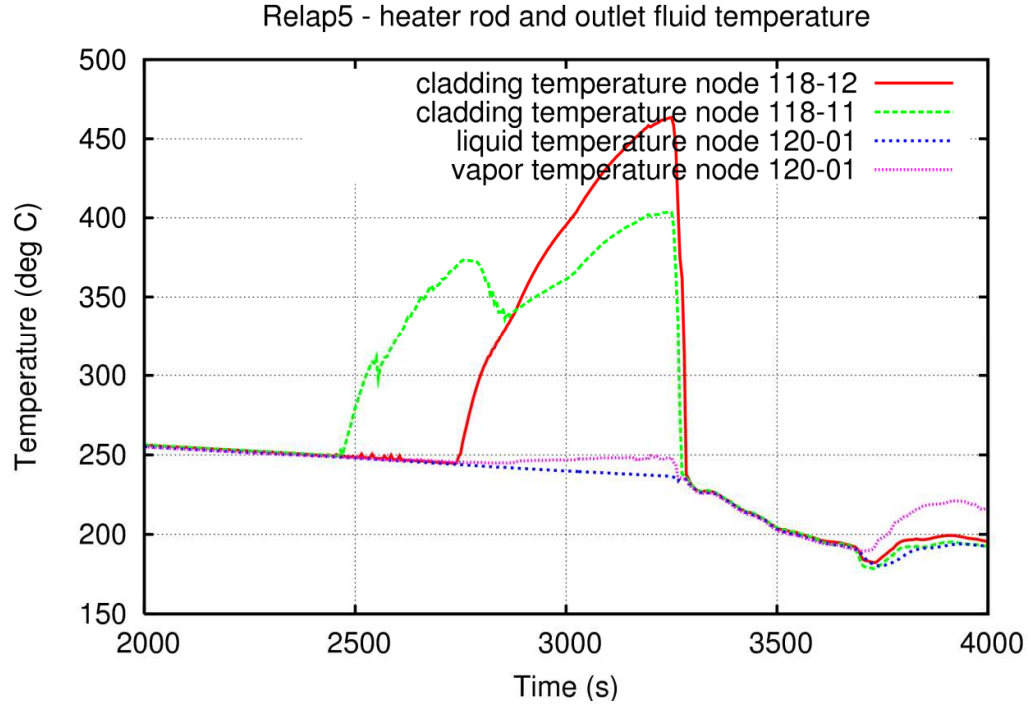
Figure 3.5.13   Relap5 – comparison between core exit fluid temperature and heater rod temperature
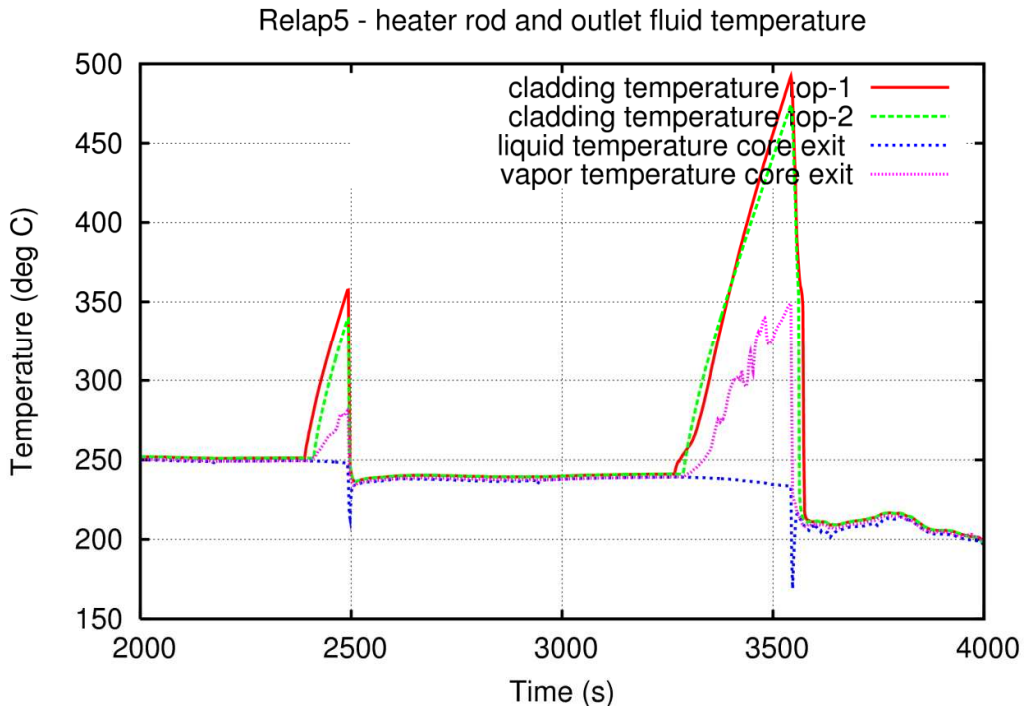
Figure 3.5.14   Cathare2 – comparison between core exit fluid and heater rod temperature
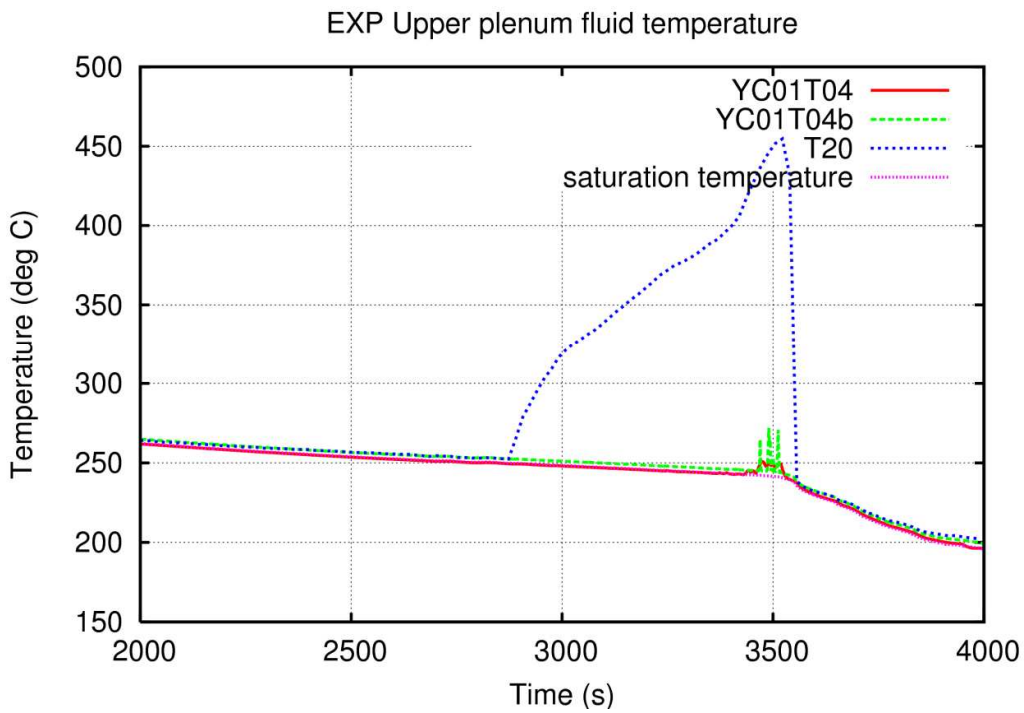
Figure 3.5.15   PSB-VVER – comparison between core exit fluid and heater rod temperature

Fluid at core outlet vs heater rod temperature
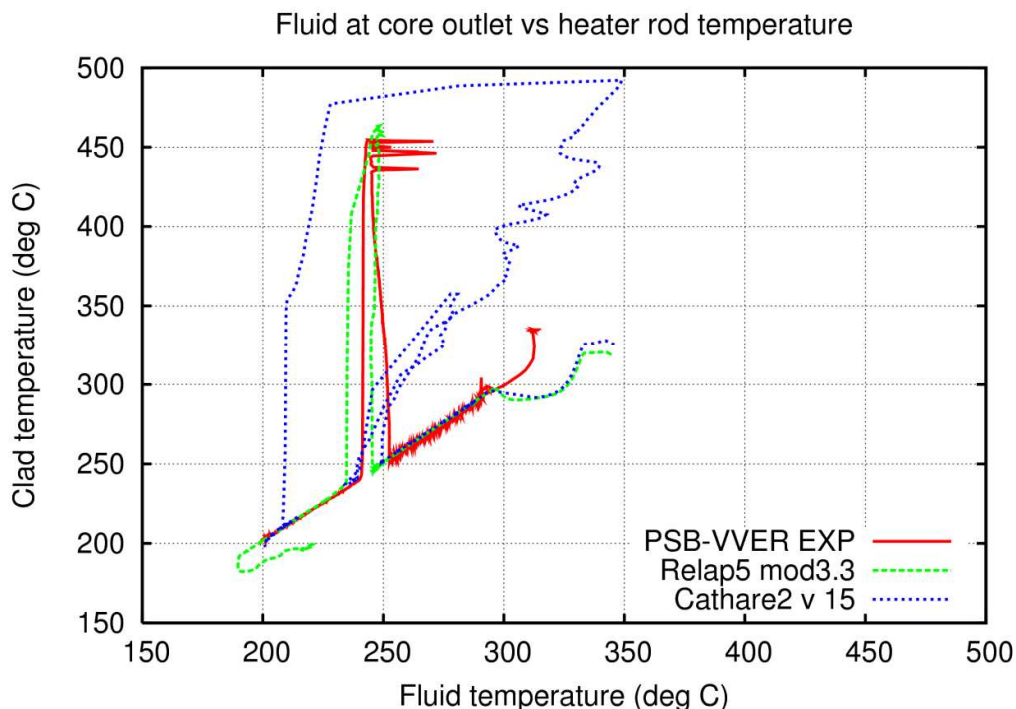
Figure 3.5.16 PSB-VVER, Relap5 and Cathare2 – fluid vs clad temperature (time evolvement from top right to bottom left).

3.5.6 Conclusions

The PSB-VVER SBLOCA experiment reported here confirms that there is a delay between increase of the heater rod surface temperature and increase at the core exit temperature readings. A postulated accident management procedure (blow down of the SG) effectively quenched the dry out, so that no statement on the rate of temperature increase of heater rod surface and core outlet fluid temperatures can be made.

Post test calculations show that without special effort of modeling the core exit thermocouples, one of the two phenomena has been reproduced qualitatively – the faster increase in heater rod surface temperature, compared with the superheated vapor temperature at the core outlet. The second phenomena, the delay between the beginning of heater rod surface temperature increase, and the appearance of superheated vapor at the node above the active structure, was not predicted by Cathare2, and by Relap5 only due to the fact that there was accumulator injection from above. A third consideration regards the uncertainty in predicting the experimental results: experience with SBLOCA analysis shows that the timing of phenomena like dryout cannot be predicted with absolute accuracy (the Relap5 calculation gives an example). The order of magnitude of the experimentally observed time delay between heater rod and core exit temperature increase is comparable to the difference between predicted and experimental dryout occurrence.

Figure 3.5.16 summarizes the results. The transient starts at the right top corner and evolves to the bottom left corner.

References

[1]   D'Auria et al., "Accident Management Technology in VVER-1000", Tacis-30303, Pacini, 2006, ISBN 88-902189-1-6

[2]   Melikov et al., "Standard Problem Definition Report, (test 1)", OECD – PSB-VVER Project, 2003

3.6   SYNTHESIS INCLUDING THE APPLICABILITY TO REACTOR SCALE

This section gives an overview of the experimental investigations, starting from a description of the various physical phenomena involved in the qualification of the CET behavior during the performed experiments. The specific geometric arrangements which largely influence the CET behavior are also summarized. The findings of the various experimental investigations are listed and synthesized in common conclusions. Individual findings specific to the different investigations are also reviewed and, if possible, explained on the basis of the specific characteristic of the corresponding experimental set-up. Finally, an attempt is made to investigate the applicability to reactor scale.

3.6.1 Important physical phenomena and influence of the geometrical arrangements

As described in detail in the former sections, the CET shall be used to get reliable information about the thermal-hydraulic state in the reactor core. The most important information concerns the quality of the cooling of the core. Any inadequate core cooling should be detected as soon as possible in order to take adequate counter-measures to re-establish a proper core cooling in a timely manner. In case of inadequate core cooling, the key information concerns the temperatures in the reactor core. The general overall temperature situation in the core is important, but the hottest fuel rod cladding temperature in the core is of paramount interest because it mainly determines the timing of AM actions.

The technical challenge consists therefore in deducing the core temperature, which is not directly measured in the reactor case, from the CET readings. That means, physically spoken, some heat from the superheated core region has to be transported to the CET measurement sensor, where it can be detected. This energy transport can only (in a timely manner and for limited temperatures) be realized through the convection of cooling fluid from the core region to the CET measurement location. In the case of a superheated core which is at least partly covered by liquid water (which is the subject of this report) the fluid consists mainly of steam or a mixture of steam and entrained water which is generated by the core decay heat. Hence, the overall energy transport from the fuel rod to the CET sensor has the following three main steps: heat transfer from the rod surface to the fluid, convective fluid transport to the CET sensor location, and heat transfer from the surrounding fluid to the CET sensor.

The heat transfer from the fuel or heater rod surface to the fluid depends on the flow regime which can vary from two-phase flow convection through the core, over quasi-stagnant water level conditions with steam flow containing entrained water in the upper core part, until pure steam flow conditions in the upper part of the core at typically very low velocities. In addition, the temperature rise in the core due to insufficient cooling is quasi starting from a single point and is afterwards restricted to a limited area, whereas the fluid is exposed to the, in particular, thermal boundary conditions along its full flow path. Due to the basic heat transfer principles, the fluid will not fully reach the rod surface temperature after having passed a restricted high temperature area. Accordingly, the fluid temperature will always be lower than for example the maximum cladding temperature in the reactor core.

An inverse situation is taking place at the CET sensor location with finally the same conclusion, that in principle the CET reading is somewhat below the temperature of the surrounding fluid. The location (e.g. distance to the upper end of the core) and the geometrical details of the CET installation can also largely influence the CET readings. The CET measurement is for example degraded and delayed if the sensor is not fully exposed to the relevant fluid flow or if the sensor is too closely connected to large structural heat capacities.

Along the fluid flow path from the reactor core to the CET location, depending on the thermal boundary conditions there will be heat transfer with the flow boundaries. These boundaries comprise the reactor core region above the maximum cladding temperature, i.e. rod parts with lower temperatures, unheated rod

parts, fuel element upper nozzles, upper core plate and even structures in the upper plenum depending on the CET location. These structural parts have quite a large heat capacity, especially compared to the energy content of steam. Therefore, they have in case of a general temperature rise in the core and reactor pressure vessel a big potential to cool down the passing fluid and the temperature rise detected in the core will not be completely "delivered" to the CET measurement, i.e. possibly only with delay and mitigation.

The fluid from the reactor core on its way to the CET measurement location is also exposed to additional thermal-hydraulic boundary conditions. These include water back-flow to the core due to condensate from the SGs and ECCS water injections, flows induced by the radial power distribution in the core, mixing effects in the core and in the upper plenum and pressure change effects which can directly change the fluid flow regime. Most of these additional flow effects are three-dimensional in their nature and therefore very hard to scale. The effect of these additional thermal-hydraulic boundary conditions results in a quasi falsified CET reading, because the original intention, to measure the temperature of the fluid coming from the reactor core, is influenced or even replaced by these additional flows. For example during certain phases of water fall-back from the hot legs the CET – especially in the vicinity of the hot leg nozzles – may indicate saturated conditions which does not necessarily represent the situation in the reactor core. Nonetheless in a full scale reactor, the water fallback may only influence the response of CET's located above peripheral assemblies in the vicinity of hot leg nozzles, but, depending on the liquid velocity at the hot leg nozzle, should not have any significant impact on CET's located above central assemblies.

Although, the above described phenomena are rather complicated and there are a variety of possible combinations and interplays, the evaluation of the pertinent experimental results helped to develop general rules of CET behavior with respect to their use for AM purposes.

3.6.2 Common findings of the experimental investigations

As described in the former sections, the CET behavior was estimated during simulated transients performed in four different facilities. The four experimental facilities have very different characteristics in various aspects like nuclear/electrical heating, volumetric scaling, pressure range and many details of the geometrical simulation especially related to and inside the reactor pressure vessel.

From the LOFT programs six tests have been considered for the evaluation of the CET performance. Three tests have been used from the PKL facility and even 13, mostly SB-LOCA, tests from the ROSA/LSTF facility. Finally, a single SB-LOCA test performed in the PSB-VVER facility was also used for the evaluation. These four facilities differ also with respect to the instrumentation, whereas due to different reasons the most detailed measurements have been available for the tests performed in PKL and ROSA/LSTF.

In the following, all the findings which are common to the evaluation of the tests in all four facilities are summarized. For convenience, if a finding was not explicitly mentioned in the conclusions for the test(s) of a facility, it was nevertheless used if its validity is obvious or if there was no evidence for that finding in the corresponding test(s).

1) The use of the CET measurements has limitations in detecting inadequate core cooling and core uncovery.

2) The CET indication displays in all cases a significant delay (up to several 100 s).

3) The CET reading is always significantly lower (up to several 100 K) than the actual maximum cladding temperature.

4) CET performance strongly depends on the accident scenarios and the flow conditions in the core.

5) The CET reading depends on water fall-back from the upper plenum (due to e.g. reflux condensing SG mode or water injection) and radial core power profiles. During significant water fall-back the heat-up of the CET sensor could even be prevented.

6) The colder upper part of the core and the cold structures above the core are contributing to the temperature difference between the maximum temperature in the core and the CET reading.

7) The steam velocity through the bundle is a significant parameter affecting CET performance.

8) Low steam velocities during core boil-off are typical for SB-LOCA transients and can advance 3D flow effects.

9) In the core as well as above (i.e. at the CET measurement level) a radial temperature profile is always measured (e.g. due to radial core power distribution and additional effects of core barrel and heat losses).

10) Also at low pressure (i.e. shut down conditions) pronounced delays and temperature differences are measured, which become more important with faster core uncovery and colder upper structures.

11) Despite the delay and the temperature difference the CET reading in the center reflects the cooling conditions in the core.

12) Any kind of AM procedures using the CET indication should consider the time delay and the temperature difference of the CET behavior.

13) In due time after adequate core cooling is re-established in the core the CET reading corresponds to no more than the saturation temperature.

Based on these common findings it is obvious that the CET behavior is qualitatively consistent in all four test facilities even if the scaling effect (loops have an important scaling effect on diameters - especially for the core) has to be taken into account when the reactor case is addressed especially in accident management procedures. For getting an indication about the similarity or differences of the quantitative behavior of the CET in the different test facilities, same or at least similar tests performed in different test facilities have to be compared. Due to the limited number of tests and the differences in the detailed information about the tests from the different facilities, only comparisons of tests from PKL and ROSA/LSTF could be chosen to get some reasonable results. Also for these two test facilities many characteristics (like e.g. pressure range or axial core power distribution) are different and there isn't any test which was performed in both facilities following the same procedure. Nevertheless, two times two similar tests executed in PKL as well as in ROSA/LSTF are chosen to compare the CET performance.

Test TR-LF-03 executed in ROSA/LSTF is a SBO transient resulting in a core heat-up due to water boil-off in the core at high pressure conditions. The observed CET behavior is characterized by a delayed detection of superheat in the core by roughly 120 s. The maximum cladding temperature at the top of the core is under-estimated by the CET measurement by approximately 40 K. This behavior is well inside a general relationship between the core superheat and the CET superheat deduced from the experimental results of eleven tests (see below, next section) performed in ROSA/LSTF. Test PKL III C5.2 simulates also a SBO transient. Following a different procedure than used for test TR-LF-03, a core heat-up during water boil-off did also take place in the later part of the transient test C5.2. Although the pressure during the core heat-up was lower in the PKL test compared to test TR-LF-03 and was further decreased into the transient, the thermal-hydraulic conditions in the core and the RPV were quit similar as in the corresponding ROSA/LSTF test. In the PKL test the CET behavior is characterized by a delay of about 100 s and an under prediction of the maximum cladding temperature at the top of the core of about 80 K.

The second comparison of the CET behavior is based on SB-LOCA transients. PKL test D1.2 was simulating a SB-LOCA transient with additional system failures resulting in a core heat-up. In this case the CET indication of the start of the superheated conditions was delayed by about 100 s. The difference between CET and the cladding temperature during the core heat-up part of the transient was about 100 K. The analysis of a series of SB-LOCA transients performed in the ROSA/LSTF facility shows quantitatively comparable results. The delay of 100 s is well covered by the range of delays observed in the ROSA/LSTF SB-LOCA tests. In addition, the deviation of the measured CET to the maximum cladding

temperatures observed in the PKL test can even be predicted by the above mentioned general relationship developed for the ROSA/LSTF tests.

The two comparisons described above confirm that in both, the PKL and the ROSA/LSTF, facilities the observed CET behavior is not only qualitatively similar and consistent, but for comparable transients also a quantitative consistency could be confirmed.

3.6.3 Specific findings of the individual experimental investigations

In this section, findings which are specific only to one experimental facility are summarized. That can be due to the fact that a specific test is only executed in one facility, but also that a dedicated evaluation of test results is only done for a single test facility.

In the OECD/LOFT fission product test LP-FP-2, so-called runaway conditions have been encountered in the core, i.e. a rapid fuel cladding oxidation took place. During this fast part of the transient the CET measurement is essentially disconnected from the core temperatures.

Regarding the tests performed in the PKL facility, there are no relevant additional conclusions to be mentioned here.

Concerning the conclusions from the 13 tests preformed in the ROSA/LSTF facility, some additional information based on a more thorough quantitative evaluation are added here:

1) For the delay of the CET response for detecting inadequate core cooling (ICC) the following general relation is valid: $t_{ICC} = a \times (t_{CET})^b$ (cf. section 3.3) except for two tests out of the 13 tests.

2) The general temperature discrepancy between the top of the core and the CET can be expressed with the following relationship based on superheats DT of averaged temperatures: DT_{AVE}(top of core) = C1 $\times DT_{AVE}$(CET) + C2 with similar values for C1 and C2 except for test TR-RH-06.

3) When the CET is measuring 623 K, a large temperature difference appears between the maximum core temperature and the CET: 70 – 190 K in eight tests. For other three tests without CET-heat-up to 623 K, the difference was even 360 – 450 K when PCT reached 923 K.

4) The delay of the CET indication becomes larger for smaller break sizes (due to the lower steam velocity).

5) High speed steam flow causes low steam superheat (encountered in the loss of RHR transient at atmospheric pressure).

6) In the test 6-1 (PV top LOCA) the CRGT steam flow bypass increases the CET indication delay time.

7) Accident scenarios in which the CET would not detect the start of inadequate core cooling that precedes core damage cannot be excluded in principal.

For the test executed in the PSB-VVER facility some post test analysis was performed for comparing the prediction with the experimental findings. It has to be mentioned here that standard system code safety analysis facility model has been used for this analysis, i.e. no special attention has been taken for modeling the CET behavior. The predictions with the codes RELAP5 and CATHARE reproduced qualitatively the faster cladding temperature increase compared to the CET measurement, but the time delay could not be predicted. The latter should be kept in mind when system code analysis is executed in relation of the CET behavior for the reactor case.

3.6.4 Applicability to reactor scale

In the following the result of the evaluation of the experimental data with respect to its application or extrapolation to the reactor scale are summarized. Again, the evaluations of the different experimental investigations result in a quite consistent picture regarding the applicability to the reactor scale.

1) Concerns about CET functionality for general use in AM are well founded.

2) Qualitative application/extrapolation of the CET response to reactor scale is possible.

3) Direct extrapolation in quantitative terms to the reactor scale is not possible in general (e.g. not all geometrical details are considered in the experimental simulations, unavoidable distortion in the scaling of the overall geometry, and scaling distortion in the fluid-specific heat capacity of structures).

4) Based on the applied scaling principles certain parameters, like for example steam generation in the core and steam velocity at the UCP may be under specific boundary conditions applicable to the reactor scale.

5) Results from transients with a significant amount of fall-back water are not generally applicable to the reactor scale because the upper plenum cannot be correctly scaled. In a test facility, due to the smaller scale the, water fall-back is more likely to affect the CET response than in the reactor case.

6) The CET measurement location and the installation details have a significant influence on the CET behavior, but are largely plant specific. Therefore, the similarity in a specific facility corresponds only to the used reference plant. That means also that no general similarity can be reached in a specific facility with respect to the location and mounting details of the CET measurement.

7) An increase in the CET is the ultimate indication of an inadequate core cooling and an already started core heat-up.

8) In some specific cases (in particular with CET's affected by water fall back), core heat up may not be detected by CET overheat.

3.6.5 Conclusions

The synthesis of the available experimental investigations results in a consistent picture regarding the behavior of the CET in relation to the maximum core/cladding temperature. The evaluation of the experimental results have also clarified the relevant physical phenomena and improved their understanding related to the CET behavior.

The variety of involved phenomena and their interplay does only allow for a qualitative general application/extrapolation to the reactor scale. In addition, the designs of the experimental facilities have always some limitations and therefore a direct extrapolation to the reactor scale is in general not possible. For certain cases or aspects under very special and restrictive boundary conditions quantitative application to the reactor scale may be possible, but only for specific parameters.

Already in the test facilities and especially at reactor scale the interplay of the different phenomena results in three-dimensional effects. The accurate prediction of the three-dimensional behavior is extremely challenging and actually no validated code is available for a reliable prediction of the behavior of all the CET located above the core during core heat-up. That means that based on the CET measurement there is presently no way to arrive at a fully covering conclusion on the cooling conditions in the reactor core. Accordingly, relevant uncertainties should be taken into account for the estimation of the cooling conditions in the reactor core. A major factor in this evaluation will be linked to the type of accident considered.

As a consequence, the available experimental results should be used to validate computer codes and models with respect to CET behavior. Definition of correct AM set points can only be expected by the use of codes and models validated in this way.

Nevertheless, taking into account the delay and the temperature difference in the CET behavior, a CET increase above saturation temperature, in particular in combination with other measurements, is well capable to detect a core heat up and is therefore an important element in the context of AM procedures.

4.   SUMMARY AND CONCLUSIONS

This section summarizes the main findings and conclusions obtained by the WGAMA Task Group on CET after a careful review of CET application for AM procedures in different countries and of pertinent experimental results focusing on CET delay times and temperature differences. Besides that, some recommendations are proposed in the next chapter: it is suggested to disseminate these among potential stakeholders.

As explained in the Introduction, the origin of the task group was a non-expected behaviour observed in Test 6.1 of the OECD ROSA Project. This experiment simulated a Reactor Pressure Vessel (RPV) Top Head Break in a PWR plant with complete failure of High Pressure Injection (i.e. beyond design basis). Preliminary analysis of the test results indicated that the observed delay between rod surface temperature and CET readings could have had a significant impact on test evolution. This concern drove WGAMA to propose to CSNI an activity which has been finally carried out by this Task Group.

4.1 SUMMARY OF THE TASK GROUP'S RESULTS

a)   CET readings use for AM in the member countries, and associated Technical Bases

The Task Group has conducted an international survey on CET use for AM (see Chapters 2.1 to 2.6). The main conclusions of this survey are as follow:

Most of the plants at the surveyed organizations use CET readings for AM. However, the scope and extent of their use is quite different from country to country; and something that is really significant, in countries using more than one unique technology (i.e. vendor), use of CET for AM could also be quite different from plant to plant.

In general, member countries have reported a generalized use of CET in EOP (preventive AM), in the transition from EOP to SAMG, in SAMG (mitigative AM) and, in some cases, in Emergency Planning.

The questions and responses to the survey were not sufficiently detailed to derive the exact technical basis for the definition of all set-point values. Criteria based on sub-cooling, saturation, onset of superheating and/or significant superheating, were reported by most of the surveyed organizations. In order to remedy this shortcoming section 2.7 provides a discussion of the technical (physical) bases for the major classes of set-point and CET usage.

Another important topic investigated in the survey was the relationship between CET Readings and Maximum Cladding Temperature. It has been noted that a significant fraction of the responses indicated that specific analysis had been performed to address this issue, but some of them felt the model validation was not fully adequate. Consistently with that, some of the responses expressed that either "delayed response" or "accuracy" was a concern.

b)   Review of experimental facilities results

The group has extensively reviewed information from different sources and experiments (see Chapter 3) where delays and differences between CET and cladding temperature readings had been observed: they included LOFT, PKL, PSB-VVER results and thirteen ROSA/LSTF experiments. ROSA/LSTF and PKL results proved to be especially useful due to more detailed instrumentation available in these facilities. The following conclusions have been obtained from this review:

- Delays in CET responses compared to actual cladding temperatures had been already identified earlier in different experiments. Especially, LOFT results had been carefully analyzed to gain insights about this issue and their impact on plant safety.

- The use of the CET measurements has some limitations in detecting inadequate core cooling and core uncovery: if CET reading indicates superheating it is in all cases with a certain time delay (ranging from 20 to several 100 s) and it is always significantly lower (up to several 100 K) than the actual maximum cladding temperature.

- CET performance strongly depends on the accident scenarios and the flow conditions in the core.

- The main causes affecting CET delays, which were present in all the experimental facilities and for most of the scenarios, are the following: radial temperature profiles (both in and above the core), cooling effect of the unheated structures in the upper part of and above the core, poor heat transfer from the rod surface to the surrounding steam due to low steam velocities during core boil-off and water backflow from the hot legs during core heat-up due to steam condensation in SG tubes, pressurizer water fall down or water from hot leg ECC injection.

- Besides that, there are other relevant aspects very specific to the facility design, like the actual CET location or behaviour that is scenario-dependent, like the hot steam chimney effect in RPV Top Head breaks and the downward core flow in the case of RPV bottom head break. It is interesting to point out that chimney effect, when present, could also produce non-conservative errors in some designs of reactor vessel water level standard instrumentation (based on "upper-to-lower heads delta-P"), because of the additional head loss produced by the steam when flowing through the CRGT up to the break. The (collapsed) liquid level reading may remain high even after the mixture level is formed. Then, such a systematic consideration should be taken into account.

- Shutdown operations: There are not many experiments from where relevant information for the importance of this issue could be compiled. However, some PKL and ROSA tests have shown that CET delays for scenarios starting from shutdown and/or low reactor water level conditions can be even more pronounced than in tests starting from nominal conditions due to colder structures in the upper part of the core. An interesting proposal deals with the convenience of using superheating rather than fixed temperature to initiate AM actions in these conditions.

c)   Applicability of experimental results to real plant conditions

Detailed conclusions with respect to the applicability of experimental results to real plant conditions have already been drawn in Chapter 3.6.4. It must be underlined that the variety of involved phenomena and their interplay allow only a qualitative extrapolation to the reactor scale. However, for certain cases and for specific parameters quantitative application to the reactor scale may be possible.

4.2 CONCLUSIONS

The evaluation of the experimental results allowed to draw up in a consistent picture regarding the behaviour of the CET in relation to the maximum core/cladding temperature. It also helped to clarify the relevant physical phenomena and improved their understanding related to the CET behaviour.

According to the results of the experiments and the subsequent analysis, and at least for scenarios starting at power conditions, it seems that the observed delays should not affect severely the effectiveness of most existing AM actions, but it must be underlined that concerns about CET functionality for general use in AM are well founded. It should be realised that an increase in the CET is the ultimate indication of an inadequate core cooling and of an already started core heat-up. No CET increase during a transient does not guarantee adequate core cooling: in some specific cases (in particular with water fall back from the hot legs), core heat up may not be detected by CET overheat, especially in CET positions affected by the water fall back. It should be emphasized that test results from transients with a significant amount of fall-back water are difficult to transpose to the reactor scale because the upper plenum cannot be correctly scaled. It can be expected that in a test facility, due to the smaller scale, the water fall-back is more likely to affect the CET response than in the reactor case.

After reviewing the different international approaches to AM, it seems that it is not possible to *a priori* fully discard the possibility of having, in a real nuclear power plant, a similar response as the one observed in ROSA Project Test 6.1, provided the applicable AM action initiation rely only on CET readings, which is not always the case.

In this sense it is interesting to remark that most of the AM strategies analyzed by the group, but not all, rely on a combination of CET readings and other instrumentation indications (normally, Reactor Vessel and/or Steam Generator water level) to define the initiation of the different AM recovery actions. This approach, when appropriately implemented, makes the AM more reliable because the specific draw-backs of each individual instrumentation system do not use to be coincident for a particular scenario. However, it is worth to recognize that not all the identified potential problems would be completely addressed by just using this type of multi-instrumentation AM approach, by the contrary specific validation for each foreseeable scenario should be carried out. Full understanding on the response of each instrumentation against the "expected" phenomena may form a basis for the validation.

Nevertheless, taking into account the delay and the temperature difference in the CET behavior, a CET increase above saturation temperature, in particular in combination with other measurements, is well capable to detect a core heat up and is therefore an important element in the context of AM procedures.

In view of the Task Group's results with respect to CET delay, the question may be raised about the consequences for the effectiveness of AM strategies relying on CET signals, widely used in the nuclear industry.

In order to judge whether the effects discussed in this report have an impact on AM measures and set-points already in place, one would need to understand whether the definition of a given CET set-point took into account all relevant effects and uncertainties listed in section 2.8. Did the AM developer use computer codes and models that were able to correctly represent these effects? Or maybe he did not address them specifically, but the set-point has included margin which would more than compensate?

Obviously, to answer these questions goes well beyond the present mandate of the Task Group and it could even be argued whether – due to a large number of plant specific aspects – it fits to the activity of an OECD task group. Based on the responses to the CET questionnaire it can be assumed that in most cases of AM procedure development the supporting analyses did not go to a detail, which would have captured correctly the complicated relationship between CET measurements and the cooling conditions in the reactor core. As a result, it can be expected that the estimation of the cooling conditions in the reactor core

includes relevant uncertainties. This calls for the validation of computer codes and models with respect to CET behavior by the available experimental results. Definition of correct AM set points can only be expected by the use of codes and models validated in this way.

5.   RECOMMENDATIONS FOR FUTURE WORK

Based on the previous conclusions the Task Group suggests to WGAMA to continue with the activities of this Task Group, including the following:

- The conclusions of the present report indicate the importance of dealing appropriately with the associated phenomena and uncertainties when performing analytical studies in support of AM strategies. Existing models used to calculate time delays between core temperature and CET readings may not be fully validated – this is also evident from the responses received to the questionnaire. Computer codes normally used for this type of analysis may not have enough "resolution" to accurately calculate some relevant phenomena affecting this particular issue. It is therefore recommended to verify whether or not state-of-the-art codes and their underlying models applied in support of AM procedure development are able to reproduce the delays and differences between rod surface temperatures and CET readings.

- The above activity could take the form of an ISP based on one or two pertinent experiments. PKL or ROSA/LSTF tests reviewed here could be candidates. The activity could have the following objectives:

    o Assessment of physical models to predict heat transfer modes affecting CET behaviour.

    o Development of a "best practice guideline" for the nodalisation approach of the uncovered core section up to the point of CET location.

    o Based on comparison with test results, assessment of the possible impact of 3D effects, not modelled in these codes.

    o If the 3D effects turn out to have an important contribution to time delay or delta-T, development of proposals, how these effects can be modelled e.g. by the help of CFD codes.

- Investigate the problem of CETs issue "scaling" (methods of extrapolating) from experimental facilities size, like LSTF, to commercial PWR reactors. The investigation could include both experimental and analytical aspects and would focus on the influence of reflux water from hot legs onto CETs as well as on the 3D flow behaviour in the upper part of the core. Large scale experiments are proposed for phenomena investigation and data preparation for code validation.

Besides that, the conclusions drawn by this group should be disseminated among stakeholders on AM (utilities, vendors, etc) in order to allow them the opportunity of reviewing the robustness of the existing AM packages to cope with situations like the ones discussed in this report.

Appendix

Abbreviations and Acronyms used in Section 4

In text:

AM	Accident Management
CAPS	CSNI Activity Proposal Sheets
CET	Core Exit Thermocouples
CRGT	Control Rod Guide Tubes
CSNI	Committee on the Safety of Nuclear Installations
ECCS	Emergency Core Cooling System
EOP	Emergency Operating Procedure
HPI	High Pressure Injection (ECC subsystem)
ISP	International Standard Problem
LPI	Low Pressure Injection (ECC subsystem)
LOFT	Loss Of Fluid Test (Integral Test Facility, USA)
LSTF	Large Scale Test Facility (ROSA Program, Japan)
PKL	Primärkreislauf (experimental facility, Germany)
PS	Primary System
PWR	Pressurized Water Reactor
PSB-VVER	OECD/NEA computer codes validation project (Russia)
RPV	Reactor Pressure Vessel
SAMG	Severe Accident Management Guideline/Guidance
SBO	Station Black-out
SG	Steam Generator(s)
WGAMA	Working Group on Analysis and Management of Accidents